EXPERIMENTAL INVESTIGATION OF ELECTROMAGNETIC BEHAVIOR OF ALUMINA REINFORCED COPPER MATRIX COMPOSITES

TARIQUL ISLAM (ROLL NO. 0418220005)

A Thesis Submitted in Partial Fulfillment of the Requirements for the Degree of Master of Science in Aeronautical Engineering

DEPARTMENT OF AERONAUTICAL ENGINEERING
MILITARY INSTITUTE OF SCIENCE AND TECHNOLOGY
DHAKA, BANGLADESH

FEBRUARY 2024

EXPERIMENTAL INVESTIGATION OF ELECTROMAGNETIC BEHAVIOR OF ALUMINA REINFORCED COPPER MATRIX COMPOSITES

M.Sc. Engineering Thesis

By

TARIQUL ISLAM (ROLL NO: 0418220005)

Approved as to style and content by the Examiners in February 2024:

_____ Dr. Shaikh Reaz Ahmed Professor Department of Mechanical Engineering, BUET	Chairman (Supervisor)
_____ Dr. Muammar Din Arif Assistant Professor Department of Mechanical Engineering, MIST.	Co-supervisor
_____ Air Cdre Md. Aminul Haque Senior Instructor & Head Department of Aeronautical Engineering, MIST.	Member (Ex-officio)
_____ Dr. Shahida Begum Professor Department of Mechanical Engineering, MIST.	Member (Internal)
_____ Dr. Md. Enamul Haque Professor Department of Biomedical Engineering, MIST.	Member (Internal)
_____ Dr. Quazi Deen Mohd Khosru Professor Department of Electrical and Electronics Engineering, BUET	Member (External)

Department of Aeronautical Engineering, MIST, Dhaka.

EXPERIMENTAL INVESTIGATION OF ELECTROMAGNETIC BEHAVIOR OF ALUMINA REINFORCED COPPER MATRIX COMPOSITES

DECLARATION

I hereby declare that the study reported in this thesis titled above is my own original work and has not been submitted anywhere for any degree or other purposes. Furthermore, I confirm that the intellectual content of this thesis is the product of my own work and that all the assistance received in preparing this thesis and sources have been acknowledged and cited in the reference section.

_____

Tariqul Islam
Student ID. 0418220005

Department of Aeronautical Engineering, MIST, Dhaka

ABSTRACT

Experimental Investigation of Electromagnetic Behavior of Alumina Reinforced Copper Matrix Composites

Copper is the third highest used metal in the industry because of its excellent electrical conductivity (100% IACS) with relatively high hardness at room temperature. However, the continuous degradation of mechanical performance of pure copper with increasing temperature eventually limits its use for electronic construction, especially for high temperature applications. Moreover, due to the conventional theoretical assumption of electromagnetic properties of metallic copper, scientists hardly made attempts to reveal the potential applicability of copper for next generation technology. In this research, attempts have been made to overcome the high temperature degradation of pure copper using trace addition of nano-crystalline Al_2O_3 particle as well as to evaluate the corresponding electromagnetic performance of copper. 99.99% pure copper was subjected to reinforcement using 0.5%, 1%, 2% and 5% white Al_2O_3 particles through conventional sand stir casting technique. The little percentage of Al_2O_3 made significant impact on the mechanical and electromagnetic properties of copper, especially when subjected to thermal treatments. The microhardness of Cu-Al_2O_3 composite increased with the increase of annealing temperature up to 600^0C according to Hall-Petch theory. The electrical conductivity was found to be very close to that of copper observed at room-temperature condition. The diamagnetic behavior of copper was transformed to paramagnetic behavior with the trace addition of Al_2O_3 particles, which was further influenced significantly by the thermal treatments. Dielectric behavior of pure copper was also investigated and the result of which were justified using Jonscher's theory of colossal permittivity. The present investigation suggested that the proper selection of composition and appropriate post thermal treatment can improve the mechanical as well as electromagnetic property of Cu-Al_2O_3 composite, thereby revealing the potential applicability of copper for future high-temperature/power applications.

সার-সংক্ষেপ

এলুমিনা মিশ্রিত তামার কম্পোজিটের তড়িৎচুম্বকীয় ধর্মের পরিক্ষামুলক গবেষণা

সাধারণ তাপমাত্রায় চমৎকার বৈদ্যুতিক পরিবাহিতার সাথে তুলনামূলকভাবে ভালো যান্ত্রিক কঠোরতা থাকার কারনে তামা শিল্পে তৃতীয় সর্বোচ্চ ব্যবহৃত ধাতু। তবে, ক্রমবর্ধমান তাপমাত্রার অবস্থার সাথে তামার যান্ত্রিক কঠোরতার ক্রমাগত অবনতি উচ্চ তাপমাত্রার পরিবেশের ক্ষেত্রে বৈদ্যুতিক যন্ত্রাংশ নির্মাণের জন্য এর ব্যবহারকে সীমাবদ্ধ করে। তদুপরি, ধাতব তামার বিদ্যুৎ-চৌম্বকীয় বৈশিষ্ট্যের প্রচলিত তাত্ত্বিক অনুমানের কারণে, বিজ্ঞানীরা পরবর্তী প্রজন্মের প্রযুক্তির জন্য তামার সম্ভাব্য প্রযোজ্যতা উন্মোচনের জন্য খুব কমই প্রচেষ্টা করেন। ৯৯.৯৯% বিশুদ্ধ তামাকে ০.৫%, ১%, ২% এবং ৫% সাদা Al_2O_3 কণা ব্যবহার করে প্রচলিত ঢালাই পদ্ধতির মাধ্যমে শক্তিবৃদ্ধি করা হয়েছে। Al_2O_3 এর সামান্য শতাংশ তাপমাত্রার অবস্থার পরিবর্তনের সাথে তামার যান্ত্রিক কঠোরতা এবং বৈদ্যুতিক চৌম্বকীয় বৈশিষ্ট্যের উপর উল্লেখযোগ্য প্রভাব ফেলেছে। হল-পেচ তত্ত্ব অনুসারে Cu-Al_2O_3 কম্পোজিটের মাইক্রোহার্ডনেস ৬০০°C পর্যন্ত বৃদ্ধি পেয়েছে এবং বিদ্যুৎ পরিবাহিতা সাধারণ তাপমাত্রার বিশুদ্ধ তামার বৈদ্যুতিক পরিবাহিতার কাছাকাছি পৌঁছে। ডায়াম্যাগনেটিক তামা Al_2O_3 যোগ করার সাথে প্যারাম্যাগনেটিক আচরণ দেখাতে শুরু করে এবং বিশুদ্ধ তামার ডাই-ইলেকট্রিক আচরণ অবশেষে উন্মোচিত হয় এবং জনসারের তত্ত্ব ব্যবহার করে লব্ধ ফলাফল ন্যায়সঙ্গত করা হয়। ফলাফলগুলি থেকে বোঝা যায় যে, মিশ্রণ এবং তাপমাত্রার যথাযথ নির্বাচন সহজেই Cu-Al_2O_3 যৌগের ইলেক্ট্রোম্যাগনেটিক প্রতিক্রিয়া বাড়িয়ে তুলতে পারে যার ফলে ভবিষ্যতে উচ্চ-শক্তি প্রয়োগের যন্ত্রাংশের নির্মাণের ক্ষেত্রে তামার সম্ভাব্য প্রযোজ্যতা প্রকাশ করে।

ACKNOWLEDGEMENTS

The author would like to extend his sincerest gratitude to Dr. Shaikh Reaz Ahmed, Professor Department of Mechanical Engineering, Bangladesh University of Engineering and Technology (BUET), Dhaka, for his patient instruction, insightful suggestions, and great encouragement throughout the research work. This work has been made possible and successful through his valuable help and guidance at every required level. The author also acknowledges the assistance of his co-supervisor, Dr. Muammer Din Arif, Assistant Professor, Mechanical Engineering Department, Military Institute of Science and Technology (MIST), Dhaka, for providing academic supervision and support to this research. The postgraduate coordinator Mahbuba Ferdous, Assistant Professor and other faculty members and staffs of the Department of Aeronautical Engineering at MIST, are gratefully acknowledged by the author for their kind assistance and support during the research. The author is also especially grateful to Dr. Mohammad Salim Kaiser, Director of the Innovation center, International University of Business, Agriculture and Technology (IUBAT), Dr. Rimi Rashid, Senior Engineer, Bangladesh Atomic Energy Commission (BAEC), Prof. Dr. Nasreen Akter and Prof. Dr. Mohammad Samirullah of the Department of Physics, Prof. Dr. Chanchal Kumar Roy of the Department of Chemistry, Bangladesh University of Engineering and Technology (BUET) for their help in various steps of the experiments.

Finally, the author would like to express his gratitude to his parents for their support and encouragement. He also thanks all the lab assistants from the Mechanical Engineering, Aeronautical Engineering and Naval Architecture and Marine Engineering Department of MIST who assisted in the experimental setup and measurements.

TABLE OF CONTENT

LIST OF FIGURES

LIST OF TABLES

LIST OF ABBREVIATIONS

MMC	Metal Matrix Composite
PMC	Polymer Matrix Composite
CMC	Ceramic Matrix Composite
MIG	Metal Inert Gas
TIG	Tungsten Inert Gas
LTI	Linear Time Invariant
MIM	Metal Insulator Metal
FCC	Face Centered Cubic
OD	Oxide Dispersed
IACS	International Annealed Copper Standard
EC	Electrical Conductivity
ER	Electrical Resistivity
FESEM	Field Emission Scanning Electron Microscope
MLT	Magnetic Loss Tangent
EIS	Electrochemical Impedance Spectroscopy
OCP	Open Circuit Potential
PVC	Poly Vinyl Chloride
ARB	Automatic Roll Bonding
ESD	Electrostatic Discharge
EM	Electro-magnetic
WEDM	Wire Cut Electronic Discharge Machine
PPMS	Physical Property Management System
DC	Dielectric Constant

CHAPTER 1
INTRODUCTION

1.1 Background

The term "metal matrix composites" (MMC) of copper refers to a class of materials that retain the desirable properties of copper, such as its high electrical and thermal conductivity, while enhancing Young's modulus, hardness, and wear resistance to outperform the extracted pure copper (Mortensen and Llorca, 2010). Due to the rapid advancement of electronic industry for the past few decades, smart phones, personal computers and other electronic devices have become a part and parcel of regular life. With the growth of technology, the characteristics required to fabricate modern complex technology, industry experts are looking for materials that perform multiple functions at the same (Seetharaman et al., 2022). The above-mentioned requirements will eradicate the use of pure substances by matrix composites like metal matrix composites, polymer matrix composites, compound composites, multifunctional materials etc. Due to the exponential increase in power requirement, per capita consumption of copper and copper-based alloy for construction of electronic components is also increasing exponentially (Gautam et al., 2018). To keep pace with the challenges, the in-built parameters of pure copper are tailored using unlike materials as reinforcement.

When it comes to high heat flux applications in fusion energy and high-power storage systems, pure copper is considered to be the prime candidate because of its excellent electrical and thermal conductivity. High heat flux is a major challenge in this regard because the material considered for construction of heat sink and wall must sustain the extreme condition of heat while maintaining optimum electrical and thermal properties (Li and Zinkle, 2012). Several researchers (Jenei et al., 2013) conducted surveys on mechanical characteristics for pure copper and found decrease in the mechanical resistance. Another critical factor influencing the usage of pure copper is its fatigue behavior with changing temperature. Copper is not a good fit for these applications because of its low yield strength and poor swelling resistance, despite its excellent thermal conductivity (Leedy et al., 1996).

Moreover, while tailoring the characteristics of pure copper, the electrical characteristics of copper like electrical and thermal conductivity must not be affected. So optimized doping material combination must be selected. Researchers are continuously putting efforts to find a solution to overcome the problems of pure copper. If the fluctuating temperature condition is selected like welding, high power energy storage applications, pure copper is known for its drastic failure. Due to this unavoidable fear, a huge potentiality of copper in construction of above-mentioned applications remains skeptical. Besides the consideration, several researchers took attempts to reveal the electromagnetic potentials of copper but those were insignificant (Benamara et al., 2024; Hossain Bhuiyan and Minary-Jolandan, 2022). The theories conventionally used for describing dielectric parameters are not applicable for highly conductive metals. Some obsolete theories like the Jonscher's predictive model, Debye model justified the co-existence of extremely large value of permittivity with high electrical conductivity in the same metal (Pérez-Madrid et al., 2017). After the initial prediction through computational modeling, progress in this field became limited within the use of copper as electrode materials. Highly recognized commercial simulation software like COMSOL even considered the value of permittivity of copper as 1 and only used it as electrode material for reference (Leelawattananon et al., 2017). Some other researchers considered the value as infinite. So, the exact character of copper in case of dielectric remained secret and confusing.

Recent advancement in the field of material science and engineering revealed the hidden possibilities of the unlike parameter combination for next generation sensing technology, resonators, memories as well as electrical contacting element construction. The sensor fabrication requires material to exert electromagnetic property with effect of signal penetration (Pei et al., 2014). The magnetic characteristics of copper known from previous investigations suggest its diamagnetic behavior and for this reason, no serious attempt was made so far to convert its repelling characteristics into attracting characteristics.

1.2 Scope of the Present Research

The present work aims to find a suitable alternative of pure copper in case of high temperature applications. To accomplish the task, it was necessary to go through the relevant previous works available so far in the literature. Some of the initiatives like using aluminum or other metallic combination were taken to cover the gap however, it was found that no individual work could cover the entire research gap. Additionally, effective attempts were not made to explore the dielectric and probable magnetic transition of the material. The present investigation differs significantly from the past investigations in this regard. The effort to reveal the electromagnetic characteristics of copper as well as the developed metal-matrix composite, especially for temperature applications will be one of the very first few experimental attempts in the literature. Finally, the mechanical strength and the electromagnetic characteristics of the developed metal-matrix composite are compared both at room and high temperature conditions for the purpose of selecting an optimum composition of the reinforcing element in copper matrix together with an appropriate post thermal treatment temperature.

1.3 Motivation of the Present Research

In the last two decades of the previous century, airships and the space shuttle's architectural design suggested a sharp increase in the use of composite materials. The primary motivation for the advancement of any material is cost optimization during manufacturing and operation. These days, composites based on copper and its alloys are becoming more significant in emerging engineering fields. Because of the superior electro-mechanical characteristics of copper, extensive steps had been taken by the researchers for proper tailoring of electro-mechanical properties of the copper-based composites specially to overcome the challenges imposed by the high temperature environment(Nomura et al., 2002). It is worth monitoring that the magnetic and dielectric characteristics of copper had hardly been explored; for example, the AC dielectric characteristics was only assumed based on conventional theoretical consideration. Because of the above-mentioned fact, the dielectric constant of copper is a confusing parameter even in this day. Moreover, the diamagnetic copper was hardly subjected

to interest by the researchers to induce para-magnetization. Therefore, this vacant area eventually imposed an invisible barrier on the practical applicability of copper for electronic construction. The primary motivation was to take the challenge of exploring the unexplored areas of copper, especially in the perspective of mechanical and electromagnetic applications, so that probable potentiality of copper could be well discovered. Steps were also taken to induce positive magnetization to copper using proper reinforcement and thermal treatment. The corrosion behavior of newly formed metal-matrix composite was also explored for examining the compatibility of the material in the adverse high temperature environments.

1.4 Objectives

To fulfill the above-mentioned requirements, the specific objectives of the research are,

I. Design and development of a copper-matrix composite reinforced with Alumina powder through conventional metal casting.
II. Comparative analysis of electrical conductivity, microhardness, corrosion characteristics and AC electromagnetic properties of the metal-matrix composite as a function of Alumina content with those of pure copper in as received state
III. Comparative analysis of the effect of isothermal and isochronal thermal treatments on the microhardness and electromagnetic properties of the Alumina reinforced Copper matrix composites

1.5 Structure of the Thesis

The conducted research is presented in this book chronologically from literature review to result analysis in such a way that a picture is easily depicted in the mind of the reader of this book so that next level attempt could be taken for further in-depth exploration.

Chapter 1 describes the fundamental concept and motivation behind the selection of this particular research

Chapter 2 is a review of the past works done in relation to the previous research

Chapter 3 describes the detailed methodology of material processing and their characterization

Chapter 4 describes the detailed analysis of the measured electro-mechanical parameters of the developed composite as well as microscopic observation of the samples

Chapter 5 portrays the analysis of the AC dielectric and magnetic characteristics of the composite

Chapter 6 describes the conventional gravimetric and electrochemical corrosion behavior of the composites

Chapter 7 includes the conclusion and the required recommendation for the future research

CHAPTER 2
LITERATURE REVIEW

2.1 Introduction

In the world of technological advancement, composites play the most crucial role in gaining the required characteristics of the designed system. Composite materials are mainly a combination of two or more unlike materials to achieve the future component's necessary properties. There are mainly three types of composites which are Metal Matrix Composite (MMC), Polymer Matrix Composite (PMC) and Ceramic Matrix Composite (CMC). The composites offer numerous benefits of which corrosion resistance, lightweight, design flexibility and better strength (Egbo, 2021). In the field of aviation, the primary characteristics required are lightweight with better stability. The most crucial feature of the Boeing 787 includes the use of composites for mechanical structure and electronic equipment's. Because of having superior properties that outperform traditional materials like the lightweight, corrosion-resistant, high strength, and stiffness, withstand high temperature, and easily formed in the manufacturing process, composite materials are continuously replacing conventional materials like metals, ceramics, and polymers (Jensin Joshua et al., 2020). In order to create a new material with new qualities that are different from the properties of the constituent materials, two or more substances must be mixed together without melting. The base metal used is known as matrix and the one used for creating a different property, submerged in the matrix is known as reinforcement. Aircrafts are subjected to a number of significant issues that might result in major accidents or degrade their performance, making the flight risky. In this research paper, a metal matrix composite is proposed which is highly applicable for avionics equipment.

2.2 Metal Matrix Composite (MMC)

MMCs are an excellent candidate for structural as well as electronic applications. It combines both the metallic and ceramic properties, resulting in higher mechanical properties required for high temperature applications and high electrical conductivity, permittivity, permeability, and

directivity (Singh et al., 2020). The comparison of mechanical and electrical attributes of MMCs is a burning area of research. The pure metals either contain high mechanical properties or high electrical properties. For example, Ag and Cu exhibit such excellent electrical properties that they are taken as reference material to compare electrical property investigation of different materials. Still, their mechanical durability and hardness properties are inferior (Studenyak et al., 2020). Any composite with electrical conductivity falls under the category of conductive composites; typically, conductive composites are made by dispersing specific volume fractions of conductive matrix with a nonconductive (or less conductive) filler. These composites exhibit a wide range of electrical conductivities required for various applications. Pure copper can't be used for component formation due to its poor machine-ability. Again, Ni focuses on mechanical properties with higher melting point (1455º C) (Karmakar et al., 2021). So, preparation of metal matrix composite requires extensive study of the mechanical and electrical properties of pure metals. The focus is kept on either high electrical property with moderate mechanical property or moderate electrical property with high mechanical property. In this research, the prepared composite's focus is kept on electrical and electronic devices such as RADAR antenna, generator-motor rotating parts, high power magnetic windings, circuit breakers, relays, and switches that require high electrical conductivity with mechanical hardness as well as thermal resistivity.

2.3 Electromagnetic Characteristics of MMC

The characteristics of a material's electromagnetic properties determine how quickly it will react to the absorption or emission of electromagnetic radiations. Radio waves, microwaves, ultraviolet, infrared, and visible light rays are a few examples of electromagnetic radiations that we are accustomed to. Due to the presence of polar molecules in materials that can react to microwave radiation, it is crucial to understand the electromagnetic characteristics of materials. Three properties of matter are the primary focus of electromagnetic analysis. These characteristics are expressed in terms of constitutive parameters, which explain how a material affects the amount of electromagnetic energy that responds to a source.

1. Permittivity (ε, F/m) measures how much matter affects how the electric field responds to an electric charge.

2. Permeability (μ, H/m) quantifies the influence of matter on determining the magnetic field in response to current.
3. Conductivity (σ, S/m) measures how matter effects on current flows in response to an electric field.

Electrical conductivity, dielectric permittivity, and magnetic permeability are examples of EM properties that are dispersive in nature. The operating frequency of the externally applied EM field determines the EM characteristics. As the polarization phenomena in a material does not change instantly with the applied EM field, there is a frequency dependence. We often require the constitutive parameters to display a few fundamental features to prevent electromagnetic theory from becoming too complex. Some of these properties are as listed below;

I. Homogeneity: It is known to hold the property or state of having a homogeneous structure or composition throughout or being of a comparable kind. A homogeneous material occupies space uniformly, meaning that the values of its constitutive parameters are consistent throughout the substance.

II. Linearity: If a substance's qualities are constant and unaffected by the strength of the sources and fields acting on it, the substance is said to be linear. For example, the permittivity of the substance separating the terminals plays a role in the capacitance of capacitors. When the applied voltage V is lower than the recommended operating voltage, this material is said to be linear. Capacitance does not considerably change with respect to V since ε is constant. The dependence on V becomes more evident when V is higher than the working voltage, and capacitance then becomes a function of V.

III. Isotropy: When a material object's physical characteristics are constant regardless of angles or directions, it is referred to as being isotropic in physical science. Certain characteristics of a material, such as its chemical, thermal, and electrical properties, are regarded as being identical (symmetrical) in all directions. As the molecular structure is the same in all directions and orientations, the material exhibits the same properties regardless of the direction or orientation. It is crucial to remember that even if a substance is described as isotropic, it is not necessarily possible for it to be

totally uniform in all respects, including dispersed characteristics and crystal symmetry.

Since they are prerequisites for superposition, linearity and time-invariance (LTI) are particularly crucial qualities to take into account. The laws of elementary circuit theory, which assume that superposition applies, do not necessarily apply to devices that are nonlinear and thus not LTI. This circumstance greatly increases the difficulty of analysis and design. Smartphones, personal computers, and other smart devices have become part and parcel of daily life due to the rapid rise of modern electronics industry. There is no truly homogenous, isotropic, linear, and time-invariant material in real world. The variation from this ideal condition is not great enough for most materials in most applications to effect engineering analysis and design. In other situations, materials might be significantly out of the box in one of these areas, but they could still be analyzed with the right modifications of the theory.

2.3.1 Concept of Dielectric Constant in Conductive Materials

Dipole or ion mobility in a material is studied through the process of dielectric analysis. Dielectric characterization is a highly effective method for assessing structural characteristics and physical alterations in a dielectric material (Nuzulia, 1967). Dielectric behavior of a medium also reveals information about the material's capacity for energy storage and energy dissipation. Electric charges do not pass through a dielectric when it is exposed to an electric field. Dielectric polarization is caused when electric charges slightly deviate from their average equilibrium positions. Positive charges move in the direction of the field while negative charges move in the opposite direction as a result of dielectric polarization. The internal electric field produced by this phenomenon lowers the overall electric field within the dielectric substance. The Maxwell- Wagner interfacial polarization model describes the interfacing reaction of two unlike molecules and the consequence in terms of polarization (Hao, 2013).

2.3.2 Concept of Colossal Permittivity

The separation of a material's positive charge center and negative charge center is referred to as electrical polarization. This type of separation occurs upon the influence of an external electric field which is the basic manifestation of dielectric behavior. For a long time, the theory of dielectric addressed the phenomenon and mechanisms of polarization in case of materials that are not essentially conductive. This focus on non-conductive materials such as ceramic and polymers was made in order to maintain the relevance of the concept of energy storage, piezoelectricity, pyroelectricity etc (Collinson, 2001). However, in connection with electrical conductors especially those with extremely high conductivity, the polarization concept received a little attention. Electronic conductors (like carbon, copper, silver) and ionic conductors (like ceramics with atomic scale channels for ions to pass through and cement-based materials, which have mobile ions dissolved in the water in the capillary pores) are types of electrical conductors. However, the conductivity of electronic conductor tends to be much higher than the ionic conductors like ceramics (Kaur et al., 2016).

Colossal permittivity refers to a situation where the material exhibits a dielectric constant higher than 10^4. As the quantitative definition is universal, the charge careers of the electronic conductor are electrons or holes. If the commonly available theory of dielectrics is considered, the colossal permittivity and high conductivity are mutually exclusive. That is where the contradiction of this research lies. The well-known physicist Jonscher successfully showed that high conductivity and colossal permittivity are inclusive in the year 1999 which is the case in this research (Tse et al., 2018).

Jonscher used complex electric susceptibility (a dimensionless complex number) which is related to dielectric constant (Wobschall, 1977) that relates with each other as given in 2.1.

$$\varepsilon_e(\omega) = \varepsilon_\infty + \varepsilon_0 x_e(\omega) - i\frac{\sigma_{dc}}{\omega} \tag{2.1}$$

Where, ε_∞ is the limiting high frequency value of the real part of the effective permittivity which is constant and real. The value describes the mechanisms of polarization that rapidly respond to the application of the applied electric field (Tuichai et al., 2017). Besides, σ_{dc} defines the value of DC conductivity of the material (constant and real) x_e is the calibrated

sum of the susceptibilities of the selected material composition that defines polarization response with respect to applied electric field.

The susceptibility of the material is defined by the universal Jonscher's equation of dielectric response as shown by the following;

$$x_e(\omega) = x_r \left(\frac{\omega}{\omega_r}\right)^{n-1} \left[1 - icot\frac{n\pi}{2}\right] \quad (2.2)$$

Where, *n* is a dimensionless parameter that characterize the change in amplitude as a function of frequency. One important consideration is that the value varies between 0 for materials with high dielectric loss and 1 for materials without dielectric loss factor.

x_r is the real part of the susceptibility of the referred frequency

ω_r is the referred frequency (arbitrarily chosen)

The ratio $\frac{\sigma_{dc}}{\omega}$ decreases with frequency and this quantity becomes negligible in the microwave range frequency. So, it can be easily neglected and the corresponding equation becomes;

$$\varepsilon_e(\omega) = \varepsilon_0 x_r \left(\frac{\omega}{\omega_r}\right)^{n-1} \left[1 - icot\frac{n\pi}{2}\right] + \varepsilon_\infty \quad (2.3)$$

To build a Jonscher model describing the permittivity of the Copper in frequency domain, the value of the mentioned three parameters (n, x_r, ω_r) is required. As the equation is used for computational prediction of dielectric parameter, non-linear algorithm for extracting them is used (Taylor et al., 2019).

2.3.3 Maxwell-Wagner Polarization Model

Capacitors made of metal-insulator-metal (MIM) are desirable passive components for analog and mixed signal applications. In this regard, various researchers recently proposed high-k dielectric stack MIM. Maxwell Wagner (M-W) dispersion can be seen in a heterogeneous system of conducting dielectrics where the ratio of permittivity to conductivity varies in the different phases. The Maxwell-Wagner phenomenon explains charge accumulation at the two-

material interface on the basis of the different charge carrier relaxation durations in these two materials as depicted in the Figure 3.1 (Xia et al., 2017).

When evaluated as a function of temperature at low frequencies, metal matrix composites typically exhibit very significant apparent dielectric constants and loss. Ionic conductivity brought on by impurities, interfacial (Maxwell Wagner-Sillars) space charge polarization buildup in heterogeneous materials, and inter-chain charge transfer are some of the mechanisms responsible for this phenomenon (Rayssi et al., 2018). The investigation of dielectric spectra obtained at low frequency may be hampered by these conductivity-related phenomena dominating the dielectric relaxation response.

This method has a few drawbacks: 1) the material's DC conductivity must be determined, or a measurement of the dielectric loss at very low frequencies must be used to approximate the conductive term; and 2) the conductive mechanisms, such as interfacial effects, may not scale linearly with frequency. In general, it is demonstrated that a number of physical factors, such as electrical and structural interactions between particles, the heterogeneity of the morphological and electrical properties of the constituent phases, the frequency dependence of electrical phase parameters, intra-particle structure, particle shape, size, orientation, and volume and surface fraction of the constituent phases, affect the dielectric properties of heterogeneous systems (Wang et al, 2008).

Depolarization field effects in heterogenous systems were first highlighted by Maxwell-Wagner and then successively by Sillars. So, the interfacial polarization is often termed as Maxwell- Wagner-Sillars effect. In a heterogenous mixture of Copper and Alumina mixture, due to differences in between dielectric characteristics and electrical conductivity, an additional charge accumulation occurs at each boundary under the influence of external electric field. The movement of charges gets attenuated out at high frequencies and the creation of depolarization fields is interrupted, the depolarization field effects in such multiphase systems disappear at sufficiently high frequencies of an applied EF.

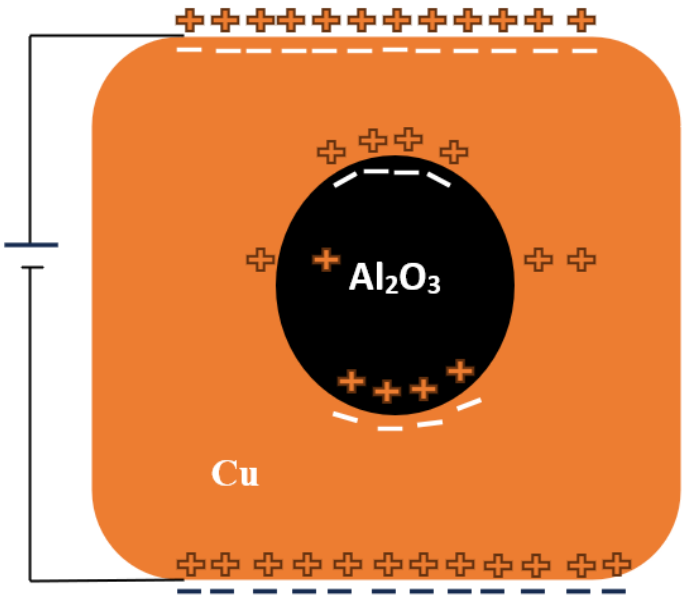

Figure 2.1: Schematic illustration of Maxwell-Wagner effect in heterogenous medium (simplest case with a single Al_2O_3 particle surrounded by solid Copper)(Rogti and Ferhat, 2014)

2.3.4 Debye Model

The Debye model is widely used to explain the dielectric behavior of materials. A distribution of relaxation times is frequently used to get a good description of the extracted experimental data. Numerous articles have focused on the dielectric behavior of materials under an external ac applied field because of its great scientific and technological significance. Measurements are performed for a variety of materials and in a very broad range of frequencies and temperatures. Jonscher provided a fairly thorough overview of the subject and presented a model for the dielectric spectroscopy called the many-body model (Mustafa et al., 2021).

Through interactions between individual dipoles in an interactive system, this model introduces the concept of correlated states in the material, which form a narrow half-filled band. Two potential wells can be used to represent the system's preferred orientations; the total polarization is determined by the relative occupancy of the two wells, and the application of an external field will excite these states, causing transitions between the two wells. However, it is generally recognized that the ideal Debye model does not accurately represent the

dielectric response of the majority of materials. As a result, different approaches to this model have been developed, including the presumption that the relaxation durations of the dipoles are distributed. It would be interesting to investigate whether a system with two or more types of dipoles, specifically dipoles with different relaxation times, described by the Debye model, would give a dielectric behavior similar to those experimentally found. This is because the many-body model predicts a region near the loss peak where the Debye description is observed (Weigand and Kemna, 2016).

Despite the success, the model has certain shortcomings. Specifically, Debye's dielectric function does not decrease quickly enough with frequency to satisfy the sum rule, which dielectric functions are required to obey. This limitation in Debye model at high frequency is related to unphysical behavior of the response function in the model. Despite having some shortcomings, its extreme simplicity and usefulness often overshadow the theoretical problems inherent in it.

Linear dielectric response for a time dependent electric field E(t) is described by,

$$D(t) = \varepsilon_\infty E(t) + \int_{-\infty}^{t} \varphi(t - t')E(t')dt' \tag{2.4}$$

Here, ε_∞ stands for instantaneous response with $\varphi(t)$ defines the time dependent input variable.

If delta function is given as input,

$$D(t) = \varepsilon_\infty E(t) + \varphi(t) \tag{2.5}$$

The Debye model response function is assumed to be,

$$\varphi(t) = \begin{cases} 0 & for\ t < 0 \\ \frac{\varepsilon_s - \varepsilon_\infty}{\tau} e^{\frac{t}{\tau}} & for\ t > 0 \end{cases} \tag{2.6}$$

This model was originally given by Debye for rotatable dipole in viscous liquid solution and then subsequently modified to extend its applicability for metallic materials (Mantas, 1999).

2.4 Copper and Copper Composites

Copper is a metal extracted from the earth. It has been vital in civilization's progress, contributing to technological development for more than 10,000 years (Jeff Doebrich, 2009). Copper is a reddish metal with a face-centered cubic crystalline structure. It reflects red and orange light and absorbs other frequencies in the visible spectrum, due to its band structure, so it as a nice reddish color (Bragg, 1914). It is malleable, ductile, and an extremely good conductor of both heat and electricity. It is softer than zinc and can be polished to a bright finish. It is found in group Ib of the periodic table, together with silver and gold. Copper has low chemical reactivity. In moist air it slowly forms a greenish surface film called patina; this coating protects the metal from further attack (Wang and Qi, 2022). Copper and copper alloys have been considered one of the best construction materials due to their high strength, excellent thermal characterization, excellent corrosion resistance, good wear resistance, and lower cost. To suit many technological applications, copper alloys are formed to find suitable characteristics. Nowadays, Aluminum bronze alloys and their composites operate effectively in electronic projects, automobile manufacturing, and military industries(Hirsch, 1997). Due to the current advancement in technology, there has been a great deal of interest in particulate–reinforced MMCs and, in particular, those based on existing copper alloys. However, their poor plasticity and limited hardness, and low reliability restricted their application in many technological fields. Copper is a tough, ductile, and malleable material. These properties make copper highly suitable for tube forming, wire drawing, spinning, and deep drawing. For the specific type of application, doping material is selected to find that material's particular characteristics.

Most metallic appearance of copper includes electrical applications, machinery production, transportation and ordinance. Tin bronzes dominated the trade throughout the entire European and middle eastern world with 300 – 400 years. (Gorman and Dzombak, 2020) conducted a statistical review on the consumption of copper in different sectors in the US between a period from 1970 to 2015. They found a significant increase in the import of copper from only 75000 tons in 1998 to 945000 tons in 2011 only form China. But the recent change in export policy of China attributed a major decrease in import by different sectors in US. A recent review conducted US geological survey has revealed that refined copper stocks in the US totaled

104,000 tons at the end of June 2023 which is 27% higher than May but 16% decrease in June 2022(U.S. Department of the Interior and U.S Geological Survey, 2022). This means researchers of US are focusing on secondary production of copper from the scrapped copper for maintaining the future mass balance and hold the per capita consumption of copper in the future.

2.5 Selection of Copper as Base Material

Before selecting the pure Copper as the base metal for this research, a thorough literature review was done considering the key properties like EC, hardness, corrosion characteristics as well as probable change with respect to changing temperature condition. The detailed description of the mentioned properties is given below;

2.5.1 Electrical conductivity

Composite materials that are conductive and lightweight are beneficial for a variety of applications, including battery parts, electrodes, shields from electromagnetic interference, electronics parts, and aviation. Composite materials must have electrical conductivity in the range of 10^{-12} and 10^{-8} S/cm for ESD applications, 10^{-8} and 10^{-2} S/cm for moderately conductive applications, and 10^{-2} S/cm and higher for shielding applications in order to be used for conductive applications (Osman and Mariatti, 2006). In comparison to any metal, copper (58 MSm^{-1}) has the best electrical conductivity other than silver. Electrical conductivity property defines the ability of a metal to carry electrical current. Electrical current will flow through all metals. However, all of them have specific resistance, which means a certain amount of force is required to push. The higher the resistance, the higher the energy needed to push the current through the metal. Because of the negligible resistance of copper, current will flow through it quickly without loss of energy (Guschlbauer et al., 2018). Since this research mainly focuses on the electronic applications of copper, the doping material was selected so that it will not affect the conductivity of copper but increase the fracture toughness.

2.5.2 Thermal conductivity

As thermal conductivity is an intrinsic property of a material, it depends on the amount of substance present. It is the ability of a material to conduct heat. Thermal conductivity occurs due to molecular agitation and contact and does not result in the solid's bulk movement. The thermal conductivity of a material is quantified based on the rate equation which is derived from Fourier's law of heat conduction. The thermal conductivity of a material varies due to factors such as temperature gradient and the path length of the heat. The conductivity of air (0.024 W/m.k) and aerogel (0.03 W/m.K) is too low whereas copper is the excellent(385 W/m.k) conductive material (Baba et al., 2012). Though diamond is the highest heat conductive material with the conductivity coefficient of 1000 but due to its low-cost effectiveness it can't be used in heating technology (Chung et al., 2014). That is why copper is the ideal material used for heat exchangers, fusion reactors. It is highly used for thermocouples as well because of the high Seebeck coefficient (Abdelaziz and Megahed, 2011). But if the application of the generator is considered, the heating process can create degradation because of the high-speed rotation of armature. So, the doping material should be selected so that the coefficient of heat conduction is reduced.

2.5.3 Hardness

To finalize a material for engineering manufacture, some vital mechanical properties must be considered. Some typical mechanical properties may include strength, toughness, hardness, ductility, brittleness. Mechanical hardness and micro-hardness are the parameters used to describe the tribological characteristics of the material. Mechanical hardness is defined as the ability of a material to resist deformation due to application of load. Hardness may include scratch hardness, indentation hardness, rebound hardness (Soundararajan et al., 2023). Micro-hardness testing and nano-indentation are standard methods of determining stress. There are many traditional methods of measuring hardness. Of them Vicker hardness is the most efficient. Pure annealed copper has micro-hardness of 40 HV and fully annealed copper has 110 HV (Poole et al., 1996). If application of rotating component like magnetic coil or armature is focused, micro-hardness is needed to be increased (Ankur et al., 2021).

2.5.4 Electrical Permittivity

Electric permittivity is one of the most important characters required for communicative equipment. Dielectric permittivity or the dielectric constant defines how strongly a material can be polarized under the influence of electric field. Relative permittivity or dielectric constant varies with respect to frequency, temperature. Copper is an excellent choice for nano-antenna (Halder et al., 2014). Researchers have hardly made significant attempt to explore the dielectric constant of copper. Because of the hackneyed theoretical assumptions that don't justify the dielectric constant of conductive metals, the exact value of pure copper remained uncovered. In the age of electronic development, the per capita usage of copper is always increasing and copper is on the most used metal in electronic engineering. Copper is best suited for base antennas as well. For permanent mount of base antenna, the fracture toughness of pure copper is needed to be increased (Valb., 1998). For this purpose, lower percentage of Alumina was added to increase the toughness of material with negligible effect on the permittivity.

2.5.5 Coefficient of Thermal Expansion

Coefficient of thermal expansion deals with the expansion characteristic of material with respect to change of temperature. In different areas of technology, an overview of the temperature dependence of the dimensions of the components of an assembly is essential before designing a piece of equipment. The ceramic phase which is generally used as reinforcement in MMC has a large difference in coefficient of thermal expansion with the metal phase. This thermal mismatch causes large residual thermal stresses near the interfaces of composite when they are cooled from the fabrication temperature. Thermal stresses are important in design because they lead to plastic yielding or failure of the material. The difference in thermal conductivity of the matrix and reinforcement generates a thermal gradient throughout the composite. The thermal mismatch of both constituents (matrix and reinforcement) plays a vital role in the thermo-mechanical reliability of devices. Some amount of thermal stress is relaxed by dislocation punching from the interface into the matrix via cooling from the processing temperature. This leads to high dislocation density and high yield strength. Thermal stress depends on: reinforcement volume fraction and morphology, matrix

crystallographic texture, void or lack of adhesion at matrix reinforcement interface. Repetitive non reversible phenomena like thermal cycling leads to permanent deformation. The reinforcement particle geometry influences the degree of thermal stress as: reducing the size of the reinforcing particles would increase thermal fatigue resistance. The copper shows a coefficient of thermal expansion of around $(16 – 16.7) \times 10^{-6}$ K^{-1} which is increased slight due to addition of some other metal (White, 1972). But Alumina (Al_2O_3) has a low thermal expansion coefficient of around 8×10^{-6} K^{-1} (Huntz et al., 2006). The application focused in this research requires decrease of coefficient of thermal expansion which is possible if Alumina is selected as doping material. The behavior of different MMC is different for different isothermal conditions when they were subjected to thermal cycling.

2.6 Selection of Alumina as Doping Material

The ceramic materials represent interesting properties and generate products that meet essential requirements for several class of applications. Over the past few decades, metal oxide nanoparticles have undergone extensive development. They have been widely used in many applications such as catalysis, sensors, semiconductors, capacitors and batteries. Corundum is commonly referred to as Al_2O_3 or alumina. Aluminum oxide is an excellent example of this class of materials being applied widely in high technology areas, especially where abrasive and erosive wear is strongly demanded. Many factors interfere with the wear of Alumina: material composition, characteristics of the used oxides and the manufacturing process. There are various phases in alumina, including gamma, delta, theta, and alpha. Among them, the alpha phase is the most stable one (Huntz et al., 2006).

In comparison to metals, ceramics are less susceptible to damage due to corrosive environments. So, Alumina can be considered as a representative of engineering ceramics which exhibits all essential properties required for engineering materials such as hardness, fracture toughness, low coefficient of thermal expansion, relatively good thermal conductivity. Though alumina’s major part is aluminum which is highly reactive in the corrosive environment but making oxides of aluminum like alumina does not react with most materials which makes it highly anti-corrosive and replaceable material over Ni (Alsoufi et al., 2016). It

is already known that copper is highly suitable for electronic applications but increasing mechanical properties to prevent thermal fatigue, cyclic loading, corrosion or melting point. If melting point becomes close to the point of subjectivity, the material will start to soften and deform. Alumina has a melting point of 2000^0C which is much higher than pure copper (Abyzov, 2019). So, addition of Alumina as reinforcement will not only increase the melting but also increase the composite's resistance to thermal fatigue and permanent deformation. Alumina is a very hard ceramic with vicker hardness of 1440 kg/mm^2 which is almost close to diamond (Bharti et al., 2020). So, it exhibits excellent wear properties. Many research already showed that wear resistance is a crucial consideration in designing rotating components. As the research focuses on the electronic application like generators, fusion reactors, MIG and TIG welding tips, increasing wear resistance will be an essential criterion for designing such equipment. Alumina is an excellent choice for this problem. Additionally, 99.5% pure alumina very high flexural strength (379 MPa), elastic modulus (375 GPa), shear modulus (152 GPa), bulk modulus (228 GPa) with low coefficient of thermal expansion (8.4 x $10^{-6}/^0$C) (Abdo et al., 2019). It works as an excellent dielectric as well with a dielectric constant of 8.9 at 1MHz frequency range(Vila et al., 1998). Some recent approaches involving the Al_20_3 as reinforcement particle is mentioned below:

(Leon-Patiño et al., 2014) carried out some experiments to join the composite Cu– Al_2O_3 (50 vol.% Al_2O_3) to electrolytic copper using the filler alloys 72Ag–28Cu and 70Cu–30Zn via brazing which was practical and successful. Mechanical performance of the joint was deviated due to temperature variation.

(Alemour et al., 2019) developed a composite taking copper as base metal reinforced with alumina and graphaite. As the researcher's focus was on marine applications, using alumina as reinforcement increased the mechanical properties .The presence of graphite gave a boost on the corrosion resistance. The samples with maximum graphite exhibited better wear resistance in the experiments under maximum load conditions.

(Hidalgo-Manrique et al., 2019) carried out a brief review on copper/graphene composite. Electrical, thermal, tribological and corrosion behavior was investigated. A description of the future prospects was given based on the specific property analysis of the composite.

(Strojny-Nędza et al., 2016) prepared a composite consisting of Cu and varied percentage of Al_2O_3. The composite was prepared using powder metallurgy technique and spark plasma sintering. As the researcher's focus was on aerospace industry such as rocket thrusters and aero-engine, thermo-mechanical tests and finite element analysis were carried out. Based on the said modeling, technological conditions for obtaining functionally graded materials were proposed.

(Ea and Ragab M, 2019) produced aluminum bronze matrix composite (ABMC) using 88% Cu, 11% Al and or hybrid composition of aluminum like Al_2O_3 and carbon nano tube. The fabrication was done using the basic powder metallurgy technique. The researcher's demonstrated the Archard rule of simultaneous enhancement of hardness and wear rate in hybrid composite alloy which attributed the synergistic reinforcement of alumina nano-particle and CNT. The research was useful for interfacing and designing of ABMCs with high strength and wear rate without decreasing the conductivity property.

(Madhusudan et al., 2016) prepared a composite using copper as reinforcement particulate in the aluminum matrix using stir cast technique. The sample form varying percentage of copper between (5-15) % was subjected to mechanical testing for both cast and homogenized condition. The CMMs responded similar to MMCs in tensile properties but strain failure and drop in strength created a barrier in mechanical application of the proposed composite.

(Mahbuba, and Chisty, 2014) investigated the relative permittivity response of silver (Ag), copper (Cu), gold (Au) and nickel (Ni) which is required for designing the metal nano-antenna. For the analysis, higher range of frequency (20-300 THz) was taken. The imaginary response of dielectric permittivity was negative where real part was positive. The gold showed the largest real part of dielectric response but other metals like copper showed moderate real part response which is applicable for reducing the size of the antenna. The gold metal got the best resonant frequency.

2.7 Thermal Ageing

Because composites are increasingly used in structural applications where higher temperatures are a prevalent environmental condition, their thermal aging behavior is of particular interest. Thermal ageing is the word used to describe long-term, irreversible changes in the structure, composition, and morphology of materials exposed to temperatures that they are generally likely to experience in service. It could be carried on by a mixture of chemical and mechanical changes, the most substantial of which is typically oxidation carried on by contact with ambient oxygen (Hamasha et al., 2022). In certain situations, or conditions, high conductivity materials such as copper or its alloys may be subjected to hot and cold work. Sudden increase in temperature may cause significant changes in the intermetallic structure which may lead to enhance certain properties as well as decrease in some other (Ju et al., 2023). This effort could have been done intentionally to create an engineering product or it could have happened when these things were being used at the user level. Cold work is defined as mechanical effort performed on a material to cause a plastic deformation at a temperature below the recrystallization temperature, which is typically approximately 40% of the melting point or somewhat lower for some materials. Face centered cubic (FCC) copper, which has a cubic crystal structure, is ductile and malleable in its annealed condition (Khan et al., 2019).

Diffusion of alloying atoms happens during thermal aging, a time- and temperature-dependent process that alters the overall microstructure of the alloyed material. By using scanning and transmission electron microscopy, the microstructure might be examined. Based on the effect of intermetallic structure of the base metal, the thermal aging temperature will be selected. The next generation fusion reactor technology requires the constructing metal to survive the harsh environment of the reactor. The Copper alloys haven't been given much thought in terms of use as structural components for fusion reactors (Gorynin et al., 1992). We have addressed a number of concerns regarding the usage of high-performance copper alloys for the CTR first-wall application and have made an effort to compare these alloys to other potential materials. Our focus is on copper alloys created using traditional casting techniques for cost effective mass production and used to achieve great strength at elevated temperatures. The process was adopted to discover the potential of copper alloy for construction of fusion reactor first wall (Zinkle, 2016). Cu based alloys depend on finely dispersed, insoluble or poorly soluble phases

that are time and temperature stable to give robust, high temperature performance and high thermal conductivity. Cu alloys with Zr+Cr (Amzirc), Mg+Zr+Cr (MZC), and CuNi-Ti alloys have lately offered various combinations of desirable properties, with slight drawbacks in each case that can be fixed by alloy and microstructural advancements (Chen et al., 2018).

2.8 Corrosion Characteristics

This property deals with the material's ability to resist the environmental impact due to its electrochemical reaction. Copper is a metal with excellent corrosion resistance with a wide variety of environment. However, stress corrosion, selective corrosion and impingement corrosion can create deterioration of copper made component. This type of corrosion can be easily overcome by efficient design of copper alloys. To prevent sea water corrosion, Ni is an excellent choice because of its high melting point and ability to resist formation of oxide layer resulted due to corrosive environment (Metikoš-Huković et al., 2010). But Ni is a metal that can reduce the electrical properties of copper. If copper is heated upon a temperature above 400º C, it essentially starts to oxidize (Mrowec and Stokłosa, 1971). So, to increase the melting point, Ni can be used for doping. But due to decrease of electrical properties, Ni is not suitable for use in electronic device.

A novel class of nanostructured materials known as metal matrix nanocomposites is composed of nanoparticles utilized as reinforcements. Researchers have given attention to develop composites in order to improve the electro-mechanical performance for use in particular applications. The manufacturing of electrodes, electronics packaging and contact terminals are some of the areas where high strength and high conductivity are required (Mazahery et al., 2009). Due to its superior corrosion resistance, lower cost, higher thermal and electrical conductivity, copper has become one of the highest employed metals for electronics application. As copper does not have adequate mechanical strength required for high temperature environment, ceramic materials are added as reinforcements. Al_2O_3 dispersion strengthened copper has remarkable mechanical stability with improved electromagnetic property at an elevated temperature (Hsieh and Tuan, 2007). The hybrid composite even exhibits electrical conductivity near Copper at elevated temperature (D. SABER, 2016). The

decrease of grain growth phenomena ensures the higher mechanical stability as per Hell-Patch relationship (Fathy and El-Kady, 2013).

Chloride salts possess many attractive properties for use as coolant and storage medium for advanced nuclear reactors and in concentrated solar power systems (Raiman and Lee, 2018). Molten salt reactors have seen a marked resurgence of interest over past few decades, highlighted by their inclusion as one of six generation iv type reactors. Scientists from oak ridge national laboratory (ORNL) have been working for the development of Molten Salt Reactor Breeder (MSBR) from the mid-20^{th} century (Kurley et al., 2019). The compatibility of halide salt for usage as storage medium is under re-examination based on their high breeding ratios and short doubling times (LeBlanc, 2010).

Salts are named mainly based on their negative ions. Salts typically used for energy applications include NaCl, $MgCl_2$, $CaCl_2$. Scientists are working extensively on Fluoride and chloride salts compatibility. But if the basics are being explored the chloride salts are the readily available and cost-effective medium. Besides that, chloride salt often exhibits almost similar behavior as fluoride salts (El-Kady et al., 2022). Generally, the corrosion of materials in chloride salts can be in the form of electrochemical corrosion, galvanic corrosion, impurities driven corrosion and corrosion due to temperature gradient. This article aims to elucidate the compatibility of Copper-Alumina composite in 3.5 wt% table salt or commonly known as "NaCl" medium which is equivalent to sea water through electrochemical Impedance spectroscopy and potentiodynamic polarization test. The Table 2.1 portrays a comprehensive review of the steps taken by researches to improve the corrosion resistance of pure copper.

Table 2.1: Review of investigations made by several authors to enhance the corrosion resistance of pure copper with variation of reinforcement and processing route

Ref No	Material	Processing Route	Corrosion Medium	Findings
(Singh et al., 2019)	1. Cu 2. A1= Cu – 1% HSSS – 1% WC – 2% Cr 3. A2= Cu – 2% HSSS – 1% WC – 2% Cr 4. A4= Cu – 4% HSSS – 1% WC – 2% Cr	Stir Casting	0.1 M NaCl	Corrosion Resistance (CR): A4 > A2 > A1 > Cu
(Medeliene et al., 2011)	1. Cu 2. Cu – CNM1 3. Cu – CNM2 4. Cu – CNM3	Coating	0.2M $CuS0_4.5H_20$ + 0.5M H_2S0_4	Corrosion: Coating possess higher CR
(Benea et al., 2000)	1. Cu 2. Cu – Zr	Coating over 6cm^2 surface	0.5M H_2S0_4	Composite coating possesses CR three times higher than pure copper
(Mohanavel et al., 2020)	1. Cu 2. Cu – 15% TC – 5% GSA	Powder Metallurgy	Not Mentioned	Corrosion rate reduced by 94.27% in comparison to copper
(Alaneme and Bodunrin, 2011)	1. Al (6063) 2. Al (6063) – 6% Al2O3 3. Al (6063) – 9% Al2O3 4. Al (6063) – 15% Al2O3 5. Al (6063) – 18% Al2O3	Stir Casting	1. 3.5 wt% NaCl Solution 2. Na-OH & 0.3 M H_2S0_4	Al_2O_3 improves the CR of Al (6063) alloy. The CR is higher in salt water than other.
(L and K. S, 2020)	1. Cu - 5% Al2O3 2. Cu - 10% Al2O3 3. Cu - 15% Al2O3	Ball Milling (Nano- Cu Micro-Al_20_3)	3.5 wt% NaCl	Corrosion Resistance: 15% Al_2O_3< 5% Al_2O_3 < 10% Al_2O_3
(D. SABER, 2016)	1. Cu 2. Cu - 10% Al2O3 3. Cu - 15% Al2O3	Mechanochemical Technique	1. 3.5 wt% NaCl 2. 0.5M H_2S0_4	15% Al_2O_3 showed lowest CR. 0.5M H_2S0_4 solution attributed higher corrosion than 3.5 wt% NaCl solution
(Allahkaram et al., 2011)	1. Cu – 16.6% Al2O3 2. Cu – 18.2% Al2O3 3. Cu – 19.3% Al2O3	DC & PC Coating	3.5 wt% NaCl Solution	CR decreased with Al_2O_3 content. PC coating improved the CR
(El-Kady et al., 2022)	1. Al 2. Al - 10Cu 3. Al – 10Cu – 2.5% Al2O3 4. Al Matrix – 0.5% GNs 5. Al Matrix – 1% GNs 6. Al Matrix – 1.5% GNs	Powder Metallurgy	3.5 wt% NaCl Solution	Corrosion Resistance is significantly improved with increase of Graphene content.

CHAPTER 3
MATERIALS AND METHODS

3.1 Introduction

The conventional way of fabrication of composite is either by casting procedure or the powder metallurgy process. The most common method adopted in industry level for manufacturing composite is by casting process. The casting process is basically accomplished by pouring the molten material into a mold of desired shape. The melting point of the material is the most important factor to be monitored while the casting process is ongoing. Existing processes for making copper-based alloy castings can be broadly classified into different categories like sand casting, centrifugal casting, chill casting and many more. Each of them has got its advantages and limitations. The conventional sand casting is the most popular in the industry because of its low cost with effectiveness if proper environment is maintained (Holman et al., 1895). As the material is subjected to environmental conditions the humidity factor of the environment is very important. In this research, stir sand casting process is applied for fabrication of composite.

3.2 Preparation of Metal-Matrix Composite by Casting

In this research, 99.99% Pure Copper was taken as the base metal as presented in Figure 3.1. The active neutral white crystalline Alumina powder with a particle size (70-230 mesh) of minimum 70% was selected. The particle had a PH value of 6.5 to 7.5 which indicated that the powder was neutral and the weight per ml at 20°C was approximately 0.9 g/ml. The Alumina particle had a purity of 99.99% as well. The casting processes technological requirements are the most significant aspect in achieving good outcomes in terms of product quality. The higher the humidity, the higher the porosity of the casted metal. The melting temperature of pure Copper is 1083 °C, and the density is 8900 kg.m-3, three times that of aluminum. Copper's heat and electrical conductivity are lower than silver, but it is 1.5 times greater than aluminum's. The casting process is selected based on the category of materials. For example,

copper-based alloy production with lower level of reinforcement with tin, aluminum, manganese is well suited in Stir sand casting with a suitable mold using sand. Before the casting process, the X-ray Fluorescence was used for to check the purity level of the base metal and reinforcement powder.

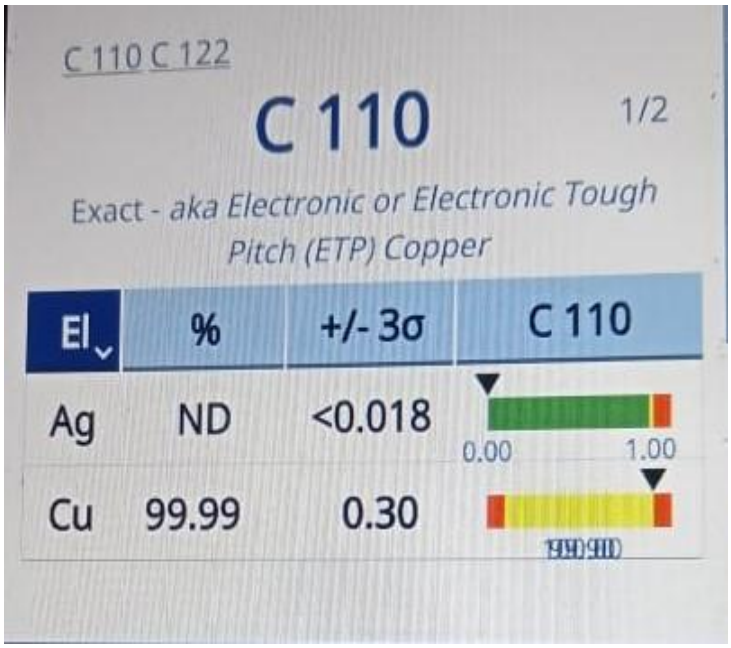

Figure 3.1: The obtained result of WD-XRF machine indicating the purity percentage of copper used in this research (99.99%) in as-received state

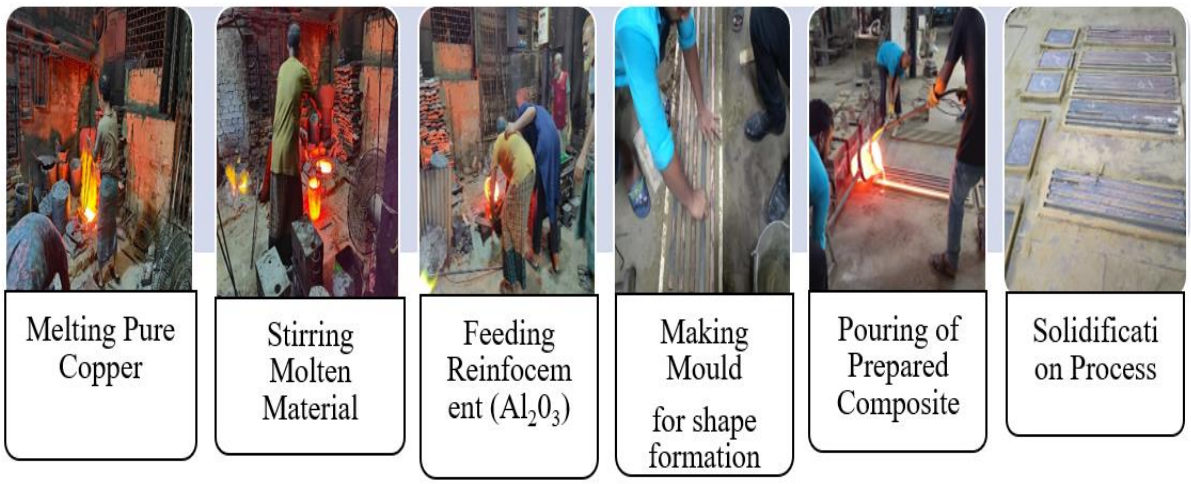

Figure 3.2: Process of manufacturing the desired composite

100 kg of pure copper was collected from commercial resources for casting. 5 kg of pure Alumina powder was collected from science laboratory ensuring that it would only be used for research purpose as dealing with pure Alumina may be hazardous to health. The casting procedure was done at Bangladesh Industrial and Technical Assistance Corporation (BITAC) maintaining proper scientific environment as depicted in the Figure 3.2. Steel molds were prepared before the start of casting process. The molds were then placed in a sand box to pour the molted composite. The melting was carried out using a clay graphite crucible in a natural gas furnace. The crucible was heat treated for 6 hours before the start of melting process. Graphite was used on the sand molds to remove the prepared composite after natural cooling.

The Alumina with melting point of 2072^0C was heat-treated at first up to a temperature of 1000°C and then molted pure copper was added as the base metal. The melting temperature of copper is 1085°C. The temperature was measured using the laser temperature sensor. The temperature was kept same at 1100°C to make sure the proper melting of pure copper. The temperature was raised to 1500°C to form the metal matrix composite. The molten metal was poured in the sand very carefully and was subjected to natural cooling as shown in Figure 3.3.

Figure 3.3: Final metal-matrix composite sample (as cast) prepared after natural cooling at environmental conditions

Five compositions of copper-based metal matrix composite were prepared with varying percentage of Alumina. The nominal percentage of the prepared composite is mentioned in the Table 3.1. The casted materials prepared for sample preparation were examined once again using the X-ray Fluorescence for ensuring the intended percentage of the composite after casting.

Table 3.1: Nominal composition of matrix (copper and reinforcing element (Al_2O_3)) in the final samples

Composition Identification No	Percentage of Copper (% weight)	Percentage of Alumina (% weight)
I	99.99% (as cast)	0
II	99.5%	0.5%
III	99%	1%
IV	98%	2%
V	95%	5%

**Reference value of the copper-as received used in this work is-O*

3.3 Machining Process

After completion of preparation of composite through sand casting route, the plates were subjected to machining to produce samples of the relevant size and shape. The specimens were mainly of five groups and their number was fixed as though it could meet all the requirements of the test. The process of fabrication of samples is described in the following article.

3.3.1 Fabrication of Plates using CNC Machine for Preparing Samples

The computer connected to the CNC (3-axis CNC milling machine VF-8/50) machine had the design loaded into it. The design of the final shape was converted by the computer into a unique numerical code that directed how the CNC shaped and cut the material. Double-sided tape was used to attach the material in order to prevent it from coming off the block during milling. The

block was then set into the CNC's vice, carefully tightening with instruments. If it is not secured, it may come away from the vice as the machine begins to cut the material. The vice travels up, down, right and left as intended when the machine is operating.

The casted plates were cleaned in terms of porosity. As the target was to produce porosity free sample which has effect on the measurement of the electrical and mechanical property. The plate was transformed into bar shape using the 20 mm spindle. The speed was maintained up to 3000 rpm. The feed was maintained up to 5 mm on both of the sides.

The reset button is typically the most significant control button. The reset button was pressed by to start the CNC machine. This "zeroes" the cutter, relocating it to the X, Y, and Z coordinates of 0, 0, 0. Initial set up was done and by changing the 3-D axis of the spindle it was placed. Although manual control of the cutter is an option, it was rarely necessary. The cutter's movement over the horizontal surfaces was managed by the 'X' and 'Y' buttons. Depth and up/down movement are controlled via the "Z" buttons. While the operation was ongoing, the coolant was sprayed on the plate. As heat generation may affect the side molecules while cutting, the unwanted heat was removed using the coolant. Finally, the transformed shape was ready for shaper machine for further progress.

3.3.2 Wire Cut Machining

The vicinity of the cutting area was heated up to 4000ºC based on the type of material (Copper) subjected to machining. The dielectric medium around this region evaporates, especially when the pressure increases. The samples were subjected to shaper machine at first. But the extra heat could change the basic characteristics of the sample by changing the micro-structure of the material. So, to maintain the accuracy level of the samples and to obtain the accurate shape and finishing CNC Wire Cut EDM Machines (Model:09AAACA1831C1ZB, Japan) was used. The wire used in the machining was 0.15 mm as per the manual subjected for metal cut with a melting point of below 3000°C. Before starting the cutting process, the sample shape and size was drawn using CAD model and was given as input to computer as shown in the Figure 3.4. After properly selecting the input parameters When the spark was extinguished and the beginning moment occurred, the pressure drop caused the metal globules that had been

discharged by the flowing dielectric medium to condense. The specifications used for fabrication of samples are illustrated in the Table 3.2.

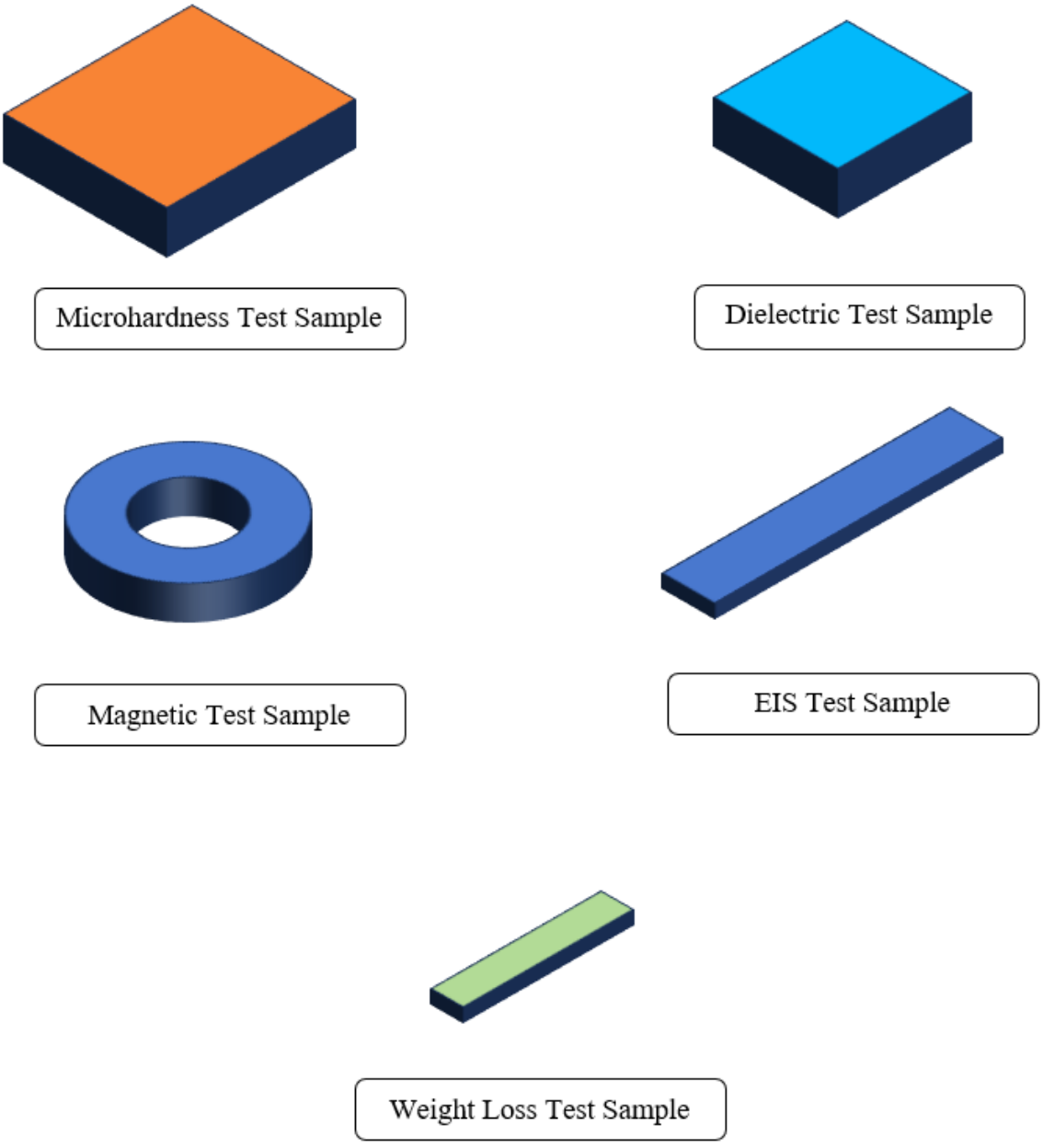

Figure 3.4: Schematic illustrations of samples used for mechanical, electrical and magnetic measurements

Table 3.2: Specimen size and Groups

Sample Groups	Size of the sample	Purpose	No of samples
Group-I	18 mm × 18 mm × 5 mm	Microhardness Test, FESEM test, DC Conductivity test	80
Group-II	15 mm × 15 mm × 5 mm	Relative permittivity test, AC impedance test	80
Group-III	D_i = 6 mm, D_o = 12 mm Thickness = 5 mm	AC magnetic test	80
Group-IV	5 mm × 5 mm × 12 cm	EIS and PDP test	30
Group-V	5 mm × 5 mm × 20 mm	Weight loss test	30

Figure 3.5: Prepared electro-magnetic test samples of the Cu-Al_2O_3 composite at a glance

The samples prepared for electromagnetic test shown in Figure 3.5 after machining the samples were subjected to heat treatment at temperatures ranging from 100° to 700° C. The designed composite was subjected to both isothermal and isochronal aging for examining the time and temperature dependency of the ceramic reinforced composite.

3.4 Characterization of prepared samples

The quantities measured for mechanical characterization was microhardness during both room temperature and thermal aging conditions in order to investigate the applicability of the specimens in the high temperature environment. The DC electrical conductivity was measured to examine the probable change in the value of conductivity with respect to changing environment. The dielectric constant and loss were plotted against a broad range of frequencies, from 100 Hz to 10^6 Hz, in order to investigate the ac and dc electric characteristics. The same range of frequencies was also used to examine the impedance characteristics. Using an impedance analyzer, the AC magnetization characteristics were once more examined in relation to the same frequency range. Finally, field emission scanning electron microscopic (FESEM) images were taken to check the surface morphology of the composite.

3.4.1 Micro-hardness

To investigate the microhardness of five study samples, square shaped specimens were used from five different combinations (both untreated and treated). 100, 300, 500, 600, 1200, 1500 and 1800 grits of SiC emery papers were used for smooth polishing of the surface. The microhardness test was carried out using a computer interfaced Micro Hardness Tester of model TM HV – 1000 DTE following ASTM E384-22 standard. According to the manual of the standard, the applied indenting load on the specimen was 1kgf for 10 seconds specified for metallic materials. The data was taken for 15 times for maintaining the reliability of the data on the both sides of the selected specimens. The 15 different values from 15 different locations are developing the data reliability here. The samples were divided into two groups both isochronal and isothermal investigation of microhardness.

3.4.2 Electrical Conductivity

The bulk conductivity of the material is perhaps the most prevalent and significant feature of electronic materials. Since the selected composition of materials have extremely high conductivities to begin with, measuring conductivity in conducting materials presents a unique problem. Therefore, careful selection of materials with porosity free surfaces were selected for the measurement of DC electrical conductivity took place.

The selected sample of each combination (Total-40) were subjected to test for up to 20 times for maintaining the data reliability of the sample. Before starting the measurement, the instrument was calibrated because of the sensitivity of the sensing probe. Two allotted samples were used between which one was pure silver and another one was pure copper. Technofour 979 digital conductivity meter set with an accuracy of ±0.1% IACS (International Annealed Copper Standard) was used for carrying out the investigation.

3.4.3 Complex Dielectric Constant and Loss Tangent

An impedance analyzer (Model: Wayne Kerr 6500B) was used to examine the materials' dielectric properties at different frequencies. For the dielectric research, the materials were modeled as parallel equivalent circuits with a purely resistive (R_P = 0.000539 Ω) element and a strictly capacitive (C_P = 16.258 μF) element in parallel as depicted in Figure 3.6. In contrast, the impedance characteristics are represented as a series equivalent circuit that consists of a series connection between a purely capacitive and a strictly resistive element.

Before starting the measurement, an automatic circuit was produced as mentioned in the Figure 3.6 for carrying out the measurement. The measured data included the capacitance of the material as well as complex permittivity and impedance characteristics of the sample. For the data extraction from capacitance, the area of the surface (A) and the thickness (d) of the sample was measured using a digital Slide-Calipers and then the value of A and d was given as input to the impedance analyzer. The data of loss tangent was directly measured from the imaginary part of the complex permittivity.

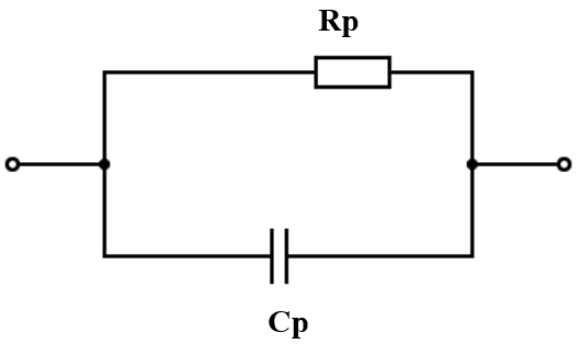

$R_P = 0.000539\ \Omega$

$C_P = 16.258\ \mu F$

Figure 3.6: Equivalent circuit used for dielectric measurement

3.4.4 AC Magnetic Permeability Test

The complex permeability, like the dielectric constant, shows how a material will behave in external magnetic fields. When a material has a complex permeability that has a low real part and a high imaginary part, it creates a strong magnetic field inside itself and stores energy without contribution to eddy current heating. On the other hand, a material that exhibits a low real part and a low imaginary part is said to have essentially little stored energy and without much lose any energy through eddy current heating. It also responds very weakly to an external magnetic field. Using the impedance analyzer, the samples' complex permeability was determined. To do this, insulated copper wire was first wounded around the toroid-shaped samples and then connected to the analyzer as shown in Figure 3.7. In this instance, every sample was modeled as an ideal resistor connected in series with an ideal inductor. From L_s/L_0 and $R_s/L_0\omega$, the real and imaginary components of permeability were determined. The average path length (l_e), cross section of the toroid (A) and number of turns (N) were entered for automatic extraction of complex permeability data from the analyzer.

(a)

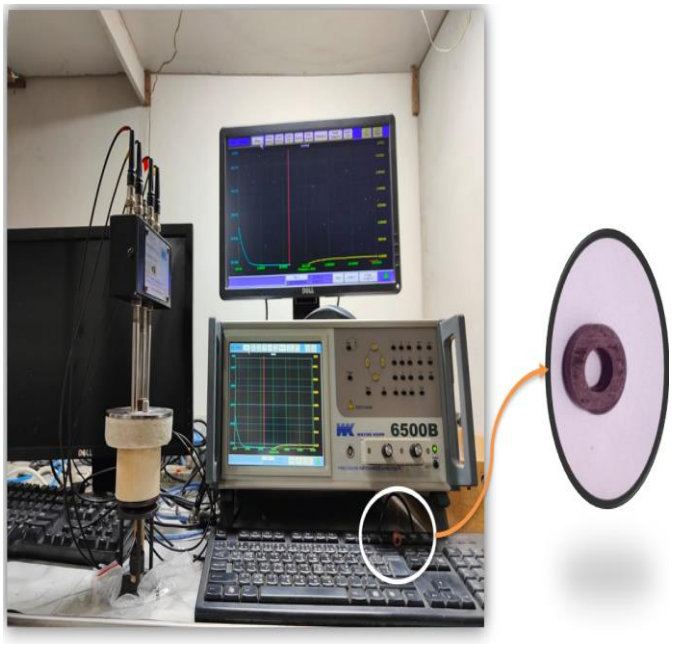

(b)

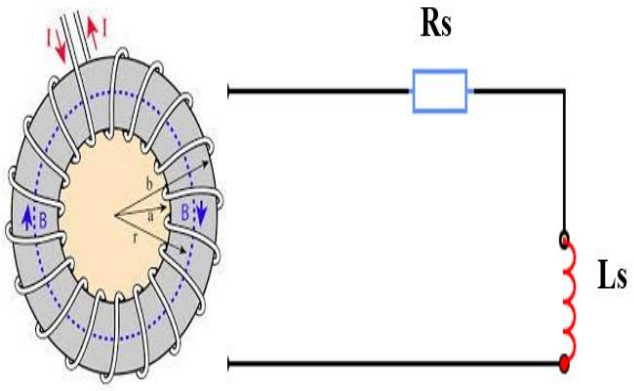

Figure 3.7: Impedance Analyzer (Wayne Kerr 6500B) used for magnetic permeability test (a) Test Set up (b) Equivalent circuit used for measurement

3.4.5 Gravimetric corrosion

The surface area of copper samples following exposure to a corrosive environment and the experimental determination of weight loss serve as the basis for the gravimetric technique used to determine the rate of corrosion.

Figure 3.8: Metal-matrix composite samples used for gravimetric corrosion test

In the present study, corrosion behavior of copper based five samples were investigated in salt water environment. The weight loss test was conducted to compare the performance between natural and forced corrosion in the same medium. The ideal sea water has a salinity percentage of 3.5% which was used as the medium for corrosion. The samples used for gravimetric corrosion is shown in Figure 3.8. The solution was prepared used 400 ml of distilled water with 3.5% NaCl mixture. Then the samples were placed separately in 5 different glass beakers at room temperature as portrayed in Figure 3.9.

Figure 3.9: Metal matrix composite samples immersed in the 3.5% NaCl salt water solution at room temperature

The composite samples were immersed up to 79 days for corrosion inhibition due to chemical reaction. Weight loss data was measured at specific interval. Weight of each specimen was measured using a high precision (0.00001 gm) digital weighing machine (model: ASB-60-220-C2) to get the initial weight before their immersion and thereafter for every specific period of immersion in the stagnant solution as applicable. Using the measured data, the weight loss of copper and Cu-Al_2O_3 was calculated as a function of time. Then the rate of corrosion was also calculated and represented in the result analysis section. SiC emery paper with 300, 600, 900, 1200 and 1500 grits were used for polishing the surface successively.

Weight loss of metal and corrosion rate were using the following equation 3.1 and 3.2.

Weight loss of metal: $$\Delta W = \frac{W_0 - W_f}{W_f} \quad (3.1)$$

Corrosion rate: $$R_{corr} = \frac{(K \times \Delta W)}{(\rho \times T)} \quad (3.2)$$

Where,

ΔW = weight loss per exposed surface area (gm/cm^2)

W_0 = Initial weight (gm)

W_f = Weight after designated period (gm)

R_{corr} = Corrosion rate

K = Unit conversion factor = 876 for corrosion rate in mm/y

ρ = Density of metal (gm/cm^2)

T = Exposed time (day)

3.4.6 Electro-Chemical Corrosion

The Cu-Al_20_3 composite containing different percentage of Al_20_3 content was prepared by conventional stir casting technique as mentioned before. The samples used for forced corrosion test is depicted in the Figure 3.10 The corrosion behavior of Cu-Al_20_3 composite was studied in 3.5 wt% NaCl solution using electrochemical impedance spectroscopy and potentiodynamic polarization technique. The Echem analyst software was used to interface with PC and all electrochemical data analysis as shown in Figure 3.11. The solution was prepared using distilled water. Analytical reagent grade NaCl was dissolved in deionized water to prepare the solutions. All experiment were carried out using computerized CH instruments – electrochemical workstation containing three electrode glass cells with 100 mL of NaCl solution. The OCP values of the sample were determined by measuring the voltage between working and reference electrode by electro-chemical workstation EIS analysis. Ag/AgCl-KCl was used as reference electrode and a platinum electrode was used as a counter electrode with the sample as the working electrode. Before EIS analysis, a sinusoidal voltage signal with ±10 mV was generated and frequency range from 100 KHz to 0.01Hz was explored. Only 5×5 mm^2 surface was exposed to the medium and the rest of the surface was coated with PVC heat shrinkable tube. The samples were immersed in the solution for 1 hour prior to allow OCP to calibrate. A thin wire used to connect the electrode and complete the circuit. The EIS experiment was performed at open circuit potential values and impedance data were collected for the above-mentioned frequency range.

Figure 3.10: Metal matrix composite samples used for electro-chemical corrosion test with the heat shrinkable tube attached with samples to avoid unwanted exposal of surfaces

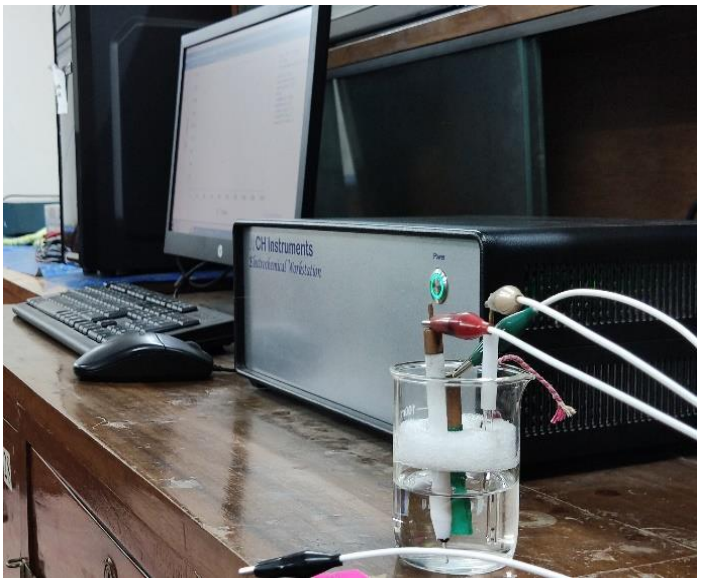

Figure 3.11: CIH workstation used for both potentiodynamic polarization and electro-chemical impedance spectroscopy test

The potentiodynamic polarization experiments were carried out using the same set-up of EIS identical to Figure 3.11. The potential range against the reference electrode was calibrated

within ±0.5V range and the scan rate of 0.01 Vs^{-1} was used for measuring the data. From the extracted data, the Tafel polarization curve was plotted and the corrosion potential (E_{corr}) and corrosion current (I_{corr}) and corrosion rate (mm/year) for each sample were calculated. After the experiment, the degradation of sample surfaces was examined through scanning electron microscope.

The corrosion rate was calculated using equation 3.4

$$Corrosion\ Rate = \frac{I_{corr}KEW}{\rho A} \text{ (ASTM standard G102)} \quad (3.3)$$

Where,

I_{corr} =Corrosion Current

K= Constant defining the unit rates of corrosion per year (here K=3272 mm (A cm year)$^{-1}$

EW= Equivalent weight in gram

ρ = Density of alloy in gm/cm^3

A = surface area in cm^2

CHAPTER 4
ELECTRO-MECHANICAL CHARACTERIZATION

4.1 Introduction

A comparative study was performed to investigate the electro-mechanical response of the designed composite in which basic micro-hardness and electrical conductivity characteristics were taken for consideration. Micro-hardness characteristics describe the localized deformation phenomena which is a primary indication of its structural resisting capability. It can synthetically display the elasticity, plasticity and strength of the designed material. The main parameter that limits the use copper in high temperature environment is its deterioration of microhardness. Besides the electrical conductivity of copper may also get changed with the changing temperature condition. This chapter portrays the behavioral change of copper primary due to addition of alumina particle and probable restoration of electrical conductivity of the specified sample with changing temperature condition. Detail description of the measuring procedure is already mentioned in section 3.4.1 and 3.4.2.

4.2 Effect of Ceramic Powder (Al_2O_3) Reinforcement on Micro-hardness

As observed from the Figure 4.1, with the addition of Al_2O_3 nanoparticle of small percentage, higher mechanical hardness is achieved. The drawback of pure copper of having low inner strength is overcome by adding a very low percentage of ceramic particle (Al_2O_3). The result shown in the graph is the average value of 15 times the value taken on different locations of both sides of the specimen. The 15 different values from 15 different locations are developing the data reliability here. Initially the value of microhardness of 99.99% pure copper was 57.3 HV which was enhanced by 8.67% due to addition of 0.5% Al_2O_3. Likewise, the micro-hardness of the other three composition also showed increased tendency of micro-hardness by 10.77%, 14.28%, 26.11% compared to pure copper because of addition of 1%, 2% and 5%

Al_2O_3 particle respectively. The Figure 4.1 shows the change of the microhardness initially slightly and in the last case rapidly due to addition of higher percentage (5%) of Al_2O_3 particle.

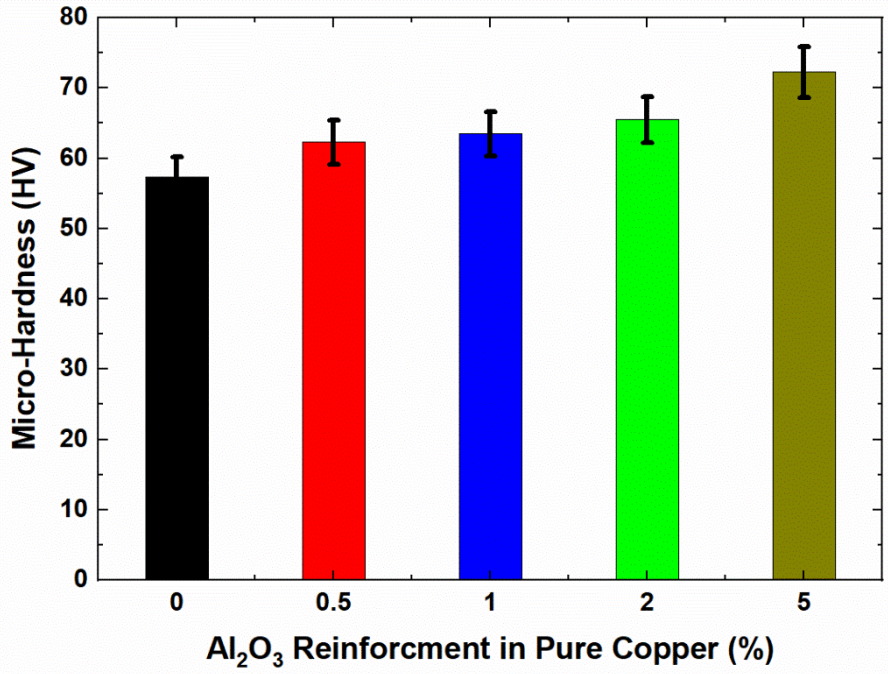

Figure 4.1: Effect of Al_2O_3 reinforcement on microhardness of copper matrix at room temperature

Jamaati and Toroghinejad (2010) also found a similar increasing trend with Alumina reinforcement but they used automatic roll bonding (ARB) process with higher percentage of Al_2O_3 particulate. From the result of microhardness test, we can say that the resultant composite shows characteristics identical to formation of non-eutectic alloy. This formation probably happened because of the higher difference (nearly 1000^0C) of the melting point between the two constituents. The Al_2O_3 particle present in MMC neither coarsen nor go into the solution rather it prevents the resultant material from softening under exposure to high temperature environment. This probable non-eutectic formation of Cu- Al_2O_3 helps to resist deformation of material under load condition. The micro-structural stability of the resultant formation helps to show the resisting tendency of the materials under point load condition. Several other researchers also found same micro-structural stability with reinforcement of Alumina (Gain et al., 2016;Simchi and Simchi, 2009).

4.3 Effect of Isochronal and Isothermal Ageing on Micro-hardness

Recent studies of the likely operational requirements of both future power-producing fusion reactors and near-term experimental systems have brought attention to the necessity of using copper and copper-base alloys. Wiffen and Reuther (1984) from the US department of energy reported the probability of using oxide dispersed copper base alloys for future fusion reactor technology but imposed a criterion of higher mechanical properties above 450^0C. As the primary goal of this research is to obtain microstructural stability in elevated temperature, thermal ageing process was adopted. The sample used were subjected to heating in hot chamber environment under temperature ranging from 25^0C to 700^0C maintaining the specific interval. The ageing process took place both isothermally and isochronally maintaining the temperature and time as variable in respective cases. Several researchers have attempted to justify the microstructural stability of the Cu- Al_2O_3 composite at elevated temperature. (Rahman et al., 2021) worked with pure copper to find reuse potential and showed the performance degradation of pure copper at elevated temperature. From the close observation of the Figure 4.2, it is found that with the increase of the temperature the same tendency of softening of pure copper is observed. The slope between points of the pure copper becomes negative with the temperature rise. The value of microhardness of pure copper drops down to 26.106 HV from the initial value of 57.3 HV. The slope between points (up-to 100^0C) was -0.0872 in case of pure copper which become positive (0.0411) due to 0.5% alumina particle addition. The other three materials exhibit the same positive slope tendency in holding the micro-hardness value. The change in hardness for the rest of the three compositions were 1.659 HV, 0.19727 HV, 0.06727 HV. The micro-hardness degradation of pure is continued with respect to temperature increase whereas the value of micro-hardness increases until 500^0C for the material-II (68.123 HV), material-III (68.533 HV), material-IV (73.84 HV) and material-V (75.56 HV). Between 500^0C and 600^0C, the micro-hardness characteristics of the material-II, material-III, material-IV, material-V show steady value. The aforementioned change in microhardness demonstrate the resisting capability with changing environment up-to 600^0C. The small percentage of alumina particles holds the material form intermetallic deformation up-to the temperature of 600^0C.

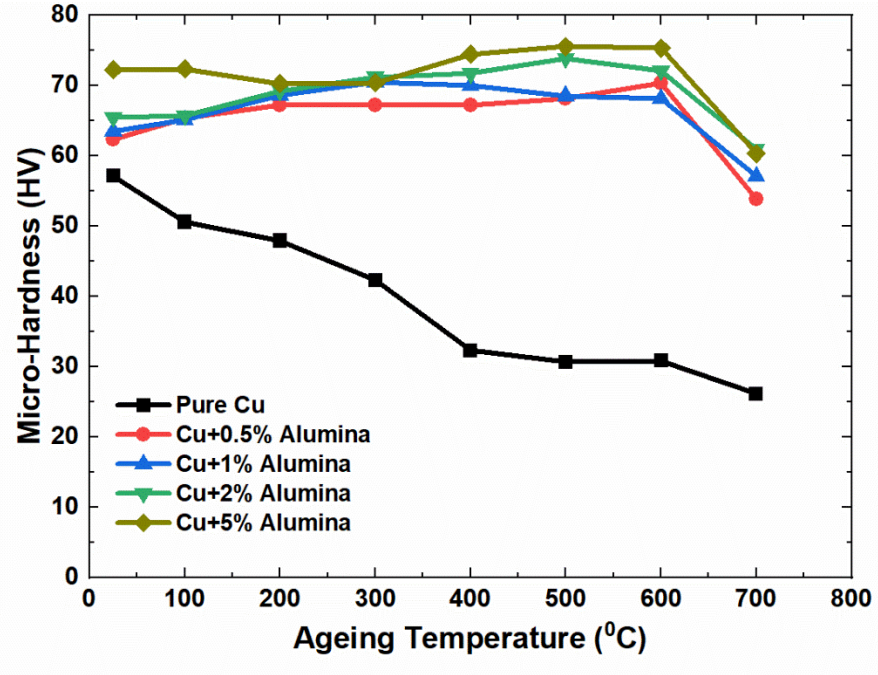

Figure 4.2: Variation of Micro-hardness of the MMC samples as a function of Isochronal ageing temperature

After close inspection, it is found that the value of micro-hardness becomes stable after 400^{0}C until 600^{0}C for material-II, material-III, material-IV and material-V compared with pure copper which has a value of 30.839 HV. The values observed from the experiment in case of 0.5%, 1%, 2%, 5% addition were 70.345 HV, 68.125 HV, 72.099 HV, 75.3145 HV respectively. After 600^{0}C temperature, the softening of material occurs in all of the five cases and higher localized deformation became evident from the value of micro-hardness. The change between 600^{0}C and 700^{0}C is in the negative direction for all of the five composites. In an attempt to justify the applicability of copper composite with low percentage (0.5 to 3.5%) of Al_2O_3 reinforcement for fusion reactor first wall construction, Harling Yu et al. (1981) got the same stabilized condition of oxide dispersed Copper up-to 650^{0}C but used stress for rupture vs temperature data for analyses. Though the change goes in the negative direction yet for 1%, 2% and 5% reinforcement with Al_2O_3 hold the value of micro-hardness (57.054 HV, 60.929 HV, 60.3246 HV respectively) higher than pure copper in room temperature condition. Saheb et al. (2012) investigated with the same constituents after manufacturing with spark plasma sintering but with higher percentage of Al_2O_3 and got the same trend.

The components made from oxide dispersed copper composite may be subjected to long term exposure to high temperature environment. Fusion reactor first wall and the welding electrode are excellent examples of such long-time exposure. For examining the compatibility of the designed composite, the samples were subjected to isothermal heat treatment at 500^0C, 600^0C and 700^0C successively. Each sample was kept in the respective temperature for 0.50, 1, 2, 4 and 8 hours cumulatively. From the isochronal ageing of samples, it is evident that the composite become structurally stabilized between 500^0C to 600^0C. After that sudden performance degradation occurred at 700^0C. This type of characteristic of increasing internal strength up-to certain temperature and then sudden reversing of strength can be easily described by Hall-Petch relationship. By reducing grain size through thermal aging, we might make materials stronger than their own theoretical strength. Based on Hall-Petch equation, the inner strength continued to rise up-to certain grain size and after attaining the peak strength due to thermal aging at 600^0C continues to decrease. This probable grain growth due to thermal ageing was also obtained by (Cho et al, 2006) which ultimately improved the strength of the material according the relationship.

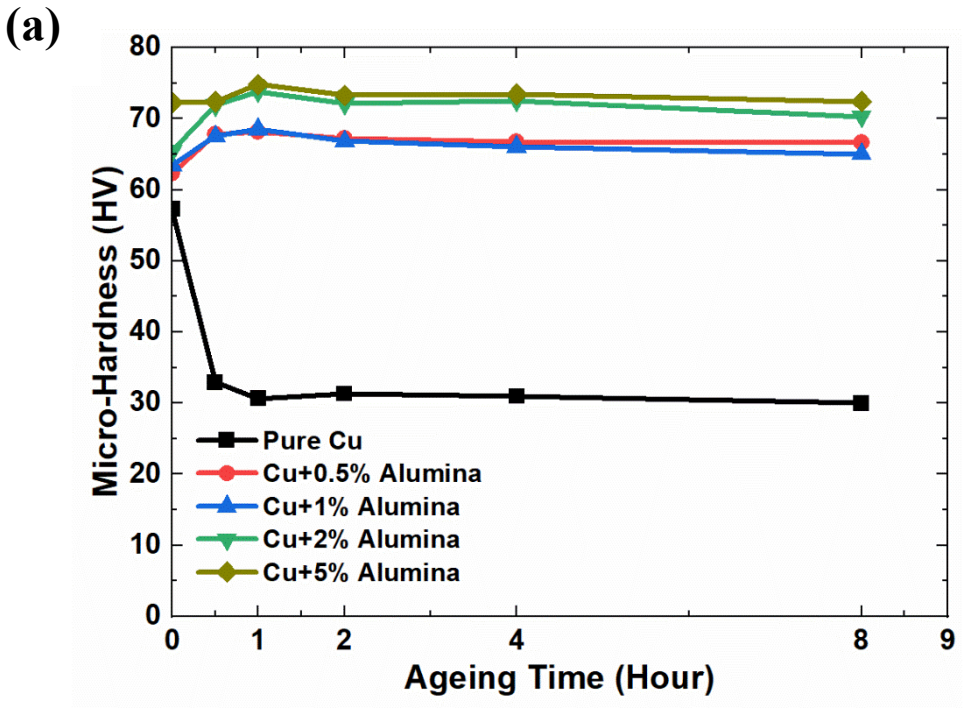

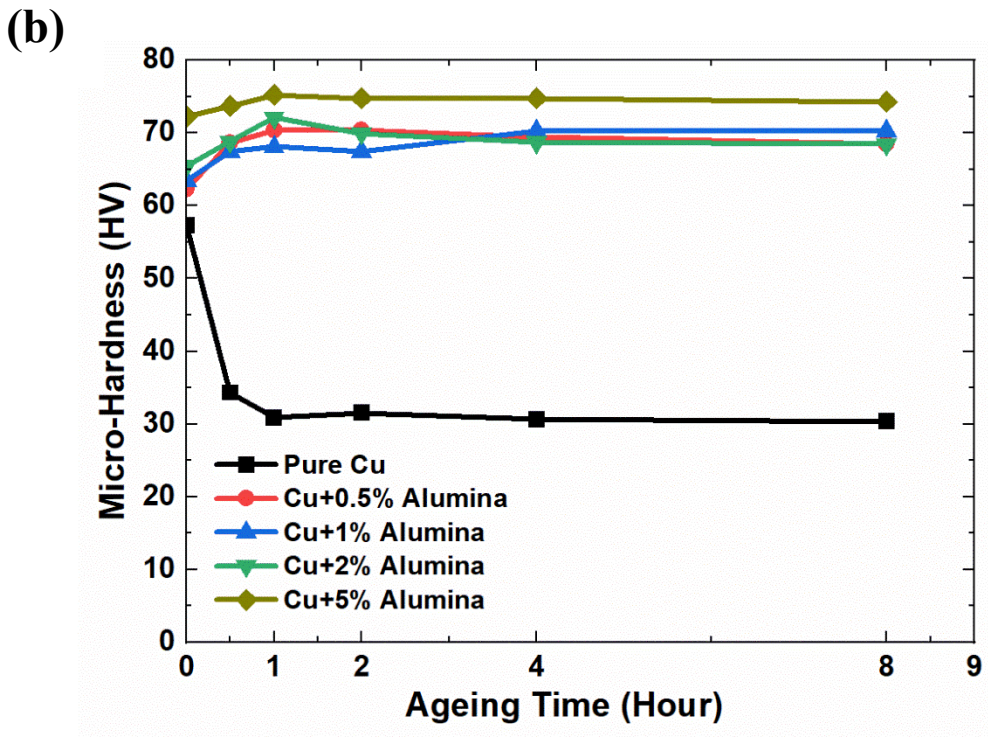

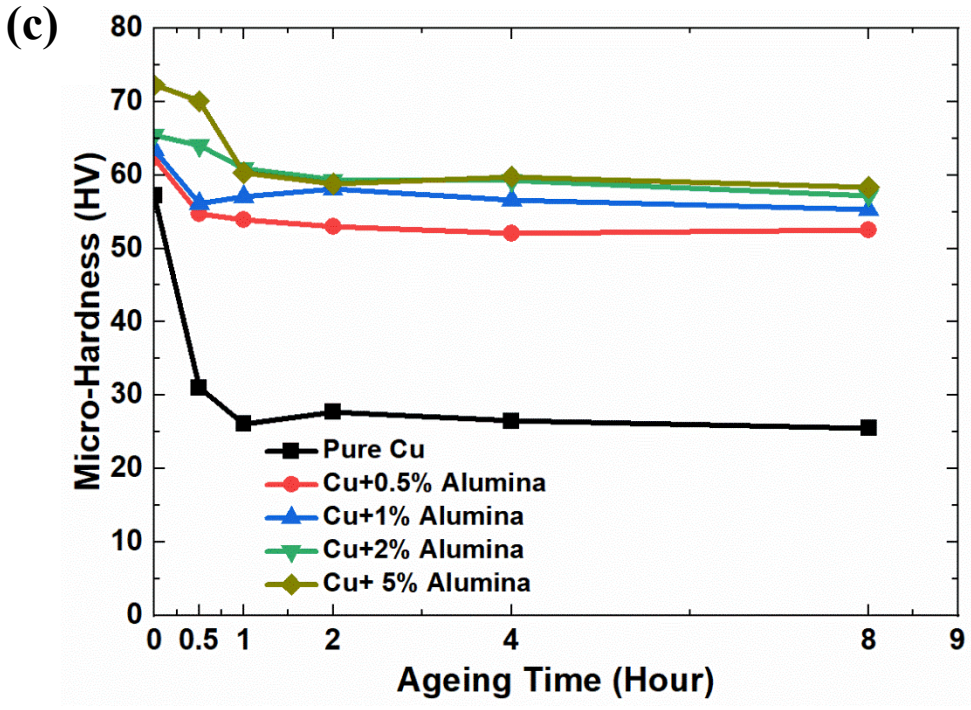

Figure 4.3: Variation of Micro-hardness of the MMC samples as a function of Isothermal ageing time at constant temperature of (a) 500^0C (b) 600^0C
(c) 700^0C

As observed from the Figure 4.3 the peak strength is observed at 1 hour of ageing time for material-II (68.121 HV), material-III (68.531 HV), material-IV (73.84 HV) and material-V (74.825 HV) in case of 500^0C temperature ageing. On the other hand, the micro-hardness of pure Copper tends to decrease up-to 1 hour and then stabilizes at a specific value of 30.645 HV. At 500^0C, after attaining the maximum microhardness the values show the tendency of softening but at a negligible range whereas for 600^0C the value of micro-hardness become almost perfectly stable after 1 hour of thermal ageing. The maximum capability of resistance (74.83 HV) against localized deformation is obtained by the composite with maximum percentage of Al_20_3 (5%). Metals and alloys' strength, hardness, and plastic deformation properties are greatly influenced by their micro- and nanoscale structural characteristics.

Because of the stable nanoscale grain size of Al_2O_3, the designed composite shows the stability in exerting resistance against local deformation at specific temperature. The value of microhardness is highest for highest amount (5%) of Al_2O_3 particle addition. As Al_2O_3 nanoparticle has got a melting point almost 1000^0C higher than the base metal, the main goal of holding the stable micro-structure is dependent on it and it is reflected from the Figure 4.3. The best performance with respect to time is obtained from 600^0C temperature isothermal ageing. In this temperature the alloy reaches at its peak performance. From a very close observation, with respect to increase in time, it observed that the all of four material-I (pure Copper), material-II (0.5% Al_2O_3), material-IV (2% Al_2O_3) & material-V (5% Al_2O_3) show the tendency to soften but at a negligible range but the micro-hardness of material-III (1% Al_2O_3) shows the opposite tendency. The value of micro-hardness of material-III reaches a value of 70.259 HV at 8 hours of ageing from the value of 68.11 HV at 1 hour of aging condition.

Due to addition of very low percentage of Al_2O_3 the prepared materials cannot hold the resisting capability at 700^0C. This recrystallization and hardness degradation is observed from all of the five cases. The micro-hardness of composites drops down to 25.521 HV, 52.48 HV, 55.265 HV, 57.1975 HV, 58.36 HV from their initial strength at room temperature. The material-III (1% Al_2O_3) shows exceptional tendency of sudden rise in micro-hardness after 1 hour of ageing and reaches 58.073 HV at 4 hours of cumulative ageing time. Even at 8 hours of ageing time, it holds the grip at a value of 55.265 HV which is close to the 5% Al_2O_3. As the isothermal ageing characteristics fulfill the purpose of portraying the performance

degradation due to long time exposure to harsh environment, the material-III (1% Al_2O_3) shows the optimum performance. The above depicted result agrees with the findings of (Madeni and Liu, 2011) on the context of intermetallic growth with effect of isothermal ageing.

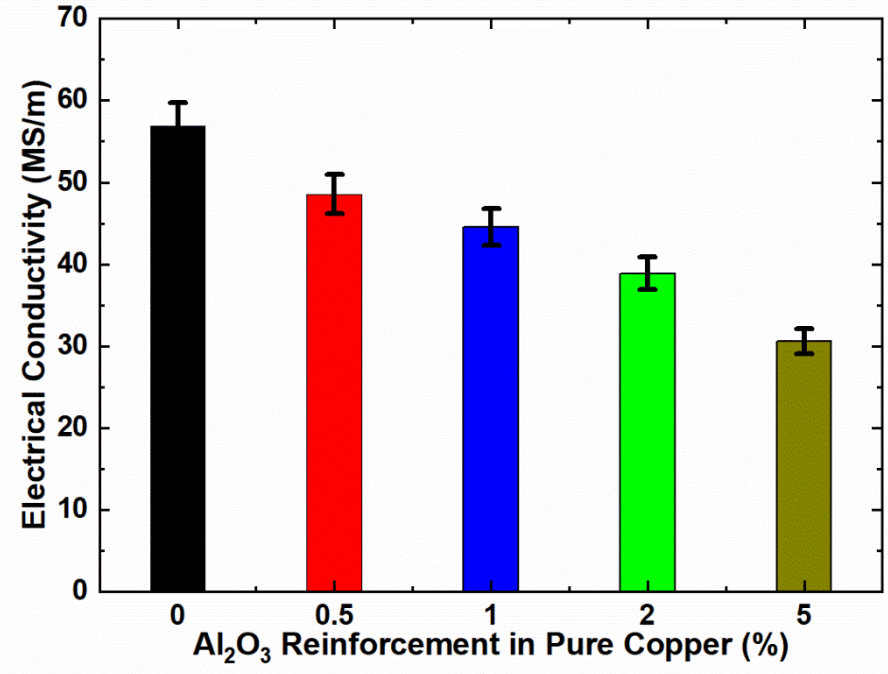

Figure 4.4: Effect of Al_2O_3 reinforcement on electrical conductivity of copper matrix at room temperature

4.4 Effect of Ceramic Powder (Al_2O_3) Reinforcement on Electrical Conductivity

The Figure 4.4 depicts the effect of Al_2O_3 reinforcement with pure copper having a purity percentage of 99.99%. The pure copper shows almost 100% IACS electrical conductivity which is equivalent to 56.91 MSm^{-1}. As the ceramic particle works as insulator mostly in the room temperature condition, the bulk conductivity shows the tendency of rapid reduction. The measured value of conductivity is 48.55 MSm^{-1}, 44.527 MSm^{-1}, 38.88 MSm^{-1}, 30.532 MSm^{-1} for material-II, III, IV, V respectively. Copper is utilized in a variety of applications because of its great electrical and thermal conductivity, including contact materials, integrated circuit connectors, lead frames, and conducting springs. Copper matrix composites are reinforced with ceramic particles and whiskers because of their outstanding thermal stability and strength. The majority of the available literature on whisker/fiber reinforced composites discusses about how

the mechanical characteristics and conductivity of the composites are affected by the types of whisker/fiber and interface optimization (Jiang et al, 2014 ;Zhang et al, 2018; Dong et al, 2015). The conventional McLachlan theoretical model developed for electrical conductivity uses filler concentration, particle size, filler conduction, interfacial region as the key factor that affects the conductivity of the composite (Zare and Rhee, 2019).

Conductivity decreases 14.67% for just 0.5% ceramic particle addition in comparison to pure copper. Likewise, 21.75%, 31.68% and 46.35% decrease is observed for 1%, 2% and 5% Al_2O_3 particle addition. The portrayed result agrees with the findings of (Fathy et al., 2012) but they worked with higher percentage of alumina ceramic particle. Several other researchers also worked in an attempt to investigate the effect of ceramic particle on electrical conductivity and found the same tendency. Several other researchers such as (Kargul et al., 2018; Cong et al., 2019; Feng et al., 2019) also worked in an attempt to investigate the effect of ceramic particle on electrical conductivity and found the same tendency.

4.5 Effect of Isochronal and Isothermal Ageing on Electrical Conductivity

As depicted in Figure 4.5, the stability of EC of pure Copper is observed though a slight deviation is still available. At a temperature of 100^0C, there is a significant drop in EC for material-II (Cu+0.5% Al_2O_3), material-III (Cu+1% Al_2O_3), material-IV (Cu+ 2% Al_2O_3) and material-V (Cu+ 5% Al_2O_3). But after that sudden reduction, the EC shows constant tendency of increasing for material-II, material-III and material-IV. Previous research work reveals that after 100^0C the electrical resistivity (ER) of Al_2O_3 shows decreasing behavior initially slowly and then in a steep slope. From the Figure 4.5, it is shown that the EC of the material-II, material-III and material-IV show values significantly higher than 100^0C and after that steep rise in EC is found with regular interval in temperature rise up to 700^0C. At the maximum temperature (700^0C) the material-II, material-III and material-IV show their respective highest level of EC (53.26 MSm^{-1}, 50.89 MSm^{-1}, 46.35 MSm^{-1}) where material-II and III almost reaches the conductivity of pure copper (55.325 MSm^{-1}). But higher percentage (5%) of Al_2O_3 creates fluctuation of electrical conductivity close to the value of room temperature which is observed from the characteristics of material-V. At the maximum ageing temperature, the EC

decreases 6.067 MSm^{-1} from the initial value of 30.532 MSm^{-1} at room temperature. It is interesting to note that higher percentage of addition of Al_2O_3 holds the EC value at a certain level but trace addition with thermal ageing creates significant improvement in the value of EC. Due to the excellent EC, Copper is used for a wide range of electrical and electronic applications. As observed from the graphical interpretation portrayed on the effect of isochronal aging, due to reinforcement with Alumina particle it was already found that the strength was significantly improved which is even better than its theoretical strength at room temperature. On the contrary, Al_2O_3 nanoparticle is almost an insulating material which in effect is the main reason for rapid decrease in EC at normal environment. Efforts have been made to overcome the limitation of lower EC for the high temperature environment. (Matsumura, 1966) made an effort to improve the electrical properties of Al_2O_3 particle for high temperature environment. His effort was extremely successful. After reviewing the research work, Cohen even classified Al_2O_3 particle as semiconductor material in high temperature environment. Cohen (1960) found significant spread in EC and activation energy for some of the ceramics including Al_2O_3.

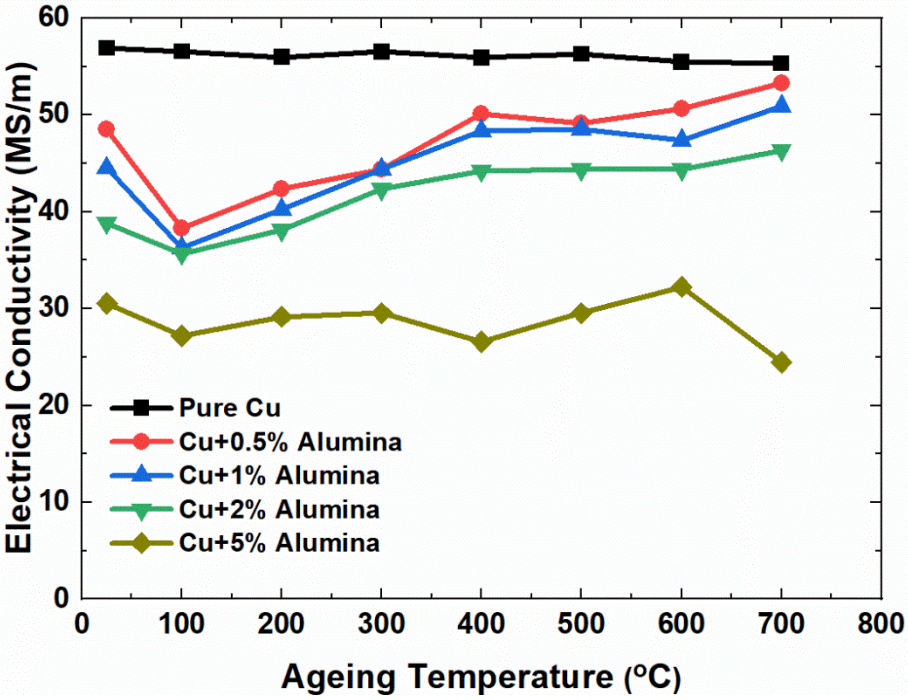

Figure 4.5: Variation of electrical conductivity of the MMC samples as a function of Isochronal ageing temperature

With the increase of temperature, electrons are able to jump from valence band to conduction band thereby increasing the overall electrical conductivity with decrease in ER. The electrical resistivity of copper matrix can be expressed as follows;

$$\rho_{Total} = \rho_{Defect} + \rho_{Impurities} + \rho_{Phonons} + \rho_{interface} \quad (4.1)$$

Here, $\rho_{Phonons}$ is the contribution of phonon scattering to resistivity, which is closely related to temperature, ρ_{Defect} is the resistivity caused by defects, dislocations and vacancies, $\rho_{Impurities}$ is the effect of impurity, $\rho_{interface}$ is the interface of scattering to resistivity. $\rho_{Impurities}$ has more obvious effect on electrical conductivity. As per the Cohen's law, Al_2O_3 nanoparticle shows semiconducting behavior which means that the electrons from valence band obtains the ability to jump to conduction band and so $\rho_{Impurities}$ decreases significantly with negligible effect on ρ_{Defect}, $\rho_{Phonons}$, $\rho_{interface}$. One important point is that, the non-conductive reinforcing element becomes conductive itself which in turn decrease the attenuation on electron flow within copper atom. So due to double effects, significant change in conductivity is observed for low percentage of reinforcement. For low temperature like 100^0C, the $\rho_{Impurities}$ becomes negligible while $\rho_{interface}$ becomes significant due to sudden scattering of atoms. The above effect is probably responsible for sudden decrease in electrical conductivity of composite (Cao et al, 2022).

The behavior of Copper matrix reinforced with 5% Al_2O_3 is also supported by the findings of (Jogi, 2014) who measured the resistivity of Copper composite with exactly 5% Al_2O_3 and got a slight increment in electrical resistivity with temperature increase up to 500^0C which in turn decreased the EC for this particular combination. It is already proved that EC of a material is significantly affected with respect to change in temperature. But if we consider a certain temperature maintained for a particular sample and the aging duration is varied then the effect of isothermal aging may have significant impact on EC. The EC was measured for samples after maintaining the temperature of 500^0C, 600^0C and 700^0C and the data was taken for 0.50, 1, 2, 4, 8 hours as shown in Figure 4.6. The EC of pure copper shows fluctuation around the EC at room temperature for all the concerned temperatures (500^0C, 600^0C & 700^0C). Samples (material-II, material-III and material-IV) thermally aged at a temperature of 500^0C achieve their respective highest value of electrical conductivity after 1 hour of aging time and after that

there is a tendency of slow reduction up-to 4 hours of aging time. After 4 hours of aging time, the EC values becomes stable for all of the composites. The EC of material-V shows unusual deflections which is sometimes opposite to the behavior of material-II, III, IV and V.

For the aging temperature of 600^0C, the value of EC rises initially at a positive slope and then gradually becomes stable after 4 hours of aging. The material-II, III IV and V attains their highest value of EC (51.39 MSm^{-1}, 47.838 MSm^{-1}, 45.098 MSm^{-1}, 32.73 MSm^{-1}) after 4 hours of aging. For temperature 600^0C, the EC values doesn't fluctuate like the cases of 500^0C and 700^0C. For 700^0C, material-II and material-III attain their highest value at 8 hours of aging which is close to the EC of pure copper at 700^0C. Material-V shows deflections around its respective EC at room temperature.

(a)

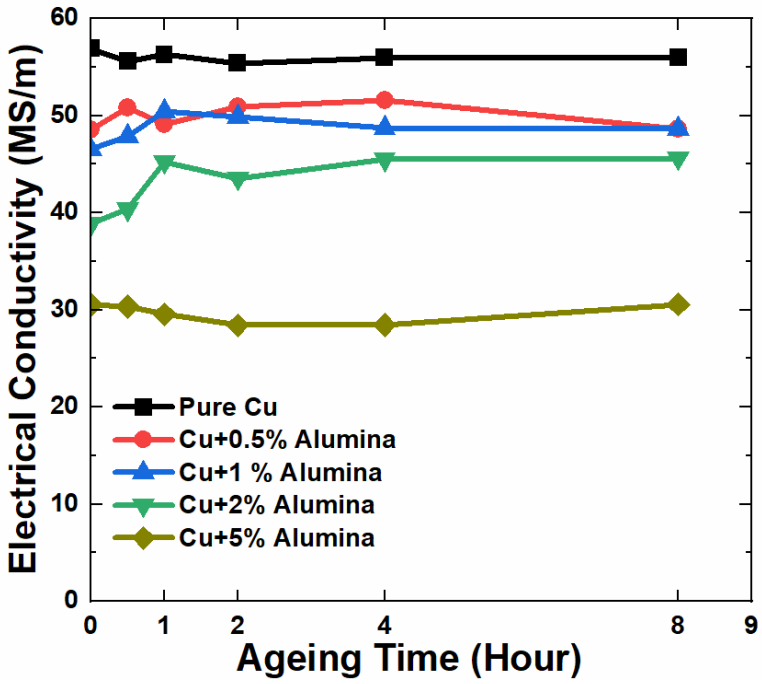

(b)

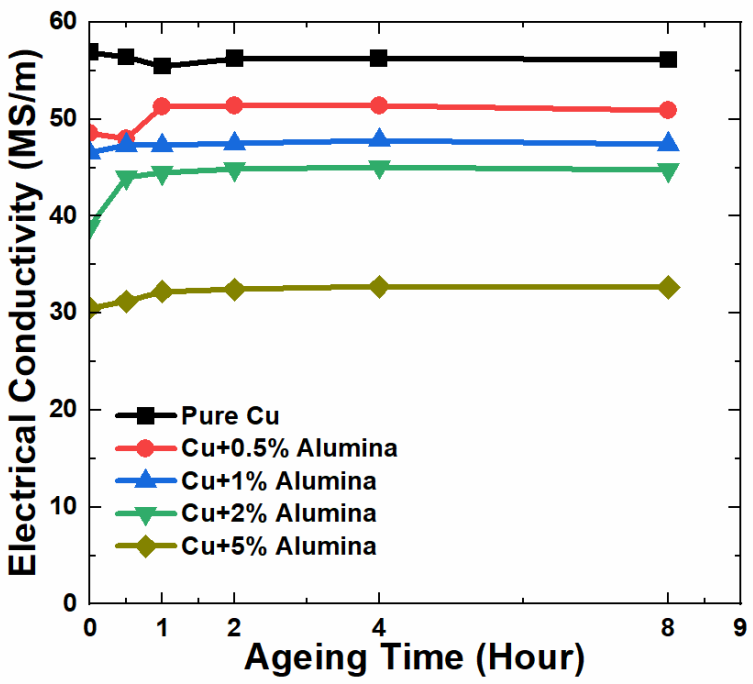

(c)

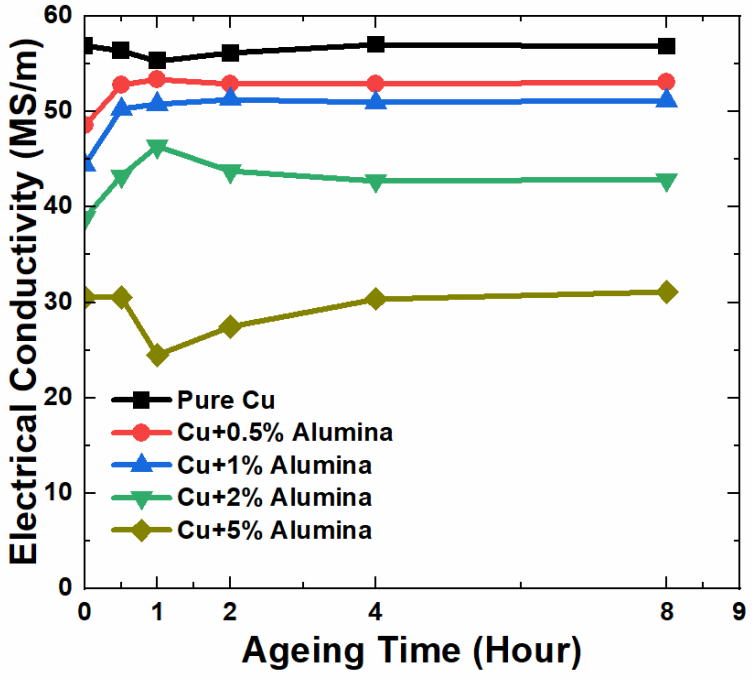

Figure 4.6: Variation of electrical conductivity of the MMC samples as a function of Isothermal ageing time at constant temperature of (a) 500^0C (b) 600^0C (c) 700^0

4.6 Microscopic observation

FESEM analysis was performed for better understanding of the surface morphology of the prepared square shaped samples. Scanning Electron Microscope (Zeiss Sigma 300 VP manufactured in Germany) was used for the image extraction. The FESEM image of material-I (Pure Cu), material-II (Cu+0.5% Al_2O_3), material-III (Cu+1% Al_2O_3), material-IV (Cu+2% Al_2O_3), material-V (Cu+5% Al_2O_3) were observed and presented in the Figure 4.7. Figure 4.7(a) depicts fine granular structure with relatively straight boundaries. Al_2O_3 reinforcement has created bright spots on the SEM images. As samples were not subjected to homogenization heat treatment, observed surfaces portrayed non-uniform distribution of reinforcement particle. The size of the Al_2O_3 particles did not vary significantly with composition, although a few agglomerated regions were observed for higher density of Al_2O_3 particles.

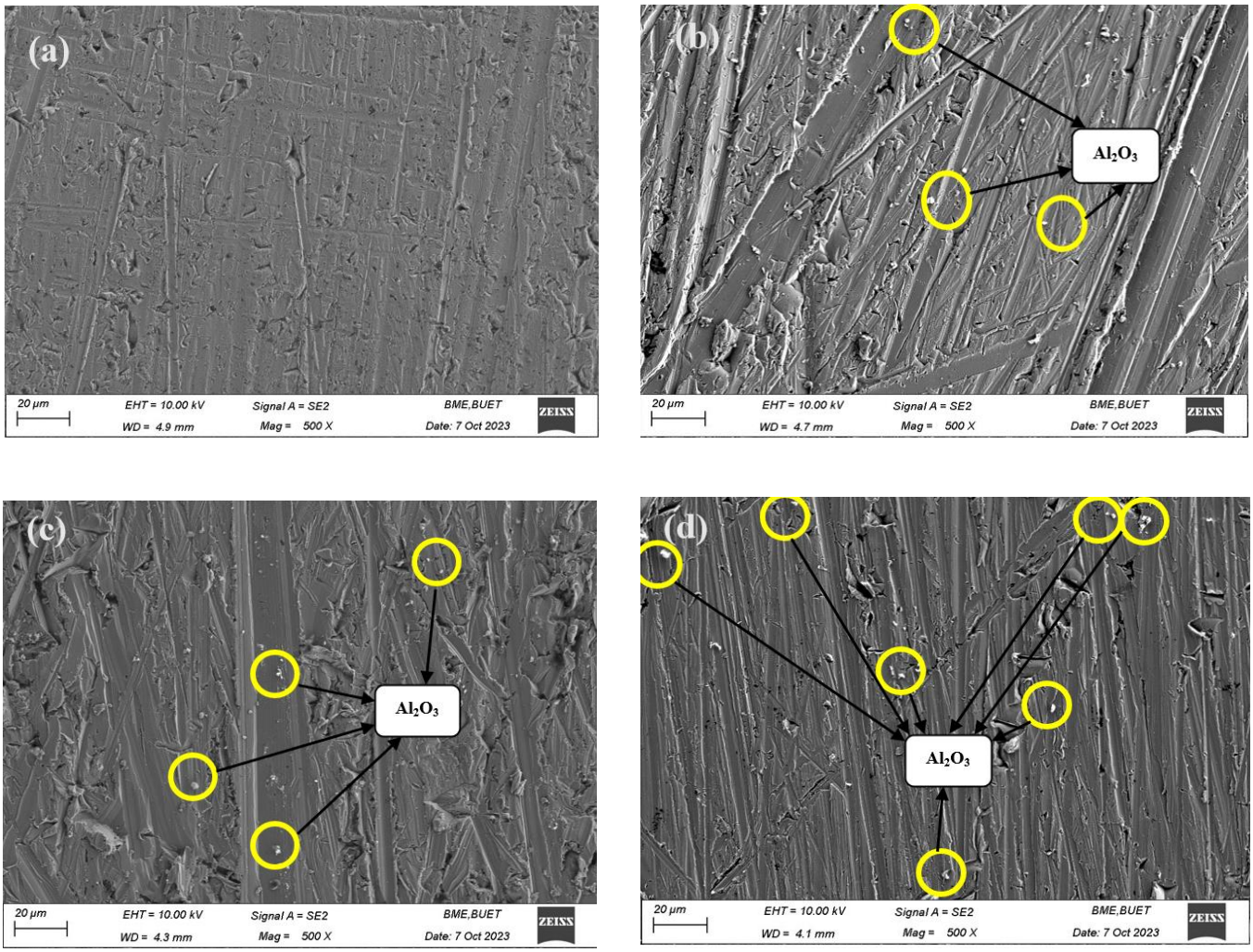

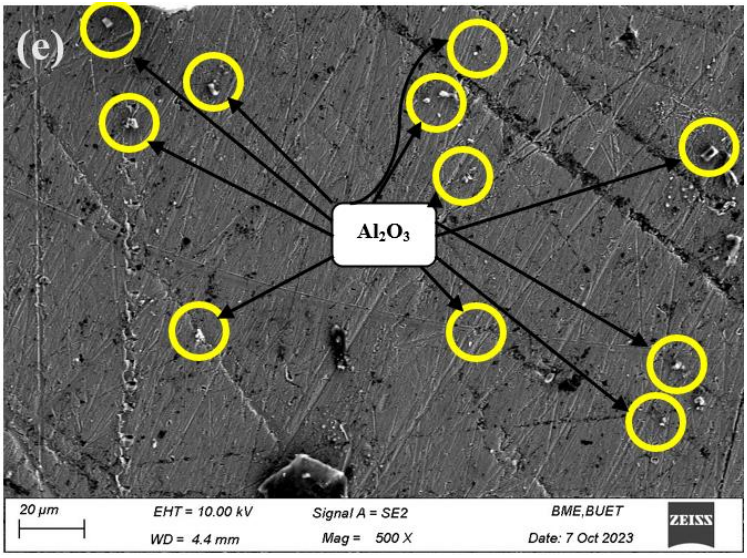

Figure 4.7: FESEM images of copper matrix with and without Al_2O_3 reinforcement at room temperature (a) pure Copper (b) 0.5% Al_2O_3 Reinforcement (c) 1% Al_2O_3 Reinforcement (d) 2% Al_2O_3 Reinforcement (e) 5% Al_2O_3 Reinforcement

Figure 4.8 shows the interface between pure copper and reinforcement Al_2O_3 particle. The reinforcement particle didn't get coarsen rather created a phase which increased the strength of the composition in comparison to pure Copper. Some empty space was observed in the interfacing region as well as porosity. Porosity was higher near the reinforcement area

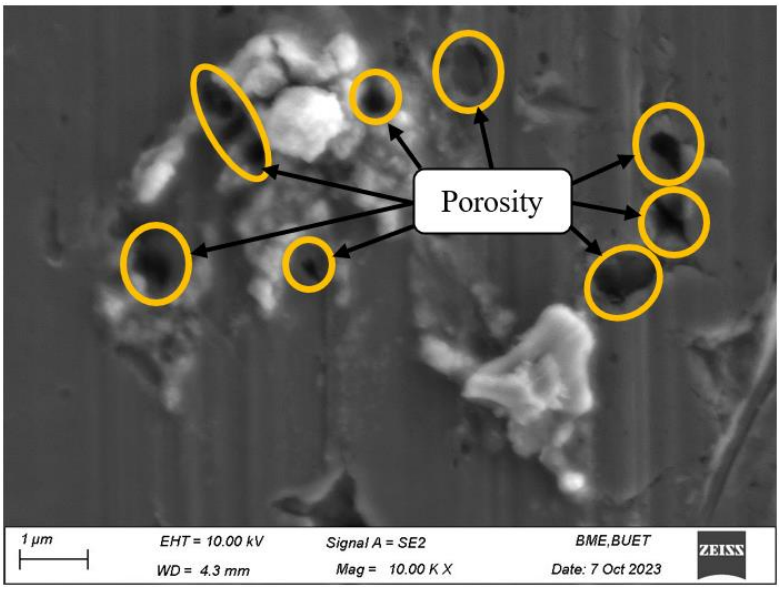

Figure 4.8: Interface between Al_2O_3 particle and bulk Copper surface

probably due to higher difference of the melting temperature between copper matrix and reinforcement particle. This apparently came from higher contraction of solidifying Copper (melting point 1085^0C) during cooling from casting temperature of 1500^0C. For low volume fraction of Al_2O_3 particle, the open porosity was low but it increased significantly with higher percentage of Al_2O_3 addition.

4.7 Summary

If the concept of parameter optimization is adopted for decision making considering the aforementioned findings, material composition-II and III shows excellent EC at high temperature thermal aging condition. The Hell-Patch theory supports the findings of micro-hardness of the designed composite which is even higher than the predicted value. The material gains strength in proportion with the percentage of Al_2O_3 reinforcement. The material-II, III, IV, V shows highest level of resistivity against localized deformation at a temperature of 600^0C. At 700^0C, all of the prepared composites show steep negative slope in incase of micro-hardness. But if EC is considered, there is no significant deviation with change in temperature in case of material-V. On the other hand, the material-II shows higher EC with temperature but its micro-hardness property is considerably low for the application. All of the considerations are fulfilled for material-III with 1% Al_2O_3 reinforcement. The micro-hardness level is considerably good for 500^0C and 600^0C. Again, for 500^0C the EC shows deflections for material-III though within a negligible range. But for 600^0C, the EC of material-III is finely stable which is the fundamental requirement for the application of welding condition. So, ultimately, Copper with 1% Al_2O_3 nanoparticle reinforcement shows the optimized performance at 600^0C with isothermal aging condition.

CHAPTER 5
ELECTRO-MAGNETIC CHARACTERIZATION

5.1 Introduction

To analyze the AC magnetic properties, the Waynekerr Impedance Analyzer was used. Toroid shaped samples with various concentration of Al_2O_3 were used. Details of experimental procedure is described in section 3.4.4. As the magnetic properties of any material is highly dependent on temperature and frequency, measurement was conducted considering variation of frequency and temperature.

The ability of a material to create a magnetic within itself is known as permeability. The dynamic response of permeability by alternating the magnetic field gives rise to the complex permeability. The complex permeability μ and the magnetic loss tangent ($tan\delta_M$) is defined by the following relationship:

$$\mu = \mu' - j\mu'' \quad \text{and} \quad tan\delta_M = \frac{\mu''}{\mu'} \tag{5.1}$$

Where, μ' is the real part of AC permeability and μ'' is the imaginary part of AC permeability

5.1.1 AC permeability of Cu-Al_2O_3 MMC

Copper is a d-block element. The magnetic behavior of d-block element depends on number of unpaired electrons in d-orbital. Copper has no unpaired electron in its outermost shell (d-orbital) and so it shows diamagnetic behavior. Because of its diamagnetic behavior, it is weakly repelled by the external magnetic field. Though there is an unpaired electron in the 4s orbital yet it doesn't contribute to the spin. From the Figure 5.1, it is depicted that the pure copper is showing the value of relative permeability approximately less than 1 (0.970821), close to that of air. With the increase in frequency, the AC relative permeability decreases rapidly and it approaches zero at higher frequencies. At 102068 MHz frequency, the relative permeability

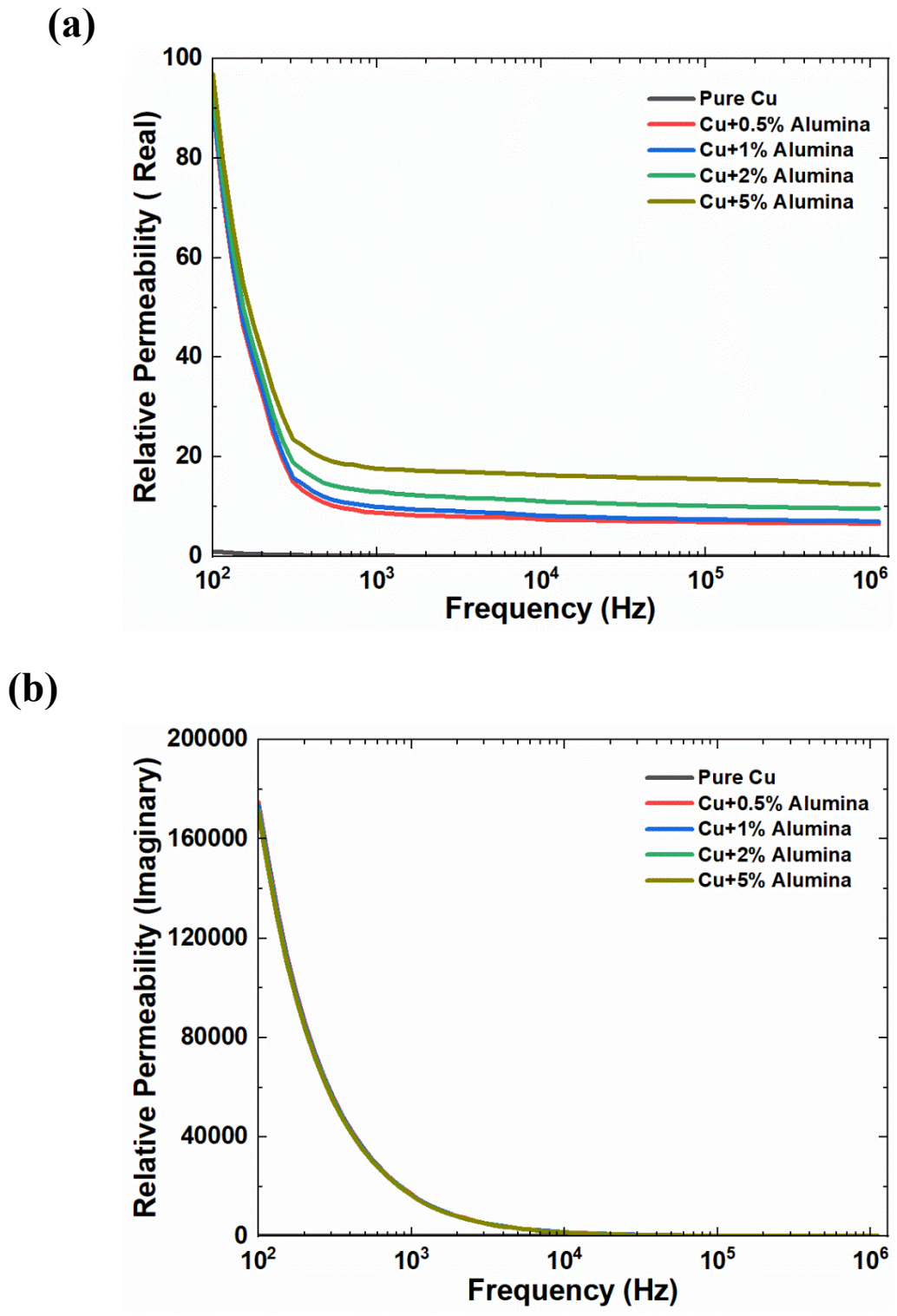

Figure 5.1: Effect of Al_2O_3 reinforcement on permeability of copper matrix as a function of operating frequency (a) real part (b) imaginary part

value reaches to 0.000273 which is essentially zero that means the pure copper loses its magnetic behavior at higher frequencies, it gets neither attracted nor repelled at higher frequencies. On the other hand, trace addition of Al_2O_3 creates significant impact on the magnetic character of pure copper. With just 0.5% Al_2O_3 nanoparticle addition, the diamagnetic behavior of base metal becomes paramagnetic in nature. The value of permeability (μ_r) becomes 90.79, 91.0572, 92.96, 96.9775 for 0.5%, 1%, 2% and 5% reinforcement with Al_2O_3 respectively. This significant change can be described as disordering magnetic character. Alumina is paramagnetic in nature and its relative permeability ranges below 10.

As the production procedure was conventional sand casting and casting creates random distribution of atomic particles, therefore the sudden change in behavior might be because of the creation of disordered magnetic system. The random distribution of Al_2O_3 has created strong deviation from the regular pattern of magnetic behavior of pure copper which has produced higher relative permeability than both of the constituents. The rise in magnetism will create dipolar orientation and wall motion. This effect is supported by Hamiltonian (Nordblad, 2016) spin effect for disordered magnetic systems. Several other researchers like (Lutsev, 2016) also agreed about the same probable findings based on the Heisenberg's model for magnetic dipole exchange. Lutsev (2016) found higher magnetic density for long wavelength (low frequency) and then initial magnetic density decreased with increase in frequency (short wavelength). The above finding using conventional casting procedure also agrees with the investigation of (Liu et al., 2014) who used strip casting for production and got higher magnetic properties for Sm-Co material because of dendritic crystal grains in micro scale range. The Figure 5.1 portrayed behavior almost identical to the findings of Lutsev. The relative permeability of material-II, III, IV and V decreased with a higher negative slope from the initial value up to 1 KHz frequency. After 1 KHz frequency, the magnetization tendency decreased with negligible negative slope and reaches to 6.54827, 6.98823, 9.48984, 14.3837 for material-II, III, IV and V respectively for Megahertz range. Higher permeability at low frequency region is already a proven factor because of Snoke's law (Acher and Dubourg, 2008). The formula is presented by the following equation:

$$f_R(\mu_0 - 1) = \frac{4}{3\gamma M_s} \tag{5.2}$$

Here, f_R is the resonance frequency, μ_0 is the initial permeability, γ is the gyromagnetic ratio and M_s is the saturation magnetization. The values also define that for higher percentage of Al_2O_3 addition, higher capability of holding the tendency of magnetization is achieved which ultimately is the resultant effect of higher domain wall motion and spin rotation.

5.1.2 Magnetic Loss Tangent (MLT) of Cu with Al_2O_3 reinforcement

The term magnetic loss tangent (unitless) refers to various forms of energy dissipation mechanism which take place when the material is subjected to frequency varying electric field. Because of the inherent irreversible nature of the magnetization process, part of the energy injected is irrecoverably transformed into heat energy.

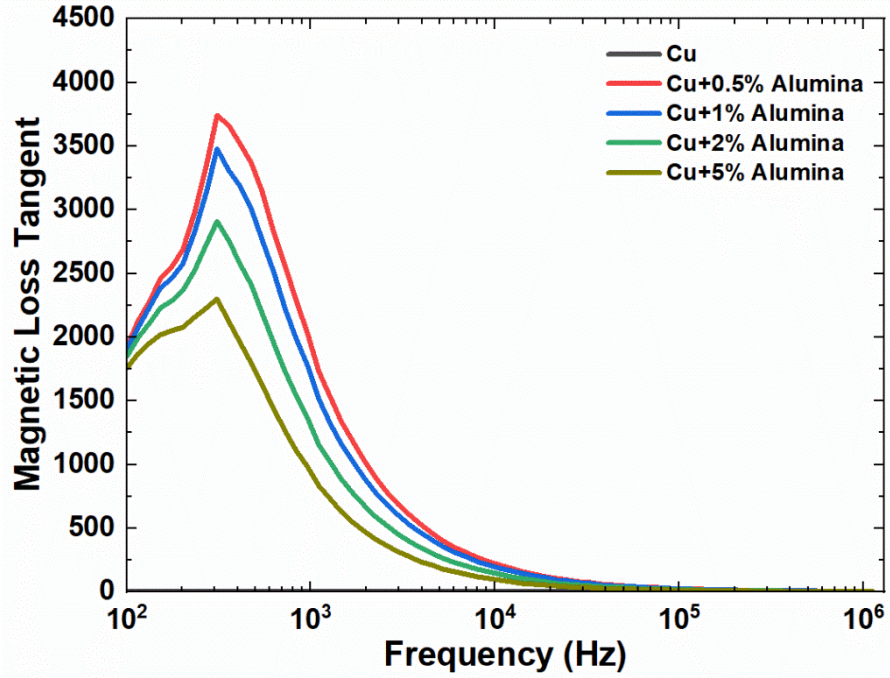

Figure 5.2: Effect of Al_2O_3 reinforcement on magnetic loss tangent of copper matrix as a function of operating frequency

The Figure 5.2 shows the dependency of magnetic loss tangent (Dissipation factor) on frequency. The pure Copper shows negligible diamagnetic behavior and hence the magnetic loss is also negligible. The MLT starts with 2.25 for low frequency and reaches 2.40 for 309 Hz and then decreases to a minimum value of 0.1419 for MHz range signal penetration. As the MLT is naturally complexly related to creation of magnetization, a rapid rise in MLT is observed for other four composites because of disordered magnetic system. Composition-II, III, IV and V show values 1928, 1906, 1848 and 1756 respectively for penetration of signal with 100 Hz frequency. The magnetic loss increased linearly up-to 309 Hz and then it decreased forming an inverse exponential curve. The magnetic loss become minimum at MHz range frequency. At a frequency of 309 Hz, the loss reaches its maximum value of 3738, 3481, 2908 and 2302 for 0.5%, 1%, 2% and 5% of Al_20_3 reinforcement respectively. This loss at that particular frequency is probably due to the heat induction associated with Joule's effect within atoms because of eddy current generation due to domain wall motion. This mechanism was probably activated by large scale instabilities accompanying the nucleation and annihilation of magnetic domains(Tsoi et al., 2003).

Though the figure displays higher level of MLT at initial point yet the decrease of loss tangent with the increase of Al_2O_3 content could easily be distinguished. Low magnetic loss is beneficial for the construction of magneto-electric devices. The increasing tendency tends to diminish itself with increase of Al_2O_3 content. For the composition-V, the MLT shows the minimum value in comparison to composition-II, III IV for 309 Hz signal penetration. The low loss suggests good magnetic insulation because of the Al_2O_3 nanoparticle. The combined effect of increasing the real permeability with low magnetic loss indicates the probability of resemblance of magnetic domain. This resemblance probably overcame the randomizing effect of atoms which in turn decreased the spin and domain wall relaxation.

5.1.3 M-H Loop Formation of Cu with Al_2O_3 Reinforcement

Hysteresis loops describe the magnetic response of a sample exposed to a magnetic field. The curves exhibited by the material clearly indicates their type of magnetic characteristics (eg. Diamagnetic, Paramagnetic ad Ferromagnetic) as well as coercive force, saturation

magnetization points and residual magnetism. The magnetic hysteresis loops were recorded at room temperature for the samples with variation (0 to 5%) of Al_2O_3 content and presented in the following Figure 5.3. The Figure 5.3(a) shows that pure copper didn't create hysteresis loop at all because of its diamagnetic behavior. The result of PPMS test is also supported by the abovementioned characteristics of pure copper in case of relative permeability and dissipation factor. The magnetization was induced directly in the opposite direction of applied field and was a linear line hysteresis. The experimental results regarding the hysteresis behavior of pure copper is supported by (Tufaile and Tufaile, 2021). They showed the same linear line behavior in case of diamagnetic substance like pure copper in this case.

The paramagnetic behavior found in the impedance analyzer investigation through complex permeability test also get supported here. Because of just 0.5% Al_2O_3 doping, the material started producing hysteresis loops and after that there was a consistency of increment of magnetic behavior mentioned in the Figure 5.3.

The saturation magnetization point was 0.01048 emu/gm which attained a value of 0.02985 emu/gm because of 5% Al_2O_3 reinforcement. The value of M_S increased by 1.5 and 2 times the saturation points of composition-II for the case of 2% and 5% reinforcement respectively. The saturation magnetization point of composition-II was almost in coincidence with composition-III. The Figure 5.3 also points that the area of the hysteresis loop becomes narrow with the increase of Alumina content. The higher the area of the hysteresis loop, the higher the magnetic loos. That means higher amount of energy will be dissipated in the form of heat if the area of the loop gets increased. The hysteresis loop become almost line hysteresis for composite-V.

Table-5.1: Magnetic hysteresis parameters of the sample in room temperature regime

Material	Saturation Magnetization, M_S (emu/gm)	Coercive Force, H_C (oe)	Residual Magnetization, M_R (emu/gm)	M_R/M_S
Copper+0.5% Al_20_3	0.01048	-112.056	1.3E-4	0.01241
Copper+1% Al_20_3	0.01054	-131.463	1.58314E-4	0.01502
Copper+2% Al_20_3	0.02664	-306.849	1.01E-05	0.00037
Copper+5% Al_20_3	0.02985	-324.087	9.68E-04	0.03243

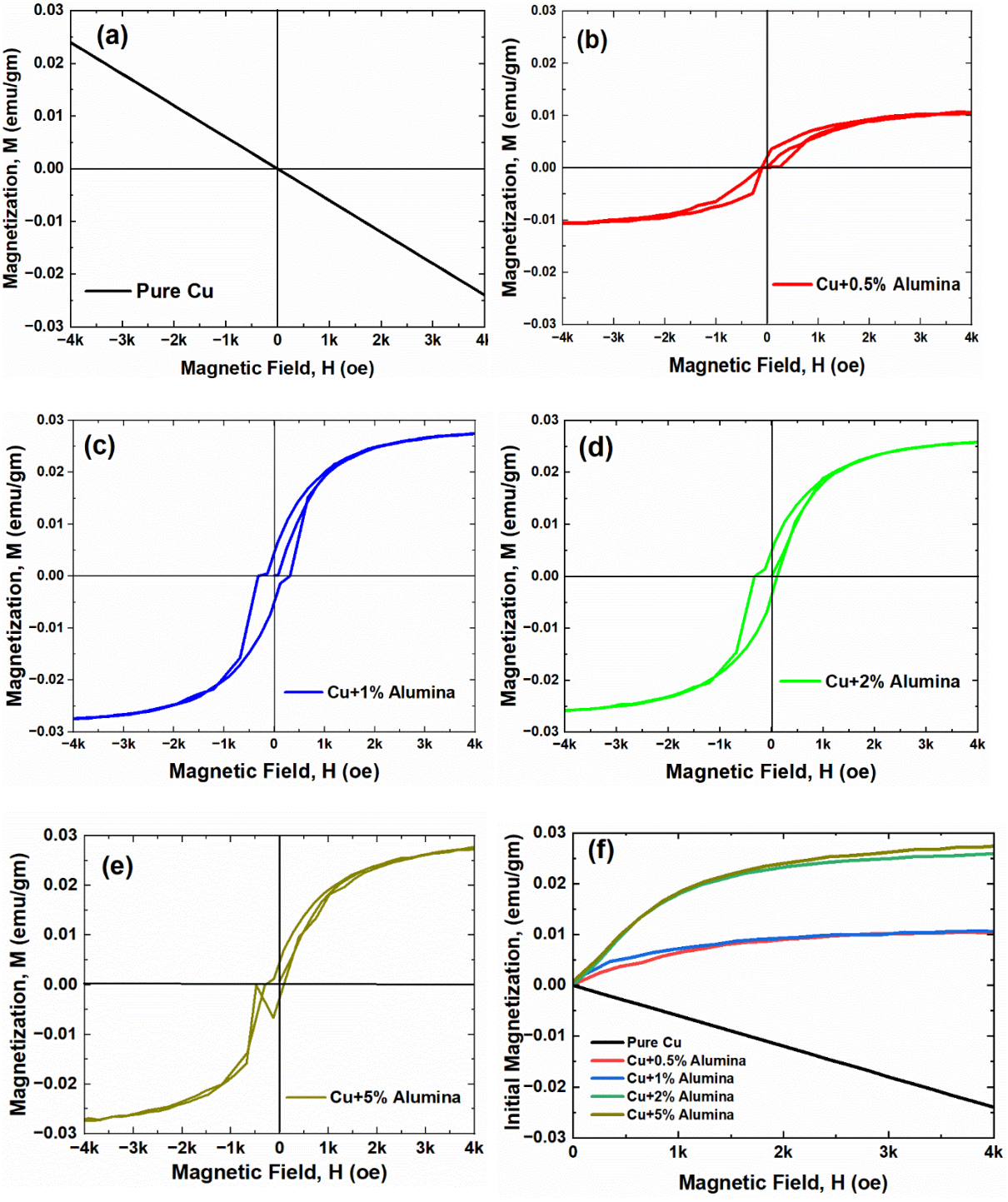

Figure 5.3: Hysteresis observation of copper matrix with reinforcement of Al_2O_3 at room temperature condition: (a) pure Copper, (b) Cu+ 0.5% Al_2O_3, (c) Cu+ 1% Al_2O_3, (d) Cu+ 2% Al_2O_3, (e) Cu+ 5% Al_2O_3 reinforcements and (f) initial M-H curves for different composites

The lowering tendency of the magnetic loss also agrees with findings of Figure 5.3. The stability of the magnetic system was also enhanced with the increase of Alumina content. The coercive force, H_C was found to be increased which demonstrates the higher stability of the magnetization. On the other hand, increasing trend of remnant magnetization defines higher requirement of external magnetic energy for ordering the magnetic moment and domain wall motion. The material with 5% reinforcement attained the highest level of retentivity. From the close observation, a deviation from the regular trend was found in case of composition-III with 2% Alumina reinforcement. The material exhibits highest level of magnetic tendency because of its saturation magnetization, coercivity with lowest remnant magnetism ratio. This phenomenon probably defines its strong potentiality for being used as soft magnet. Lower remnant magnetism of composite-III overcomes the limitation of higher strength requirement of external magnetic field for arranging the spin of magnetic moment.

If the application of fusion reactor is considered, then fusion energy is required to be confined. The confinement of fusion energy requires separation of hot plasma from the first wall. The most effective approach is to use magnetic field for the separation of hot plasma. The fusion power produced in Tokamak was proportional to the strength of the magnetic field to the fourth power (Acher and Dubourg, 2008).

That's why the magnetic characteristics of the construction material becomes a crucial parameter for achieving the condition and it will provide insulation of the stable hot plasma from material surface. So, the construction material has to act like an electromagnet where large electric currents will flow in loops surrounding the plasma. The current must flow through a material with extremely high electrical conductivity (low resistance) for which copper composite reinforced with alumina has become an excellent choice. The low resistance is required because of the generation of magnetic field indefinitely without supply of electrical power. Therefore, the size, timeline and economics of magnetic confinement are strongly dependent on electromagnets (Degrave et al, 2022). The above-portrayed findings of Table 5.1 of the Copper composite strongly justify the induction of paramagnetic behavior of Copper-Al_2O_3 composite in the room temperature with the influence of external magnetic field. But the fusion reactor first wall construction requires the material to hold this magnetic behavior

at high temperature. As a result, the isochronal permeability effect was investigated to observe the magnetic characteristics of material up-to 700^0C at various frequency.

5.1.4 Effect of Isochronal Aging on Relative permeability

Temperature in the crystal structure can have significant impact on the magnetic behavior of the material. The super-exchange energy works to keep the magnetic lattices aligned, on the other hand the temperature acts to randomize the electrons which in turn affects the magnetic moment. At the curie temperature, the temperature randomizing effect becomes greater than the super-exchange energy. Below the curie temperature, the magnetic remanence or spontaneous magnetization acts to hold the magnetic stability. Impurities with metallic oxides like Al_2O_3 works to hold the magnetic lattices in their position after sudden thermal shock. Tarasenko et al (2010) found decreased magnetic susceptibility of Al_2O_3 with the increase in temperature which is the resultant effect of higher magnetic tendency. Figure 5.4 portrays the isochronal magnetic behavior of Cu- Al_2O_3 composite as a function of temperature with frequency as a constant value. The toroid samples were thermally aged up to 700^0C temperature to investigate the magnetic remanence for high temperature environment. When an AC signal with 100 HZ frequency is applied, the tendency of reducing the magnetic permeability with temperature increase is observed as observed from the Figure 5.4. After sudden thermal shock, the atomic particles might get displaced which in turn decreased the magnetic permeability of the composite. The depicted results show the common characteristics of decreasing permeability from low to high frequency signal. Generally, the magnetic losses are due to spin rotation relaxation and domain wall relaxation. The nano-sized grain and crystal morphology also might contribute in this magnetic reaction.

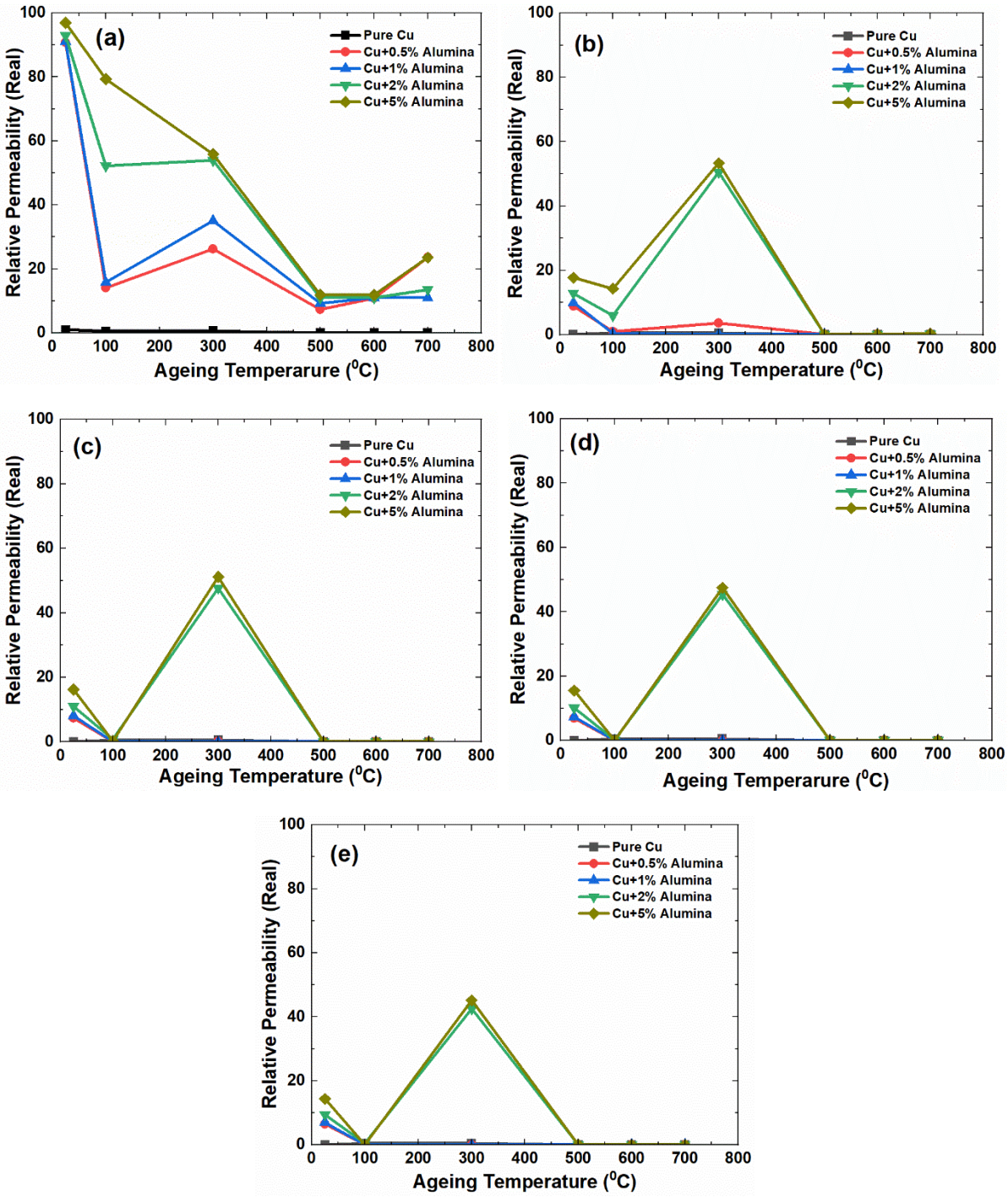

Figure 5.4: Variation of relative permeability (real part) of the MMC samples as a function of Isochronal ageing temperature maintaining constant frequency of (a) 100 Hz (b) 960 Hz (c) 10626 Hz (d) 102068 Hz (e) 1129240 Hz

From close observation, it is found that for 100^0C aging, the relative permeability decreased with steep negative slope for all the frequencies. It is interesting to note that there is a common tendency to restore the magnetic atoms to their respective order at temperature of 300^0C. The same drop-down effect was observed in case of Vicker micro-hardness, EC for 100^0C and restoring tendency after that. The sudden thermal shock has probably displaced the atomic particle or the atoms might get trapped within their interstitial place because of 100^0C aging. For 300^0C, reverse effect is observed. The higher the percentage of Al_2O_3 nanoparticle, the higher the capability of restoration is found. The notable fact is that the positive slope of attaining higher permeability at 300^0C of aging diminishes for 0.5% and 1% Al_2O_3 reinforcement with the progress in frequency. But the Copper alloy with 2% and 5% Al_2O_3 reinforcement showed the isochronal recovery of shape of normal magnetization. Thermal aging below curie temperature may have created residual thermal shock which have successfully restored the behavior at room temperature due to a decrease of magnetic anisotropy as shown in Figure 5.5. The same tendency is also observed for 700^0C temperature thermally aged sample. But the effect of isochronal recovery at 700^0C is negligible in comparison to that of 300^0C.

The findings portraying the recovery tendency of achieving the normal behavior through isochronal shock is supported by the findings of Crowe and Rose (1971). They used Nickel composite and found the same level of isochronal recovery at different temperature for different Nickel compound through the approach of heat treatment. The curie temperature of pure copper is around 1043^0F and due to addition of Al_2O_3 nanoparticle might have slightly deviated from the empirical assumption. Though there may be a probable tuning of curie temperature to a higher value but still much lower in comparison to Nickel. The same fine tuning of Curie temperature was also accomplished by (Teixeira and Araujo, 2022). Through isochronal aging and impurity doping with different concentrations of copper, fine tuning of curie temperature to a lower value was probably obtained which supports the above depicted behavior of the composite at 300^0C and 700^0C. After 300^0C of ageing the magnetic permeability decreases once again to a lower value with steep negative slop. For heat treatment at 500^0C and 600^0C, there is a negligible positive slope. Between 500^0C and 600^0C, the relative permeability increases with slope 0.035705, 0.017039, 0.000051, 0.00082 for material-II, III, IV and V.

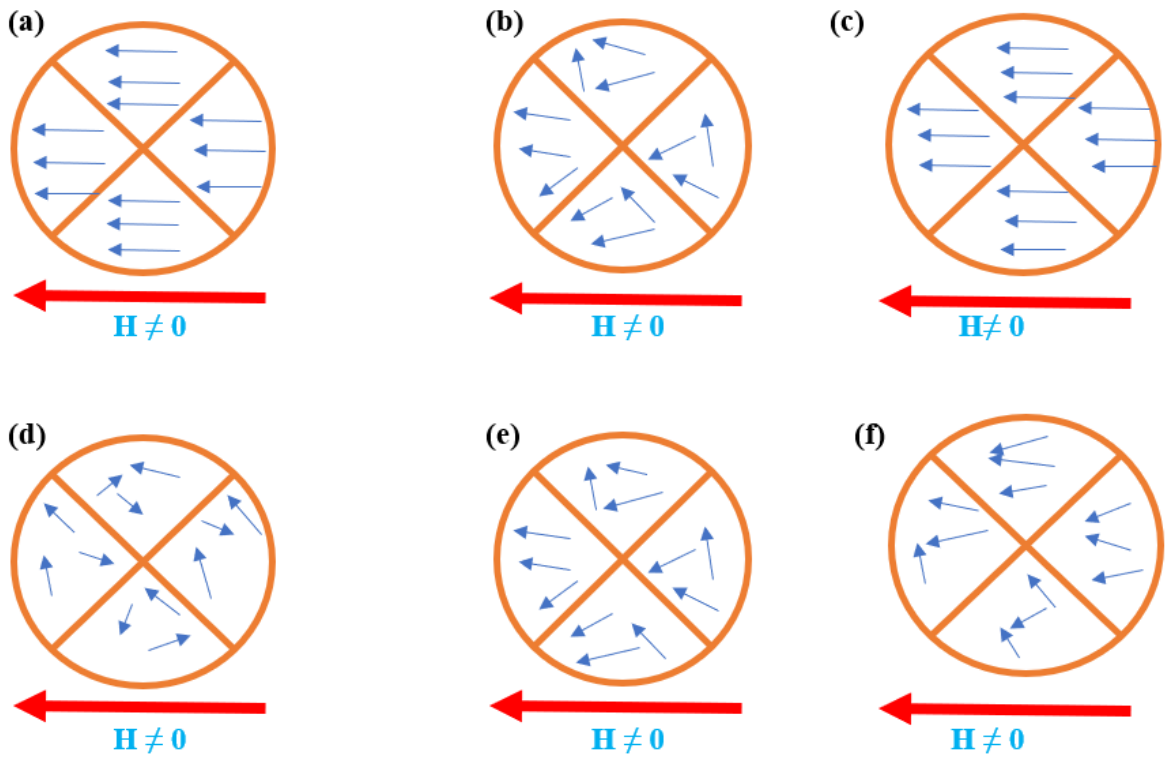

Figure 5.5: Schematic diagram domain wall prediction for Material-II, III, IV and V after thermal aging at (a) Room Temperature, (b) 100^0C, (c) 300^0C, (d) 500^0C, (e) 600^0C and (f) 700^0C

It is interesting to observe that in case of 100 Hz signal propagation there is a tendency of becoming stable between 500^0C and 600^0C with the increase in percentage of Al_2O_3 doping. This slope almost becomes zero with increase in frequency. But at 700^0C of thermal aging, the relative permeability shows the isochronal recovery tendency identical to 300^0C. The spin and domain wall motion relaxation between 500^0C and 600^0C were once again recovered in low frequency region. The electrons scattering may have created this rise in permeability. Unlike 300^0C of aging, 700^0C thermally aged samples couldn't hold the permeability for higher temperature region (KHz to MHz region). The positive slope attained at 100 Hz frequency gets diminished in the high frequency region.

5.2 AC Dielectric Characterization

The dielectric characteristics of the designed material was investigated at various frequencies using the Waynekerr Impedance Analyzer (6500B). The square shaped samples were used to construct a parallel equivalent circuit with a purely resistive and a purely capacitive element. The study of electromagnetic waves propagating in metals have become complex due to interaction between wave and matter. The dielectric permittivity of metal is affected by frequency and temperature mainly and partially due to moisture content. The relative permittivity becomes a complex number with the penetration of frequency varied signals.

5.2.1 Relative Permittivity of Cu with Al_2O_3 Reinforcement

Figure 5.6 portrays extremely high value of dielectric constant in case pure copper ($\times 10^6$). Though it may seem opposite to the regular theoretical assumption yet high permittivity in highly conductive metals has been shown theoretically by the well- known physicist Jonscher (Zaidi and Jonscher, 1999). The initial prediction was even upto 10^8 but the experimental approach validated the value upto 10^6 (Chung and Xi, 2022). The value stated by Chung is equivalent to the value of our findings (1.4×10^6) provided here. For low frequency, the colossal permittivity of pure copper attributes charge-carrier polarization and space charge polarization associated with carrier-atom interaction. The pure nano-crystalline Al_2O_3 ceramic shows insulating characteristics and hence it is a good dielectric (DC ranges between 8-9)`(Marco et al, 2016). Due to the addition of the Al_2O_3 nano-particle, the composite-II, III, IV and V showed lower value in comparison to pure copper. The insulating characteristics of Alumina particle showed considerable influence on the dielectric characteristics of pure copper. The findings of the relative permittivity at 100 Hz frequency also got supported by the initial investigation of electrical conductivity shown in Figure 4.5 which showed considerable decrease of EC due to addition of alumina particle. The relative permittivity shown by the composite-II, III, IV & V were 1230230, 963732, 776652, 727939 respectively. The reduction probably defined the disturbance caused in between the charge-carrier interaction due to doping of insulating ceramic material.

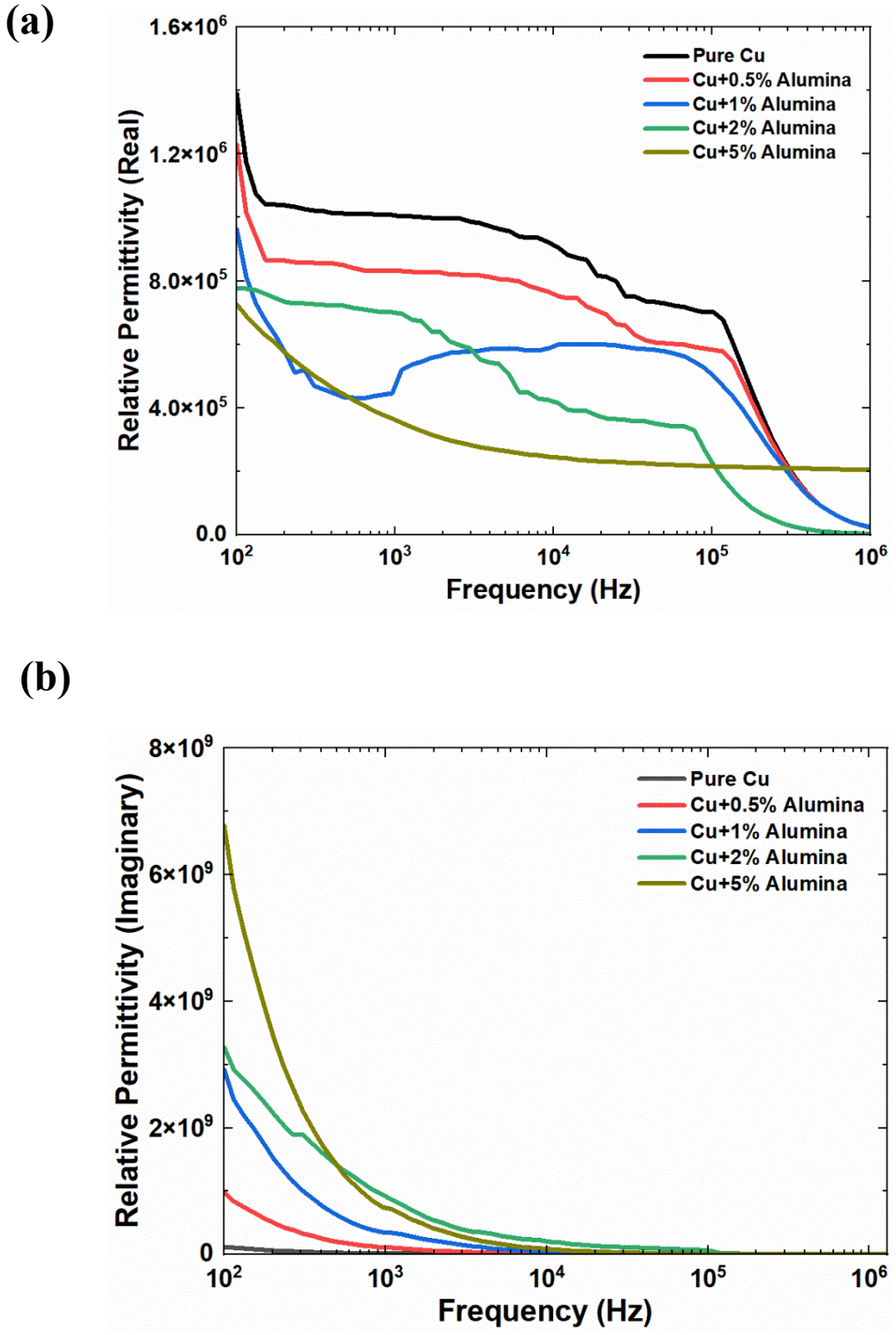

Figure 5.6: Effect of Al_2O_3 reinforcement on permittivity of copper matrix as a function of operating frequency at room temperature (a) real part (b) imaginary part

With increase in frequency, the DC decreased rapidly up-to KHz range frequency. This decreasing trend could be justified by Maxwell- Wagner interfacial polarization model which is dominant in low frequency (≤ 10 KHz) region (Karthik and Tummala, 2017).

The variation among the composites is assumed to cause the inhomogeneity of charge careers across the grain boundaries. After the initial decrease, the DC value was relatively stable up-to 100 KHz frequency and at HF range (3 to 30 MHz) it decreased with a steep slope. In the high frequency range, the steep slope was attained probably due to high power loss. From close observation, the stability of DC at relatively higher value for composite-V was found. In the higher frequency region (10^5-10^6 Hz), the permanent dipole probably did not follow the orientational polarization for this particular case. A competition between orientational polarization and space charge polarization might take place where the first one tried to go down and second one tried to go up. As a result, the DC was constant at higher value (>2000) at HF region for case-V (Ojha et al, 2021).

5.2.2 Dielectric Loss Tangent of Cu with Al_2O_3 Reinforcement

Dielectric loss factor is a measure of the energy absorbed in a certain medium as the EM wave passes through it. Dielectric materials possess dielectric loss factor primarily due to extrinsic and intrinsic losses. These two types of losses arise due to electrical conduction, dielectric relaxation and resonance. Figure 5.7 depicts the lowest dielectric for pure copper. The imaginary part of the dielectric primarily justifies the increasing tendency of loss factor of pure copper with increasing percentage of alumina content. Pure copper shows lowest loss among the five cases because of the highest conduction capacity. The findings regarding pure copper are justifies by the theory of intrinsic dielectric loss in crystals developed by (Gurevich and Tagantsev, 1991). According to Gurevich (1991), the AC electric field alters the equilibrium of the phonon system and subsequent relaxation is associated with energy dissipation.

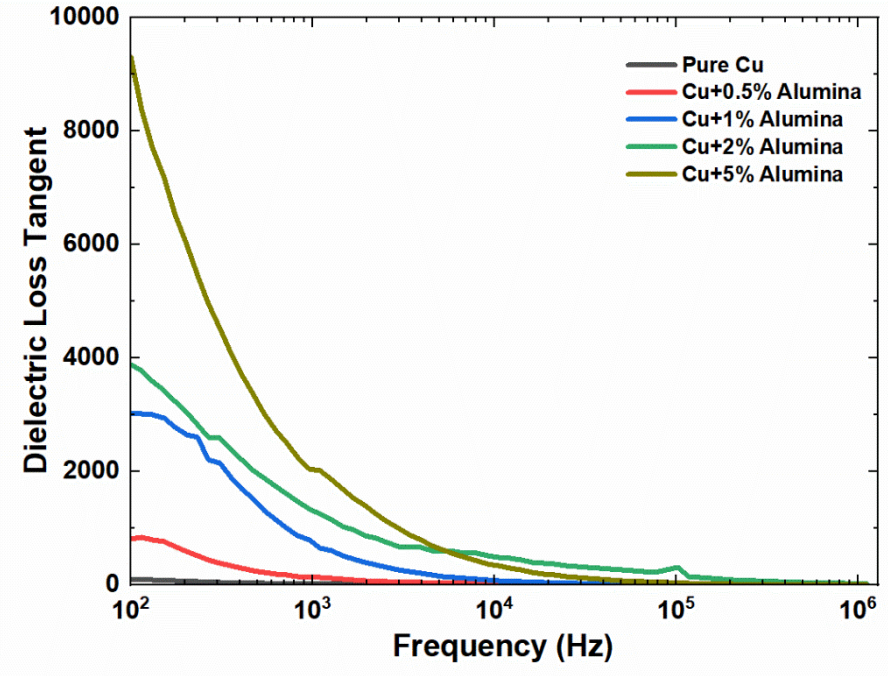

Figure 5.7: Effect of Al_2O_3 reinforcement on dielectric loss tangent of copper matrix as a function of operating frequency at room temperature

The imaginary part of relative permittivity shows higher value with increase of Al_2O_3 content. Dielectric loss increased to 803.10136 from 87.64935 which is almost 10 times the value of pure copper for 0.5% percent addition. Consecutively, 34 times, 80 times and 105 times increase were observed for 1%, 2% and 5% reinforcement. The ceramic particle shows insulating nature which affects the electrical conductivity of the copper. The Al_2O_3 nanoparticle may have created perturbation in electron flow within crystals which generate heat inside the crystals. The addition of reinforcement in copper may have created imperfection among crystals. As conventional casting process was adopted, the micro-cracks, random crystal orientation, dislocations and porosities might be created due unavoidable environmental condition. Also, the Debye effect gets enhanced due to frictions between the copper and Al_2O_3 atoms in the interfacial region (Mantas, 1999)

5.2.3 AC Impedance Characteristics of Cu with Varying Percentage of Al_2O_3 Reinforcement

Figure 5.8 shows the impedance variation of the designed material with the increase in frequency. The impedance response of such material may consist of contribution of grains to the conduction mechanism. Electromagnetic wave excitation induces microscopic motion in materials at the molecular and atomic level which may attribute the chemical change and material structure. The square shaped samples were excited with electrical energy over the frequency range of 100 Hz to 100 MHz. The measured single frequency response at each level provided the abovementioned continuous spectra. The designed composite exhibited complex impedance characteristics representing energy dissipation (resistive) characteristics and storage (reactance) parts.

(a)

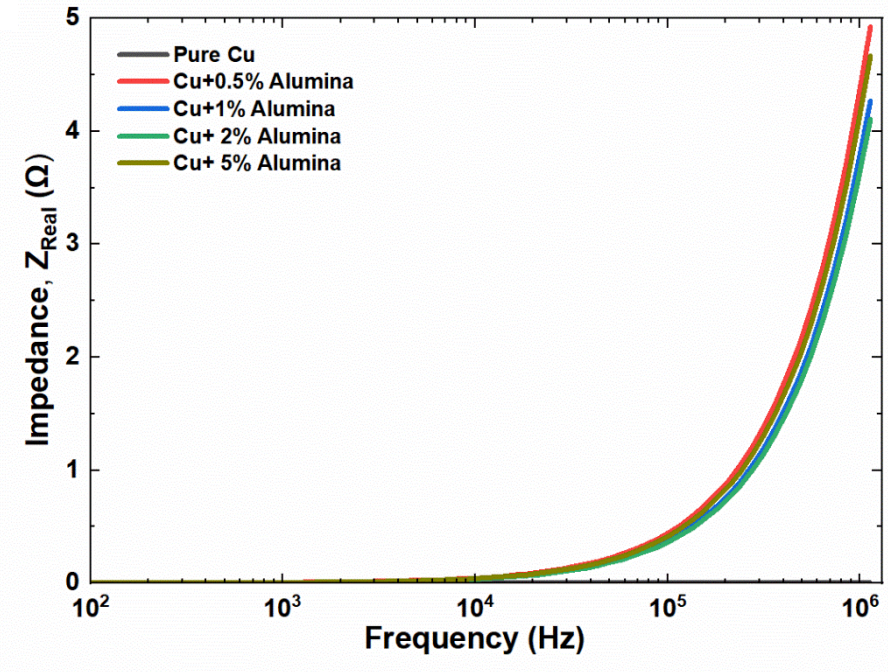

(b)

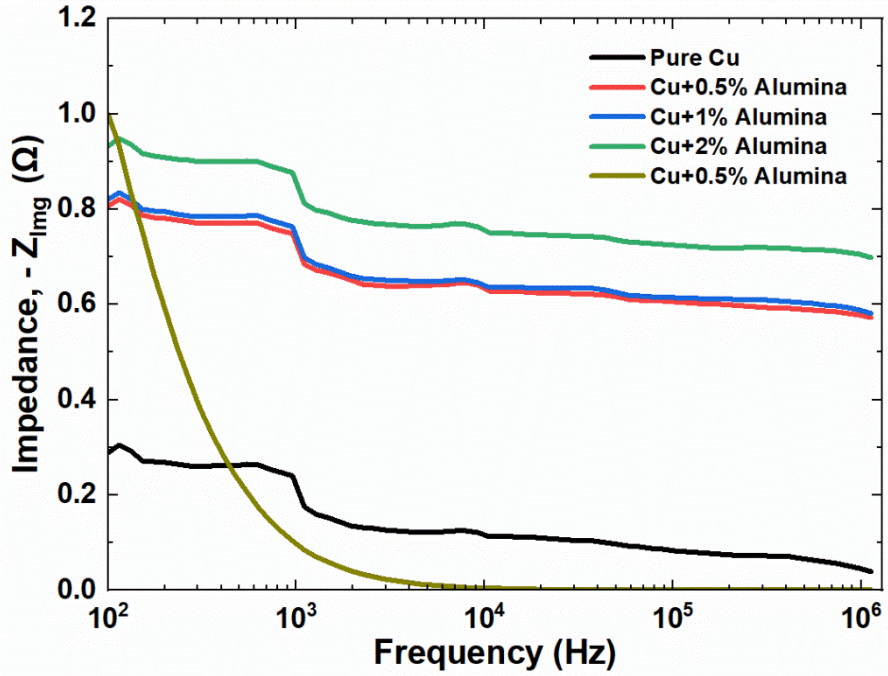

Figure 5.8: Effect of Al_2O_3 reinforcement on AC impedance of copper matrix as a function of operating frequency at room temperature (a)Real part (b) Imaginary Part

From the Figure 5.8, the resistivity exhibited by the pure copper (0.000118 Ω) is negligible because of its perfect conduction characteristics. With the trace addition, rise in resistivity of the composite was observed. At 100 Hz frequency, the resistivity characteristics exhibited were 0.000753 Ω, 0.000893 Ω, 0.00091 Ω, 0.00092 Ω respectively for 0.5%, 1%, 2%, 5% addition of Alumina. On the other hand, an exponential rise was observed in the high frequency range due to trace addition of Alumina ceramic. The inherent impurities configured at the grain boundaries in a way that caused electric field across the boundaries to resist the flow of electrons between atoms. This phenomenon can be described using Maxwell-Wagner interfacial polarization model which depicts the dielectric phase change due to interaction between unlike molecules. Because of the separate dielectric phase with respect to excitation of electric field, probably a difference between voltage drop was produced in the high frequency region which made the rise in resistivity observed. The footprints that the impurities leave on the overall resistance closely resemble the thermodynamic effects due to collision of atoms at higher frequencies according to the understanding of several scientists. Based on our

findings, the resistance at the grain boundaries might be calibrated by inserting materials intentionally that negate the effect of impurities.

The reactance of the material showed stability tendency with increase in frequency for the pure copper, 0.5%, 1%, and 2% alumina addition. On the contrary, 5% Alumina addition created significant drop in reactivity of copper. This is due to the probable domination of ceramic nanoparticles on the charge transport characteristics of copper atoms. Most importantly, the material gained charge storage capability due to addition of Alumina reinforcement. If impedance magnitude is considered, contribution of resistivity property was negligible. The overall drop in impedance characteristics upto 10^5 Hz could be justified by the Koops phenomenological theory in the conduction band. The resistive grains were more active in the low frequency region preventing the electronic charge careers from hopping between them. However, the conductive grains probably became more active in the high frequency region which contributed in the fall of impedance magnitude of the material.

5.2.4 Effect of Isochronal Aging on Relative permittivity

The temperature dependance of relative permittivity of pure copper and its composition is shown in Figure 5.9. The formation of bathtub effect was clearly observed in the Figure 5.9. For low frequency (100 Hz), the real part of relative permittivity was extremely high and with frequency it was having a decreasing trend. At a temperature of 100^0C, significant drop in permittivity was found. In a crystalline solid, certain orientations are permitted by the lattice which was probably oscillated and dislocated from the equilibrium condition due to sudden energy injection that led to dipole loss. After the sudden decrease in relative permittivity, the value remains stable up to the temperature of 500^0C. The composites were probably isostructural in this temperature region (100^0C – 500^0C). Thermal aging at 500^0C probably overcame the energy barriers and the disturbed orientation at 100^0C was corrected thereby contributing to rise in the permittivity. With the increase in temperature after 500^0C, a tendency towards restoring the initial relative permittivity was observed thereby creating the bathtub curve.

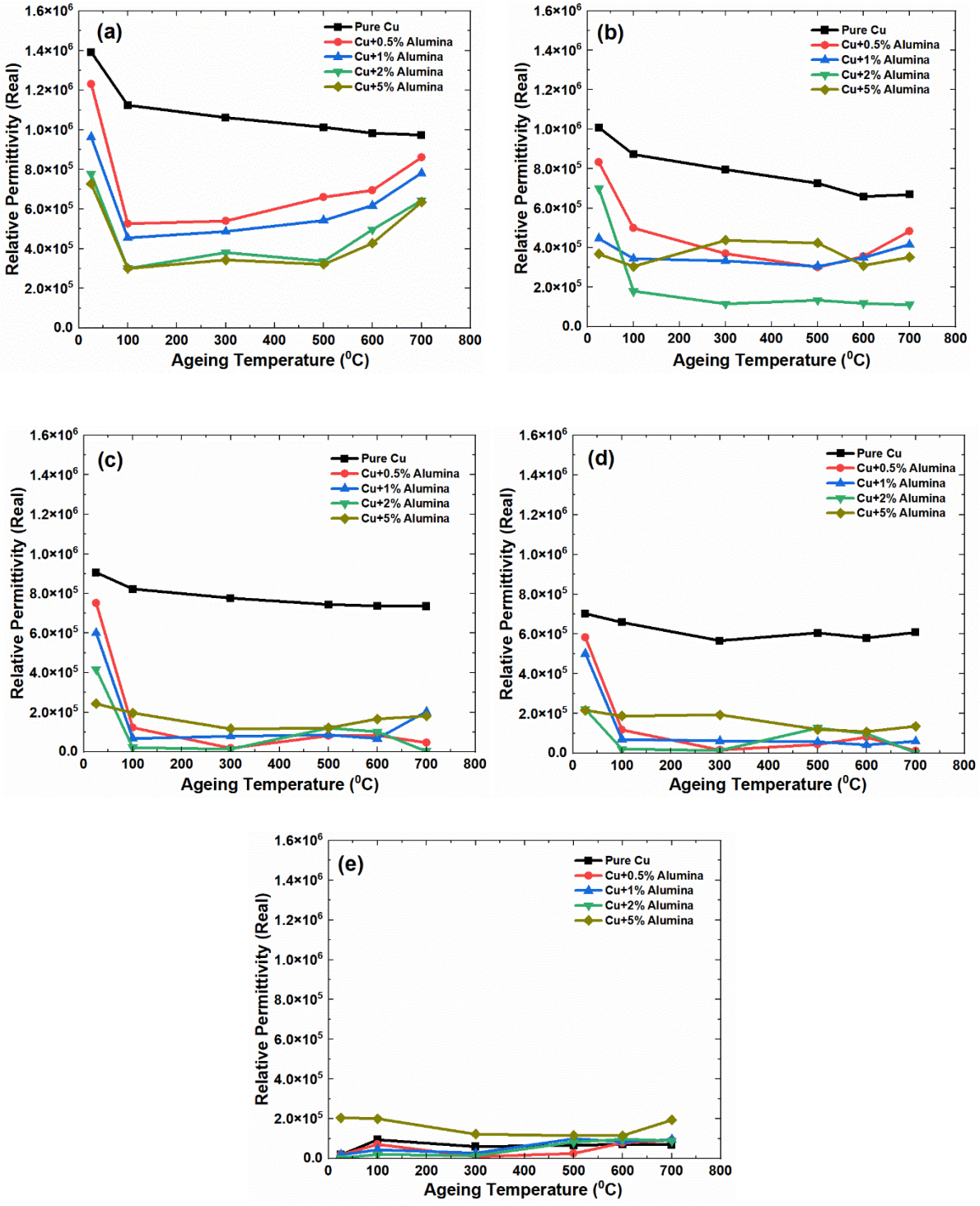

Figure 5.9: Variation of relative permittivity (real part) of the MMC samples as a function of Isochronal ageing temperature maintaining constant frequency of (a) 100 Hz, (b) 960 Hz, (c) 10626 Hz, (d) 102068 Hz, and (e) 1129240 Hz

One very important point to note that, for constant frequency the relative permittivity of pure copper doesn't show steep slope with temperature increase whereas, 0.5%, 1% and 2% addition of reinforcement created steep negative slope defining the significant impact of Al_2O_3 particle on the characteristics of copper. The aforementioned effect after 500^0C happened probably due to the semiconductive nature of Al_2O_3 at high temperature according to the Cohen's law. Besides that, the composition-V with 5% addition of ceramic particle showed stability characteristics with the frequency rise. The initial dislocation of lattice was probably attenuated due to higher percentage of reinforcement. The oscillating characteristics was applicable for trace addition of Al_2O_3 up to 2%. The initial reduction denoted the probability of composing the lattice structure with highly resistive grains surrounded by poor conductive grains whereas higher temperature aging denoted the possible formation of lattice with highly conductive grains by poor resistive grains of ceramic. This happened due to influence of external energy. As a result, localized accumulation of charges was obtained which led to interfacial polarization. The highest percentage (5%) of addition probably held the lattice formation thereby stabilizing the relative permittivity with temperature rise. Only space charge polarization contributed in this particular case.

CHAPTER 6
ELECTRO-CHEMICAL CORROSION BEHAVIOR

6.1 Introduction

Sea water is a severe corrosion agent because of its complex electrolytic behavior. Copper has the status of membership of noble metal family and it is not immune to corrosion damage in the corrosive environment. As this research focuses on the potential application on copper composite like fusion reactor where salt is the proposed medium of energy storage, ideal sodium chloride salt water was taken as the electrolyte. The gravimetric method of measuring weight loss is the most conventional way of determining the possible damage due to corrosion attack. So, the gravimetric approach was adopted along with potentiodynamic polarization and electrochemical impedance spectroscopy for examining the corrosion behavior of pure copper and copper matrix with alumina reinforcement in the room temperature condition. In the laboratory, sea water was ideally formed using a mixture of 3.5% NaCl in the distilled water.

6.2 Weight Loss of Cu with Al_2O_3 Reinforcement

Figure 6.1 portrays the detailed effect of Al_2O_3 reinforcement on the corrosion behavior of copper. Lowest weight loss in case of pure copper was observed in comparison to copper matrix with reinforcement. As the percentage of reinforcement increased, the weight loss due to gravimetric corrosion was also increased. The initial weight loss due to corrosion was 0.000595219, 0.000710187, 0.001947504, 0.002062301, 0.002682403 respectively for pure copper, 0.5% Al_2O_3, 1% Al_2O_3, 2% Al_2O_3, 5% Al_2O_3 for 1 day of immersion. After that with increase in day count, marginal slope was observed for all the cases. A steep slope was found for the 22 and 43 days of immersion of the samples. The peak value of weight loss was extracted at the time count of 43 days.

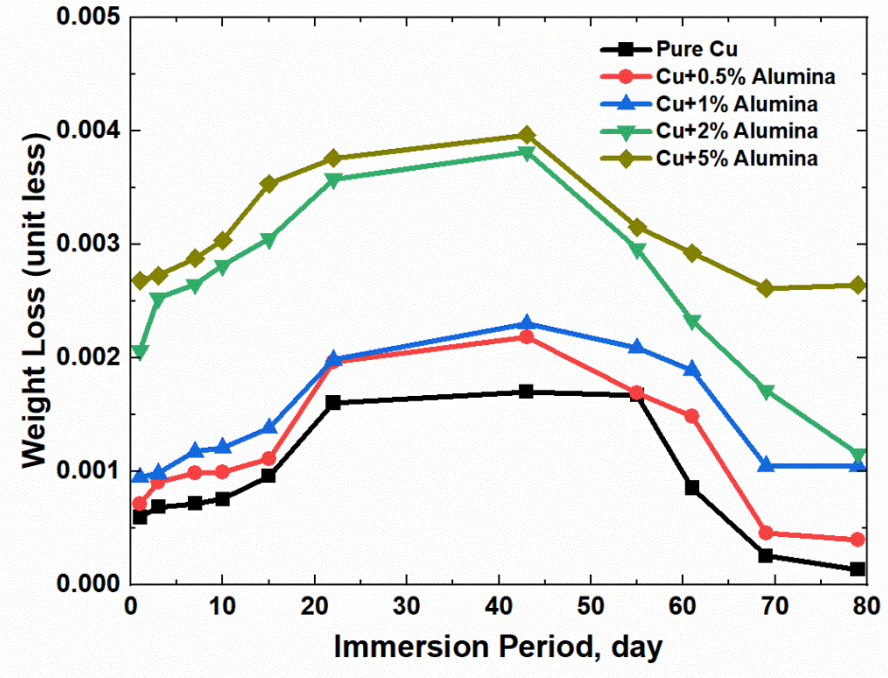

Figure 6.1: Variation of weight of copper matrix with and without reinforcement of Al_2O_3 in 3.5% salt (NaCl) water solution at room temperature

After 43 days of immersion, negative slope was observed, that means the tendency of corrosion reduced. The 5% reinforcement showed the behavior of holding the highest corrosion characteristics with the increase in time count. Probably after the highest amount of weight loss, the formation of passive films (Cu based oxide or hydroxide) on the exposed surface of the sample reduced the weight loss level by significant amount. The porosity formed due to casting contributed to the increase in surface exposal which probably made the sample with 5% alumina reinforcement vulnerable. That means the reinforcement of ceramic particle like alumina led to the increased corrosion tendency of the composite.

6.3 Potentiodynamic Polarization Curve of Al_2O_3 Reinforced Copper Matrix

The influence of mass transport condition on the rate of copper electro-dissolution reaction is of particular interest to corrosion scientist. The focus specially indicates to chloride media due to its applicability in sea water. Figure 6.2 shows the polarization curves of pure copper and reinforced copper matrix with varying percentage of Al_2O_3 reinforcements in 3.5% NaCl solution. The calculated values from the Tafel diagram are shown in table 6.1. The corrosion current was found from the extrapolation between anodic and cathodic behavior. In the PDP test, the potential was applied on the test electrode of our interest and the surface of the metal got oxidized and reduction reaction happened. Because of the electron transfer due to ionization resulted into generation of corrosion current. From the theoretical assumption, corrosion current should be lower for justifying the compatibility of composite in corrosive media. Researchers have already proven the strong influence of chloride ion on corrosion of copper. The table 6.1 describes the corrosion formation on copper ion which actually defines the anodic reaction of highly favorable complexation of cuprous ion with chloride ion. On the other hand, the cathodic reaction was dominated by the oxidation of surface which is irreversible. The influence of anodic and cathodic reaction creates formation of artificial film. Automatically created films probably blocked the surface of the metal with insulating materials.

On the contrary, it is seen that the corrosion current of pure copper increased with the addition of Al_2O_3. The I_{corr} was recorded as 0.7798 μA in the corrosive medium which increased by 1.79% due to 0.5% Al_2O_3 addition.

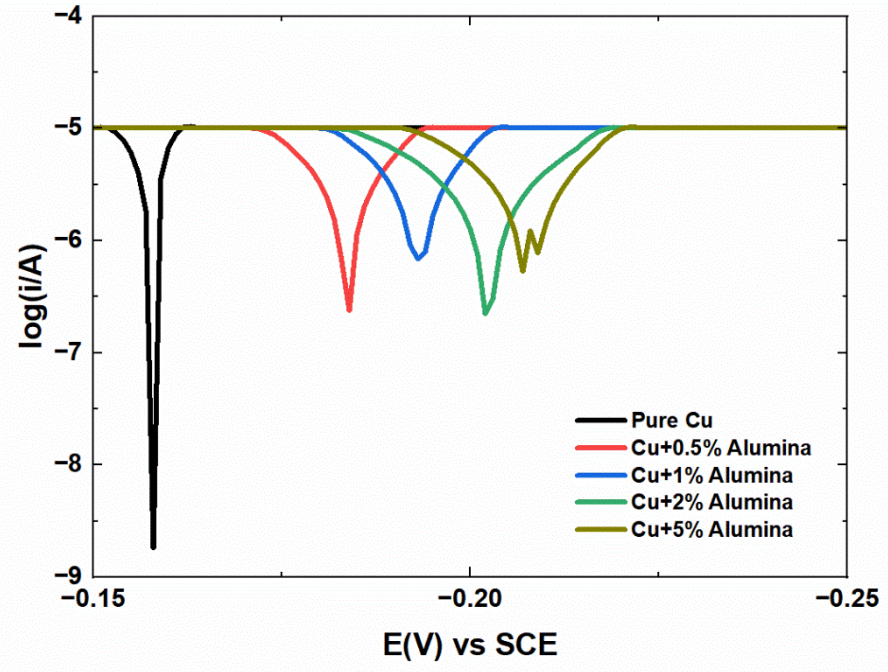

Where, log(i/A) = Log current density

E(V) = Potential in volt

SCE = Saturated calomel electrodes

Figure 6.2: Tafel polarization curve of Copper and Copper matrix composites with varying percentage of Al_2O_3

As the percentage of Al_2O_3 reinforcement increased, the corrosion resistance decreased initially at a lower percentage and then dramatic increase (21.85% for 2% Al_20_3 and 36.086% for 5% Al_2O_3 reinforcement) was observed. This increase in corrosion current probably justifies the formation initial stage of passive film formation that ultimately led to higher level of corrosion. Again, creation of higher corrosion potential shifted the polarization curve to larger negative value. This shifting towards higher negative value is resulted from susceptibility to pitting corrosion.

Table 6.1: Corrosion parameters resulted from potentiodynamic polarization analysis

Material	Corrosion Current I_{corr} (µA)	Corrosion Potential E_{corr} (V)
Pure Cu	0.7798	-0.158
Cu + 0.5% Al_2O_3	0.7938	-0.184
Cu + 1% Al_2O_3	0.7991	-0.192
Cu + 2% Al_2O_3	0.9502	-0.202
Cu + 5% Al_2O_3	1.0612	-0.207

This pitting corrosion is extremely dangerous in the interfacing region between base copper and reinforcement. The corrosion process normally starts from the defects of the composite surface. As conventional stir casting process was adopted for fabrication of composite, probably the unavoidable defects (Figure 4.8) formed due to difference in thermal expansion in changing temperature condition is mainly responsible for the shifting of open circuit potential and made the material vulnerable to pitting corrosion. The result portrayed above agrees with the findings of several other researchers as mentioned in the Table 2.1. Saber et al (2016), Kumar et al (2018), Allahkaram et al (2011) examined corrosion behavior of copper-alumina composite through the same chloride media. Even though they used different ways of production (Mechanochemical Technique, Ball Milling, DC & PC deposition) of composite with varying percentage with Al_2O_3 reinforcement yet none of them could reach the corrosion rate of pure copper in room temperature condition.

6.4 Electrochemical Impedance Spectroscopy

The importance of EIS over other electrochemical technique lies in its ability to discriminate and thus provide a vast amount information regarding physio-chemical processes taken place in a real electro-chemical system. EIS was performed to investigate the effect of inhibitors in 3.5% NaCl media. Nyquist and bode diagram of copper with and without various concentrations of Al_2O_3 are shown in Figure 6.3 and 6.4. The data extracted from the

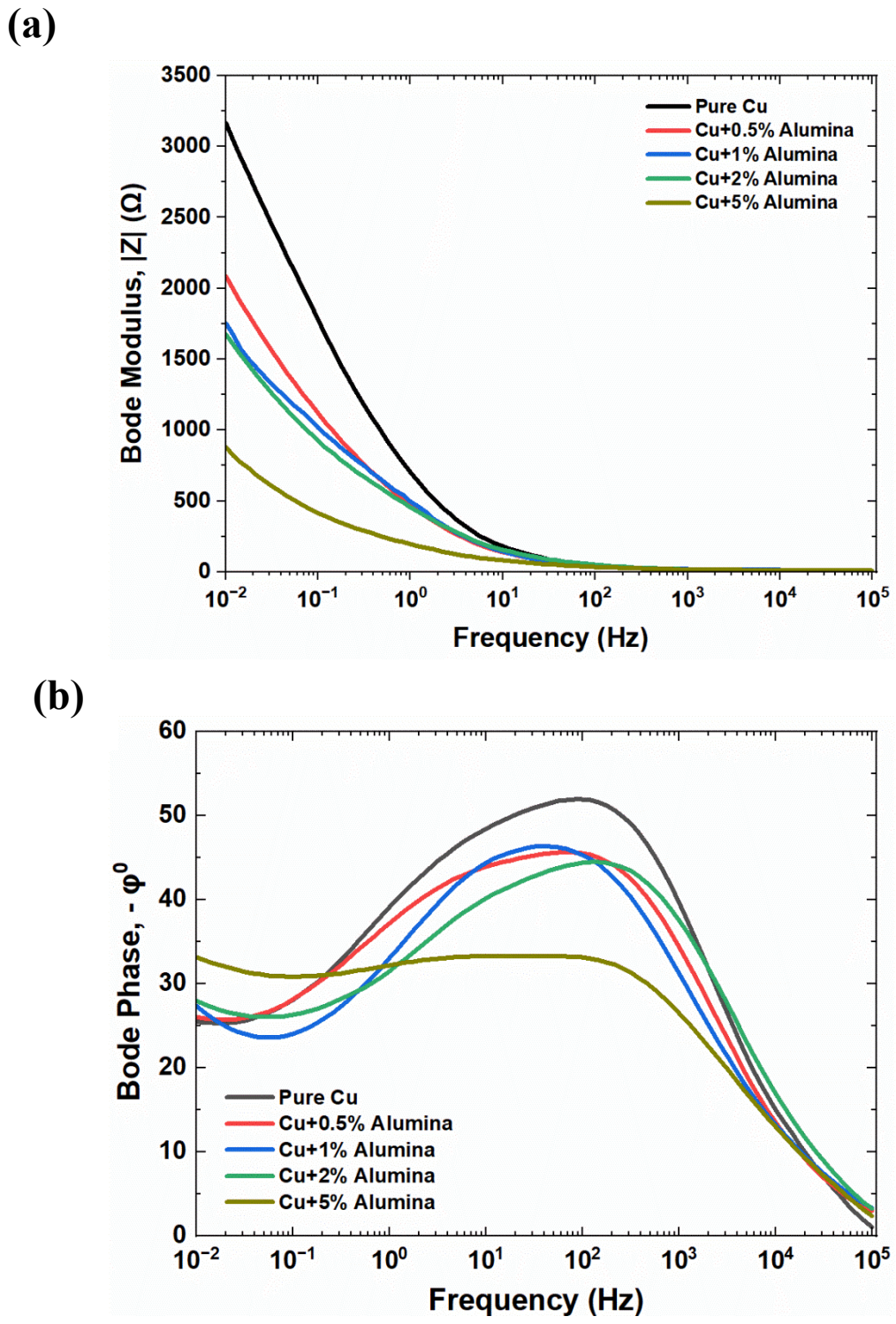

Figure 6.3: Variation of electro-chemical corrosion impedance and phase of copper matrix with and without various percentage of Al_2O_3 reinforcement at room temperature. (a) Bode Modulus (b) Bode Phase

experiment was fitted into an equivalent circuit model using EC lab software. The obtained Nyquist plot became complicated with the addition of Al_2O_3 content due to passive metal electrolyte solution interface, metal- inhibitor interface etc. As observed from the figure, the plot became depressed with Al_2O_3 reinforcement. The pure copper showed incomplete semicircular tendency in the high frequency region whereas linearity in the low frequency region. These two different behaviors in two different regimes are due to the existence of Warburg impedance and capacitive resistance. With the increase in Al_2O_3 content, the Warburg impedance dominated over the capacitive loop and its slope increased. This is probably due to decrease in charge transfer resistance and increase in oxygen transport from solution to copper surface.

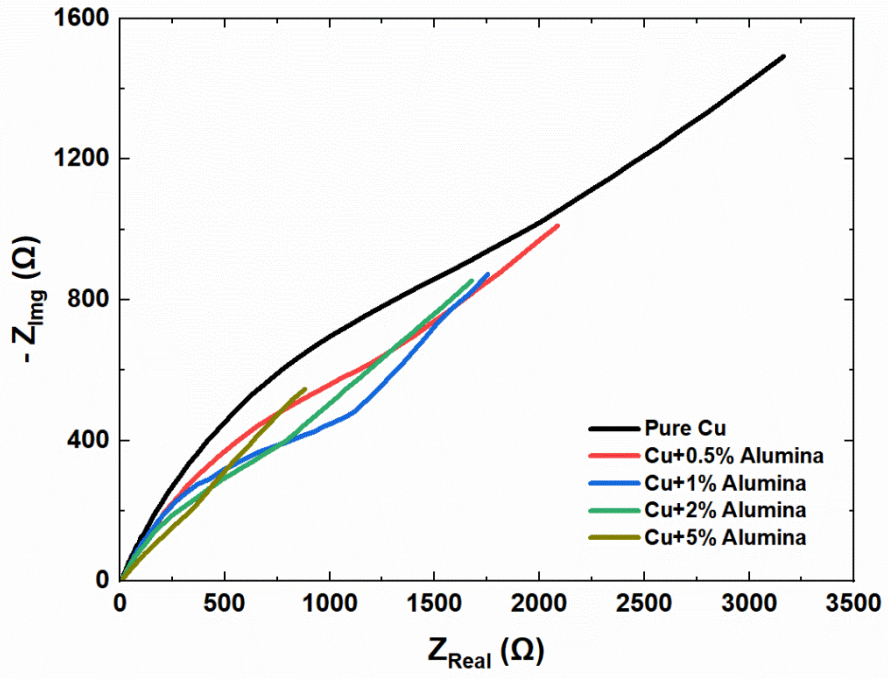

Figure 6.4: Variation of Nyquist diagram of electro-chemical corrosion impedance of copper matrix with and without various percentage of Al_2O_3 reinforcement at room temperature.

The diffusion of electroactive species in the solution probably increased with increase of Al_2O_3 reinforcement. For that reason, the corrosion of copper gets increased significantly with Alumina addition. The obtained Nyquist plot reveals the fact that Warburg impedance started

dominating the higher frequency region as well because of the Al_2O_3 addition while the charge transfer resistance gets decreased. The behavior is well described by the equivalent circuit model presented in the Figure 6.5 below. The observed finding also reveals the increase in diffusion process with addition of reinforcement and thereby corrosion phenomenon. The Randles circuit is commonly considered to estimate polarization resistance and oxygen transport resistance represented in the impedance spectrum. The polarization resistance usually combines the effect of resistance due to charge transfer and passivation in between the working electrode and the electrolyte.

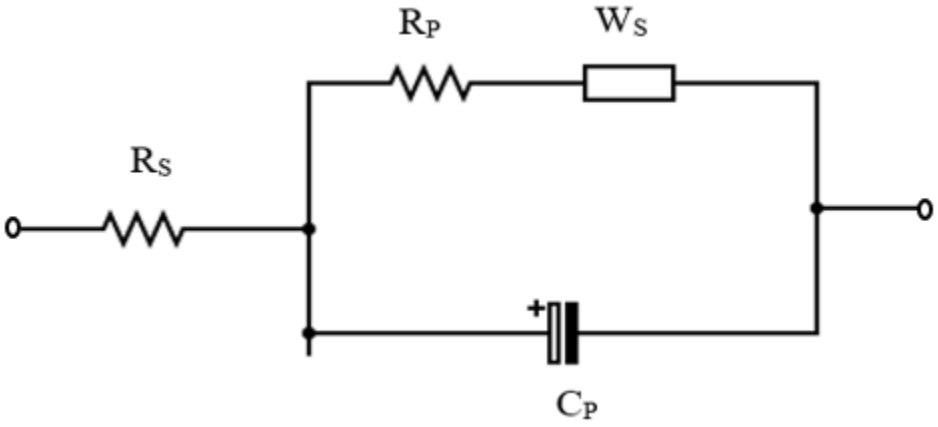

Figure 6.5: Equivalent Circuit used for the EIS data fitting

Table 6.2: Parameters of Equivalent circuit used to fit the EIS data

Material	R_S (Ω)	R_P (Ω)	C_P (μF)	Warburg Impedance W_s (Ohm.s^-1/2)
Pure Cu	0.0101	800	0.1154	150
Cu + 0.5% Al_2O_3	0.12364	459	0.1194	206
Cu + 1% Al_2O_3	0.6523	500	0.0814	198
Cu + 2% Al_2O_3	0.98745	436	0.0369	256
Cu + 5% Al_2O_3	1.3698	345	0.0325	400

The Randles circuit perfectly portrays the effect of Warburg impedance shown in the Nyquist diagram. The solution resistance of the circuit is negligible in comparison to charge transfer resistance. For the case with pure copper, the current probably went through the working

electrode by capacitive current caused by electro-chemical double layer and because of that the double layer capacitance and charge transfer resistance were highest among all the cases. After that the effective capacitance and charge transfer resistance decreased with increase in alumina addition. For 5% Al_2O_3, the Nyquist diagram became linear with 45^0 angles. This domination was probably due to the pitting corrosion of the exposed surface to the salt water medium. As the sand casting was adopted for production, the unavoidable porosity caused an increase in the exposed surface and vulnerability of composition-V occurred.

CHAPTER 7
CONCLUSIONS AND RECOMMENDATIONS

7.1 Conclusions

This thesis provides a cohesive assimilated view of the electromagnetic behavior of pure copper as well as with trace Al_2O_3 reinforcement processed through sand casting route. Four distinctive groups were formulated for improvement of the performance of the pure copper. To evaluate physical, mechanical and electro-magnetic characteristics of the prepared composite, a number of tests were carried out. Complementing these tests, an in-depth characterization was carried out using FESEM analysis. Following conclusions can be drawn from the analysis:

- The electrical conductivity of the pure copper decreased by 14.67% due to addition of just 0.5% Al_2O_3 which reached up to 46% for 5% addition at room temperature. The possible reason of the sudden deterioration was the interference of non-conductive grains in between the hopping of electrons among copper molecules. But higher temperature aging converted the non-conductive grains into conductive ones following the Cohen's law of conduction for semiconductive Al_2O_3 particle up to 2% reinforcement at higher temperature.

- The advantage of gaining higher electrical conductivity was added by the recovery of strength of copper up to 600^0C of thermal ageing condition according to Hall-Petch effect. After this temperature, the reinforcement material could not hold the microstructure of the prepared composite and the microhardness dropped significantly. Best possible hardness and conductivity for the MMC was found with trace-addition of Al2O3 ($\geq$ 1%) together with post-thermal treatments at 400 ~ 600 ^{o}C.

- Huge permittivity in highly conductive metals was predicted long before by Jonscher which is once again proved in this research in case of copper (1.4×10^6). This is the one of the first approach of its kind to explore the relative permittivity characteristics of highly conductive metals like copper. Because of being an ideal dielectric material,

the Al_2O_3 addition created a decreasing trend of the permittivity of pure copper. The colossal permittivity of copper is attributed to charge carrier polarization and space charge polarization due to carrier atom interaction at heterogeneities. For VHF range frequency, the 5% Alumina could hold the dielectric constant close to RT Duriod polymer used for micro-strip patch antenna

- The value of impedance was also affected by the above-mentioned phenomena which justified the higher activity mode of the resistive grains in the low frequency conduction band. With the temperature rise, initial disturbance of lattice orientation was disturbed but after a temperature of 500^0C, the dipole loss due to sudden external energy was overcome thereby tendency to restore the relative permittivity at room temperature was observed.

- One very interesting point was the transition of magnetic behavior of copper from diamagnetism to paramagnetism due to formation of unpredicted disordered magnetic system because of low percentage reinforcement of Al_2O_3.

- The saturation magnetization reached higher point with the increase of Al_2O_3 content and the hysteresis loop became thinner which demonstrated the lower dissipation of energy therefore higher magnetic stability. The isochronal recovery phenomena at temperature 300^0C and 700^0C reveals the potential applicability of the material for high temperature sensor construction because of the probable shifting of curie temperature to a higher point.

- Corrosion resistance tends to decrease, but it is very close to that of pristine Cu with trace addition of Al2O3 (≤ 1%). Conventional sand casting may make the MMC sample susceptible to pitting corrosion.

- From overall perspective, addition of 1% Al2O3 in Cu appears to be the optimum composition for high-temperature electromagnetic applications

With the present findings, it is expected that the Al_2O_3 affected copper will now be free from fears of deterioration in terms of electrical conductivity which was affecting the end users skeptical to accept the use of ceramic doped copper for high temperature environment. This will open the potential use of copper composite for a number of applications like high power electrical applications, fusion reactor first wall, microstrip patch antenna and sensors construction for high temperature sensing.

7.2 Recommendations

- The present research was concerned with as-cast, conventional sand-casting formed MMCs. The manufacturing process might have significant impact on the prepared composite. So other precision approach like powder metallurgy, strip casting etc could also be explored.
- Micro-hardness characteristic was mainly explored, but the embrittlement behaviour induced by trace-addition of ceramic particles may be explored by the tensile test.
- The antenna construction demands the optical reflectance and directivity of the signals based on their type. The designed MMC would be an excellent candidate for thermocouple construction if thermal conductivity could be explored.
- The isochronal and isothermal characterization of properties like AC impedance and loss tangent (dielectric and magnetic) could be undertaken which could led to enhancement of its behavioral spectrum further and thus new potentiality of copper-alumina composite might be discovered.
- The corrosion characteristics of copper composite focused only the room temperature environment with sodium chloride media. The vulnerability of copper matrix reinforced with alumina could also be explored in the isothermal and isochronal environment condition. For next generation fusion-reactor technology, high temperature corrosion characteristics is an essential requirement. EIS and PDP test in the molten salt-water medium would be a potential area to be explored

REFERENCES

Abdelaziz, Y.A., Megahed, F.M. (2011). Realization of copper melting point for thermocouple calibrations. Sensors and Transducers., Vol.131,pp. 61–67.

Abdo, B.M.A., Anwar, S., El-Tamimi, A.M., Nasr, E.A. (2019). Experimental analysis on the influence and optimization of μ-RUM parameters in machining alumina bioceramic. Materials (Basel)., Vol. 12.

Abyzov, A.M. (2019). Aluminum Oxide and Alumina Ceramics (review). Part 1. Properties of Al2O3 and Commercial Production of Dispersed Al2O3. Refract. Ind. Ceram., Vol. 60, pp. 24–32.

Acher, O., Dubourg, S. (2008). Generalization of Snoek's law to ferromagnetic films and composites. Phys. Rev. B - Condens. Matter Mater. Phys., Vol. 77.

Alaneme, K.K., Bodunrin, M.O. (2011). Corrosion Behavior of Alumina Reinforced Aluminium (6063) Metal Matrix Composites. J. Miner. Mater. Charact. Eng., Vol. 10, pp. 1153–1165.

Alemour, B., Badran, O., Hassan, M.R. (2019). A review of using conductive composite materials in solving lightening strike and ice accumulation problems in aviation. J. Aerosp. Technol. Manag., Vol. 11, pp. 1–23.

Allahkaram, S.R., Golroh, S., Mohammadalipour, M. (2011). Properties of Al2O3 nano-particle reinforced copper matrix composite coatings prepared by pulse and direct current electroplating. Mater. Des., Vol. 32, pp. 4478–4484.

Alsoufi, M.S., Alhazmi, M.W., Ghulman, H.A., Munshi, S.M., Azam, S. (2016). Surface roughness and knoop indentation micro-hardness behavior of aluminium oxide (Al2O3) and polystyrene (C8H8)n materials. Int. J. Mech. Mechatronics Eng., Vol. 16, pp. 43–49.

Ankur, Bharti, A., Prasad, D., Kumar, N., Saxena, K.K. (2021). A Re-investigation: Effect of various parameter on mechanical properties of copper matrix composite fabricated by powder metallurgy. Mater. Today Proc., Vol. 45, pp. 4595–4600.

Baba, Y., Inoue, T., Sugioka, K.I., Kobatake, H., Fukuyama, H., Kubo, M., Tsukada, T. (2012). Thermal conductivity measurement of molten copper using an electromagnetic levitator superimposed with a static magnetic field. Meas. Sci. Technol., Vol. 23.

Benamara, M., Iben Nassar, K., Rivero-Antúnez, P., Essid, M., Soreto Teixeira, S., Zhao, S., Serrà, A., Esquivias, L. (2024). Study of Electrical and Dielectric Behaviors of Copper-Doped Zinc Oxide Ceramic Prepared by Spark Plasma Sintering for Electronic Device Applications. Nanomaterials Vol. 14.

Benea, L., Mitoseriu, O., Galland, J., Wenger, F., Ponthiaux, P. (2000). Corrosion study of copper composite coating by impedance spectroscopy method. Werkstoffe und Korrosion., Vol. 51, pp. 491–495.

Bharti, S., Ghetiya, N.D., Patel, K.M. (2020). Micro-hardness and wear behavior of AA2014/Al2O3 surface composite produced by friction stir processing. SN Appl. Sci., Vol. 2, pp. 1–16.

Bragg, W.L. (1914). XLII. The crystalline structure of copper . London, Edinburgh, Dublin Philos. Mag. J. Sci., Vol. 28, pp. 355–360.

Cao, Zhang, Cai.P., Jiang.Y. (2022). Effect of Reaction Temperature and Heat Treatment Time on Electrical and Mechanical Performance TiB_2 particles and TiB Whiskers Reinforced Copper Matrix Composites. Metals, Vol. 12, pp. 592

Chen, Z.X., Hillairet, J., Turq, V., Song, Y.T., Laloo, R., Bernard, J.M., Vulliez, K., Lombard, G. (2018). Characterizations of thermal stability and electrical performance of Au-Ni coating on CuCrZr substrate for high vacuum radio-frequency contact application. Thin Solid Films., Vol. 659, pp. 81–88.

Cho, J.H., Rollett, A.D., Cho, J.S., Park, Y.J., Moon, J.T., Oh, K.H. (2006). Investigation of recrystallization and grain growth of copper and gold bonding wires. Metall. Mater. Trans. A Phys. Metall. Mater. Sci., Vol. 37, pp. 3085–3097.

Chung, C.Y., Lee, M.T., Tsai, M.Y., Chu, C.H., Lin, S.J. (2014). High thermal conductive diamond/Cu-Ti composites fabricated by pressureless sintering technique. Appl. Therm. Eng., Vol. 69, pp. 208–213.

Chung, D.D.L., Xi, X. (2022). A review of the colossal permittivity of electronic conductors, specifically metals and carbons. Mater. Res. Bull., Vol. 148, pp. 111654.

Cohen, J. (1960). Polarization effects in electrical “conductivity” of artificial sapphire at high temperatures. J. Phys. Chem. Solids., Vol. 16, pp. 285–290.

Collinson, M.M. (2001). Handbook of Advanced Electronic and Photonic Materials and Devices. Handb. Adv. Electron. Photonic Mater. Devices., Vol. 4, pp. 163–194.

Cong, D., Huimin, L., Shan, F., Yuan, Q., Qilong, H., Jiachen, J. (2019). Effect of La2O3 addition on copper matrix composites reinforced with Al2O3 ceramic particles. Mater. Res. Express., Vol. 6.

Crowe, C.R., Rose, M.F. (1971). Isochronal recovery of the shape of the normal magnetization curve of nickel shocked at 400 kbar. J. Appl. Phys., Vol. 42, pp. 4319–4323.

D. SABER, K.A.E.-A.& A.F. (2016). Corrosion Behavior of Copper–Alumina Nanocomposites in Different Corrosive Media. Int. J. Mech. Eng., Vol. 5, pp. 1–10.

Degrave, J., Felici, F., Buchli, J., Neunert, M., Tracey, B., Carpanese, F., Ewalds, T., Hafner. (2022). Magnetic control of tokamak plasmas through deep reinforcement learning. Nature., Vol. 602, pp. 414–419.

Dong, S., Zhou, J., Hui, D., Wang, Y., Zhang, S. (2015). Size dependent strengthening mechanisms in carbon nanotube reinforced metal matrix composites. Compos. Part A Appl. Sci. Manuf., Vol. 68, pp. 356–364.

Ea, E., Ragab M. (2019). Modern Approaches on Material Science Synergetic Reinforcement of Cu-11.0 wt.% Al Alloy with Al 2 O 3 Nano-Sized Particles and Carbon Nanotubes CNTs. pp. 186–194.

Egbo, M.K. (2021). A fundamental review on composite materials and some of their applications in biomedical engineering. J. King Saud Univ. - Eng. Sci., Vol. 33, pp. 557–568.

El-Kady, O.A., Yehia, H.M., Nouh, F., Ghayad, I.M., El-Bitar, T., Daoush, W.M. (2022). Enhancement of Physical Properties and Corrosion Resistance of Al-Cu-Al2O3/Graphene Nanocomposites by Powder Metallurgy Technique. Materials (Basel)., Vol. 15.

Fathy, A., El-Kady, O. (2013). Thermal expansion and thermal conductivity characteristics of Cu-Al2O3 nanocomposites. Mater. Des., Vol. 46, pp. 355–359.

Fathy, A., Shehata, F., Abdelhameed, M., Elmahdy, M. (2012). Compressive and wear resistance of nanometric alumina reinforced copper matrix composites. Mater. Des., Vol. 36, pp. 100–107.

Feng, J., Liang, S., Song, K., Guo, X., Zhang, Y., Li, G., Volinsky, A.A. (2019). Effects of Particle Characteristic Parameters on the Electrical Conductivity of TiB2/Cu Composites: A Modified Model for Predicting Their Electrical Conductivity. J. Mater. Eng. Perform., Vol. 28, pp. 4316–4323.

Gain, A.K., Zhang, L., Quadir, M.Z. (2016). Thermal aging effects on microstructures and mechanical properties of an environmentally friendly eutectic tin-copper solder alloy. Mater. Des., Vol. 110, pp. 275–283.

Gautam, Y.K., Somani, N., Kumar, M., Sharma, S.K. (2018). A review on fabrication and characterization of copper metal matrix composite (CMMC). AIP Conf. Proc. 2018.

Gorman, M., Dzombak, D. (2020). Stocks and flows of copper in the U.S.: Analysis of circularity 1970–2015 and potential for increased recovery. Resour. Conserv. Recycl., Vol. 153, pp. 104542.

Gorynin, I. V., Fabritsiev, S.A., Rybin, V. V., Kasakov, V.A., Pokrovskii, A.S., Barabash, V.R., Prokofiyev, Y.G. (1992). Radiation-resistant properties of copper alloys intended for fusion reactor applications. J. Nucl. Mater., Vol. 194, pp. 401–406.

Gurevich, V.L., Tagantsev, A.K. (1991). Advances in Physics Intrinsic dielectric loss in crystals. Adv. Phys., Vol. 40, pp. 719–767.

Guschlbauer, R., Momeni, S., Osmanlic, F., Körner, C. (2018). Process development of 99.95% pure copper processed via selective electron beam melting and its mechanical and physical properties. Mater. Charact. Vol. 143, pp. 163–170.

Halder, K., Paul, B.K., Bagchi, B., Bhattacharya, A., Das, S. (2014). Copper Ion Doped Mullite Composite in Poly (vinylidene Fluoride) Matrix: Effect on Microstructure, Phase Behavior and Electrical Properties. J. Res. Updat. Polym. Sci., Vol. 3, pp. 157–169.

Hamasha, K., Hamasha, M.M., Hamasha, S. (2022). Effect of Thermal Aging on the Mechanical Properties of SAC305. Materials (Basel)., Vol. 15.

Hao, X. (2013). A review on the dielectric materials for high energy-storage application. J. Adv. Dielectr., Vol. 03, pp. 1330001.

Harling Yu, O.G., Grant, N., Meyer, J. (1981). Holland PublisbingGompany APPLICATION OF HIGH STRENGTH COPPER ALLOYS FOR A FUSION REACTOR FIRST WALL. JournalofNuclear Mater., Vol. 103, pp. 127–132.

Hidalgo-Manrique, P., Lei, X., Xu, R., Zhou, M., Kinloch, I.A., Young, R.J. (2019). Copper/graphene composites: a review. J. Mater. Sci., Vol. 54, pp. 12236–12289.

Hirsch, J. (1997). Aluminium alloys for automotive application. Mater. Sci. Forum., Vol. 242, pp. 33–50.

Holman, S.W., Lawrence, R.R., Barr, L. (1895). Melting Points of Aluminum. Source Proc. Am. Acad. Arts Sci., Vol. 31, pp. 218–233.

Hsieh, C.L., Tuan, W.H. (2007). Thermal expansion behavior of a model ceramic-metal composite. Mater. Sci. Eng., Vol. A. 460–461, pp. 453–458.

Huntz, A.M., Maréchal, L., Lesage, B., Molins, R. (2006). Thermal expansion coefficient of alumina films developed by oxidation of a FeCrAl alloy determined by a deflection technique. Appl. Surf. Sci., Vol. 252, pp. 7781–7787.

Jamaati, R., Toroghinejad, M.R. (2010). Application of ARB process for manufacturing high-strength, finely dispersed and highly uniform Cu/Al2O3 composite. Mater. Sci. Eng. A 527, 7430–7435. https://doi.org/10.1016/j.msea.2010.08.038

Jeff Doebrich. (2009). Copper — A Metal for the Ages How Do We Use Copper ? Where Does Copper Come From ? USGS Sci. a Chang. World. pp. 1–4.

Jenei, P., Gubicza, J., Yoon, E.Y., Kim, H.S., Lábár, J.L. (2013). High temperature thermal stability of pure copper and copper-carbon nanotube composites consolidated by High Pressure Torsion. Compos. Part A Appl. Sci. Manuf. Vol. 51, pp. 71–79.

Jensin Joshua, J., Venkatanarayanan, P.S., Singh, D. (2020). A literature review on composite materials filled with and without nanoparticles subjected to high/low velocity impact loads. Mater. Today Proc. Vol. 33, pp. 4635–4641.

Jiang, Q., Wang, X., Zhu, Y., Hui, D., Qiu, Y. (2014). Mechanical, electrical and thermal properties of aligned carbon nanotube/polyimide composites. Compos. Part B Eng. Vol. 56, pp. 408–412.

Jogi, T.D. (2014). Alumina copper composites for thermoelectric applications.

Ju, H., Liu, J., Zhuo, S., Wang, Y., Li, S. (2023). Effect of Thermal Aging on the Microstructure and Mechanical Properties of ER308L/Z2CND18.12N2 Dissimilar Welds. Materials (Basel). Vol. 16.

Kargul, M., Borowiecka-Jamrozek, J., Konieczny, M. (2018). The effect of reinforcement particle size on the properties of Cu-Al 2 O 3 composites. IOP Conf. Ser. Mater. Sci. Eng. Vol. 461, pp. 6–12.

Karmakar, R., Maji, P., Ghosh, S.K. (2021). A Review on the Nickel Based Metal Matrix Composite Coating. Met. Mater. Int. Vol. 27, pp. 2134–2145.

Karthik, R., Tummala, V. (2017). Voltage dependent Maxwell-Wagner polarization in dielectric heterostructures. Mater. Today Proc. Vol. 4, pp. 8751–8757.

Kaur, S., Sandhu, M., Kaur, J. (2016). Dielectric Theory and Its Properties. Int. J. Emerg. Technol. Eng. Res. Vol. 4, pp. 145–150.

Khan, M.A.R., Ahmed, T., Islam, M.K., Dhar, S.A., Qadir, M.R. (2019). Effect of copper content on thermal and mechanical properties of eutectoid Zn-Al alloy. arXiv.

Kurley, J.M., Halstenberg, P.W., McAlister, A., Raiman, S., Dai, S., Mayes, R.T. (2019). Enabling chloride salts for thermal energy storage: Implications of salt purity. RSC Adv. Vol. 9, pp. 25602–25608.

L, R. kumar, K. S, A. (2020). Corrosion and wear behaviour of nano Al2O3 reinforced copper metal matrix composites synthesized by high energy ball milling. Part. Sci. Technol. Vol. 38, pp. 228–235.

LeBlanc, D. (2010). Molten salt reactors: A new beginning for an old idea. Nucl. Eng. Des. Vol. 240, pp. 1644–1656.

Leedy, K.D., Stubbins, J.F., Singh, B.N., Garner, F.A. (1996). Fatigue behavior of copper and selected copper alloys for high heat flux applications. J. Nucl. Mater. Vol. 233–237, pp. 547–552.

Leelawattananon, T., Locharoenrat, K., Chittayasothorn, S. (2017). Simulation of copper thin film thickness optimization for surface plasmon using the finite element method. SIMULTECH 2017 - Proc. 7th Int. Conf. Simul. Model. Methodol. Technol. Appl. pp. 188–195.

Leon-Patiño, C.A., Aguilar-Reyes, E.A., Braulio-Sánchez, M., Rodríguez-Ortiz, G., Bedolla-Becerril, E. (2014). Microstructure and shear strength of sintered Cu-Al2O3 composite joined to Cu using Ag-Cu and Cu-Zn filler alloys. Mater. Des. Vol. 54, pp. 845–853.

Li, M., Zinkle, S.J. (2012). Physical and Mechanical Properties of Copper and Copper Alloys. Compr. Nucl. Mater. Vol. 1-5, pp. 667–690.

Liu, L., Liu, Z., Chen, R., Liu, X., Yan, A., Lee, D., Li, W. (2014). Effect of strip casting on microstructure and magnetic properties of 2:17 type Sm-Co sintered magnets. IEEE Trans. Magn. Vol. 50, pp. 2–5.

Madeni, J.C., Liu, S. (2011). Effect of thermal aging on the interfacial reactions of tin-based solder alloys and copper substrates and kinetics of formation and growth of intermetallic compounds. Soldag. Inspeção Vol. 16, pp. 86–95.

Madhusudan, S., Sarcar, M.M.M., Rao, N.B.R.M. (2016). Mechanical properties of Aluminum-Copper(p) composite metallic materials. J. Appl. Res. Technol. Vol. 14, pp. 293–299.

Mahbuba, M., Chisty, N.A. (2014). Study of the Relative Permittivity Response of Metal Nanoantenna at Optical Frequency. Int. J. Eng. Res. Vol. 3, pp. 584–587.

Mantas, P.Q. (1999). Dielectric response of materials: Extension to the Debye model. J. Eur. Ceram. Soc. Vol. 19, pp. 2079–2086.

Marco, D. Di, Drissi, K., Delhote, N., Tantot, O., Geffroy, P.M., Verdeyme, S., Chartier, T. (2016). Dielectric properties of pure alumina from 8 GHz to 73 GHz. J. Eur. Ceram. Soc. Vol. 36, pp. 3355–3361.

Materials, N., Alloys, C., Fusion, F.O.R., Applications, R. (1984). Vol. 199, pp. 799–801.

Matsumura, T. (1966). the Electrical Properties of Alumina At High Temperatures. Can. J. Phys. Vol. 44, pp. 1685–1698.

Mazahery, A., Abdizadeh, H., Baharvandi, H.R. (2009). Development of high-performance A356/nano-Al2O3 composites. Mater. Sci. Eng. A Vol. 518, pp. 61–64.

Medeliene, V., Stankevič, V., Grigucevičiene, A., Selskiene, A., Bikulčius, G,(2011). The study of corrosion and wear resistance of copper composite coatings with inclusions of carbon nanomaterials in the copper metal matrix. Medziagotyra. Vol. 17, pp. 132–139.

Metikoš-Huković, M., Škugor, I., Grubač, Z., Babić, R. (2010). Complexities of corrosion behaviour of copper-nickel alloys under liquid impingement conditions in saline water. Electrochim. Acta. Vol. 55, pp. 3123–3129.

Mohanavel, V., Vinoth, T., Iyankumar, R., Vinoth, N. (2020). Mechanical and corrosion behaviour of copper matrix composites fabricated by powder metallurgy process. Mater. Today Proc. Vol. 33, pp. 3394–3398.

Mortensen, A., Llorca, J. (2010). Metal matrix composites. Annu. Rev. Mater. Res. Vol. 40, pp. 243–270.

Mrowec, S., Stokłosa, A. (1971). Oxidation of copper at high temperatures. Oxid. Met. Vol. 3, pp. 291–311.

Mustafa, E., Németh, R.M., Afia, R.S.A., Tamus, Z. (2021). Parameterization of debye model for dielectrics using voltage response measurements and a benchmark problem. Period. Polytech. Electr. Eng. Comput. Sci. Vol. 65, pp. 138–145.

Nomura, Y., Suzuki, R., Saito, M. (2002). Strength of copper alloys in high temperature environment. J. Nucl. Mater. Vol. 307, pp. 681–685.

Nordblad, P. (2016). Disordered Magnetic Systems. Ref. Modul. Mater. Sci. Mater. Eng. pp. 1–6.

Nuzulia, A. (1967). Non-native Intramolecular Radical CyclinizationCatalysed by a B_{12}-Enzyme. Angew. Chemie Int. Ed. 6(11), Vol. 30, pp. 5–24.

Ojha, S., Ali, M.S., Roy, M., Bhattacharya, S. (2021). Hopping frequency and conductivity relaxation of promising chalcogenides: AC conductivity and dielectric relaxation approaches. Mater. Res. Express. Vol. 8.

Osman, A.F., Mariatti, M. (2006). Properties of aluminum filled polypropylene composites. Polym. Polym. Compos. Vol. 14, pp. 623–634.

Pei, X., Kang, W., Yue, W., Bange, A., Heineman, W.R., Papautsky, I. (2014). Disposable copper-based electrochemical sensor for anodic stripping voltammetry. Anal. Chem. Vol. 86, pp. 4893–4900.

Pérez-Madrid, A., Lapas, L.C., Rubí, J.M. (2017). Multiscale Model for the Dielectric Permittivity. Zeitschrift fur Naturforsch. - Sect. A J. Phys. Sci. Vol. 72, pp. 109–114.

Poole, W.J., Ashby, M.F., Fleck, N.A. (1996). Micro-hardness of annealed and work-hardened copper polycrystals. Scr. Mater. Vol. 34, pp. 559–564.

Rahman, M.M., Ahmed, S.R., Kaiser, M.S. (2021). On the investigation of reuse potential of SnPb-solder affected copper subjected to work-hardening and thermal ageing. Mater. Charact. Vol. 172, pp. 110-115.

Raiman, S.S., Lee, S. (2018). Aggregation and data analysis of corrosion studies in molten chloride and fluoride salts. J. Nucl. Mater. Vol. 511, pp. 523–535.

Rayssi, C., El Kossi, S., Dhahri, J., Khirouni, K. (2018). Frequency and temperature-dependence of dielectric permittivity and electric modulus studies of the solid solution Ca0.85Er0.1Ti1-: XCo4 x /3O3 ($0 \leq x \leq 0.1$). RSC Adv. Vol. 8, pp. 17139–17150.

Rogti, F., Ferhat, M. (2014). Maxwell-Wagner polarization and interfacial charge at the multi-layers of thermoplastic polymers. J. Electrostat. Vol. 72, pp. 91–97.

Saheb, N., Iqbal, Z., Khalil, A., Hakeem, A.S., Aqeeli, N. Al, Laoui, T., Al-qutub, A. (2012). Spark Plasma Sintering of Metals and Metal Matrix Nanocomposites : A Review.

Seetharaman, S., Subramanian, J., Singh, R.A., Wong, W.L.E., Nai, M.L.S., Gupta, M. (2022). Mechanical Properties of Sustainable Metal Matrix Composites: A Review on the Role of Green Reinforcements and Processing Methods. Technologies, Vol. 10.

Simchi, H., Simchi, A. (2009). Tensile and fatigue fracture of nanometric alumina reinforced copper with bimodal grain size distribution. Mater. Sci. Eng. A Vol. 507, pp. 200–206.

Singh, H., Singh Brar, G., Kumar, H., Aggarwal, V. (2020). A review on metal matrix composite for automobile applications. Mater. Today Proc. Vol. 43, pp. 320–325.

Singh, M.K., Gautam, R.K., Ji, G. (2019). Mechanical properties and corrosion behavior of copper based hybrid composites synthesized by stir casting. Results Phys. Vol. 13, pp. 102319.

Soundararajan, S., Muthukutti, G.P., Kumarasamy, S.P., Vijayananth, K., Barik, D., Sharma, P., Paramasivam, P. (2023). Investigating the tribological characteristics of copper surface composites reinforced with high entropy alloy (AlCoCrCuFe) through friction stir processing. Sci. Rep. Vol. 13, pp. 1–16.

Strojny-Nędza, A., Pietrzak, K., Węglewski, W. (2016). The Influence of Al2O3 Powder Morphology on the Properties of Cu-Al2O3 Composites Designed for Functionally Graded Materials (FGM). J. Mater. Eng. Perform. Vol. 25, pp. 3173–3184.

Studenyak, I.P., Pogodin, A.I., Studenyak, V.I., Izai, V.Y., Filep, M.J., Kokhan, O.P., Kranjčec, M., Kúš, P. (2020). Electrical properties of copper- and silver-containing superionic (Cu1−xAgx)7SiS5I mixed crystals with argyrodite structure. Solid State Ionics. Vol. 345, pp. 3–8.

Tarasenko, R., Orendáčová, A., Orendáč, M., Kajňaková, M., Feher, A. (2010). Experimental study of magnetic properties of alumina ceramics. Acta Phys. Pol. A Vol. 118, pp. 1067–1068.

Taylor, N.T., Davies, F.H., Davies, S.G., Price, C.J., Hepplestone, S.P. (2019). The Fundamental Mechanism Behind Colossal Permittivity in Oxides. Adv. Mater. Vol. 31.

Teixeira, H.A., Araujo, C.I.L. d. (2022). Magnetic properties and Curie temperature tuning in copper-Permalloy alloys obtained by electrodeposition. J. Magn. Magn. Mater. Vol. 561, pp. 169702.

Tse, M.Y., Wei, X., Wong, C.M., Huang, L.B., Lam, K.H., Dai, J., Hao, J. (2018). Enhanced dielectric properties of colossal permittivity co-doped TiO2/polymer composite films. RSC Adv. Vol. 8, pp. 32972–32978.

Tsoi, M., Fontana, R.E., Parkin, S.S.P. (2003). Magnetic domain wall motion triggered by an electric current. Appl. Phys. Lett. Vol. 83, pp. 2617–2619.

Tufaile, A.P.B., Tufaile, A. (2021). Hysteresis Loops, Dynamical Systems and Magneto-Optics. Springer Proc. Complex. pp. 981–993.

Tuichai, W., Danwittayakul, S., Chanlek, N., Srepusharawoot, P., Thongbai, P., Maensiri, S. (2017). Origin(s) of the apparent colossal permittivity in (In1/2Nb1/2)xTi1−xO2: clarification on the strongly induced Maxwell-Wagner polarization relaxation by DC bias. RSC Adv. Vol. 7, pp. 95–105.

U.S. Department of the Interior, U.S Geological Survey, (2022). Mineral Industry Surveys: copper 2023.

Valb, R., n.d. ill I., VTT. (2024). Tensile and Fracture Toughness Properties of Copper Alloys and Their HIP Joints with Austenitic Stainless Steel in Unirradiated and Neutron Irradiated Condition.Vol. 7, pp. 505-506

Vila, R., González, M., Mollá, J., Ibarra, A. (1998). Dielectric spectroscopy of alumina ceramics over a wide frequency range. J. Nucl. Mater. Vol. 253, pp. 141–148.

Wang, C., Qi, C. (2022). Revealing the structural and chemical properties of copper-based nanoparticles released from copper treated wood. RSC Adv. Vol. 12, pp. 11391–11401.

Wang, C.C., Lu, H.B., Jin, K.J., Yang, G.Z. (2008). Temperature-dependent dielectric strength of a Maxwell-Wagner type relaxation. Mod. Phys. Lett. B Vol. 22, pp. 1297–1305.

Weigand, M., Kemna, A. (2016). Debye decomposition of time-lapse spectral induced polarisation data. Comput. Geosci. Vol. 86, pp. 34–45.

White, G.K. (1972). Thermal expansion of platinum at low temperatures. J. Phys. F Met. Phys. Vol. 2.

Wobschall, D. (1977). A Theory of the Complex Dielectric Permittivity of Soil Containing Water: The Semidisperse Model. IEEE Trans. Geosci. Electron. Vol. 15, pp. 49–58.

Xia, X., Zhong, Z., Weng, G.J. (2017). Maxwell–Wagner–Sillars mechanism in the frequency dependence of electrical conductivity and dielectric permittivity of graphene-polymer nanocomposites. Mech. Mater. Vol. 109, pp. 42–50.

Zaidi, S.H., Jonscher, A.K. (1999). Dielectric Relaxation in Solids: Andrew K Jonscher. J. Phys. D Appl. Phys. Vol. 32, pp. 57.

Zare, Y., Rhee, K.Y. (2019). Simplification and development of McLachlan model for electrical conductivity of polymer carbon nanotubes nanocomposites assuming the networking of interphase regions. Compos. Part B Eng. Vol. 156, pp. 64–71.

Zhang, C., Yao, D., Yin, J., Zuo, K., Xia, Y., Liang, H., Zeng, Y.P. (2018). Effects of whisker surface modification on microstructures, mechanical and thermal properties of β-Si3N4 whiskers reinforced Al matrix composites. Mater. Des. Vol. 159, pp. 117–126.

Zinkle, S.J. (2016). Applicability of copper alloys for DEMO high heat flux components. Phys. Scr. Vol. 4, pp. 14004.